CDU 53 (469) (05)

PORTUGALIAE PHYSICA

VOLUME 9
1974-1975

INSTITUTO DE ALTA CULTURA
CENTROS DE ESTUDOS DE FÍSICA DAS UNIVERSIDADES PORTUGUESAS

PORTUGALIAE PHYSICA

Fundadores: A. Cyrillo Soares, M. Telles Antunes, A. Marques da Silva, M. Valadares.

VOLUME 9 1974 75

VOLUMES PUBLICADOS:

Vol. 1 — 1943-45 — 326 pp.
Vol. 2 — 1946-47 — 256 pp.
Vol. 3 — 1949-54 — 173 pp.
Vol. 4 — 1965-66 — 304 pp.
Vol. 5 — 1967-70 — 194 pp.
Vol. 6 — 1970-71 — 316 pp.
Vol. 7 — 1971-72 — 210 pp.
Vol. 8 — 1972-73 — 266 pp.
Vol. 9 — 1974-75 — 182 pp.

Redacção: Laboratório de Física da Faculdade de Ciências — Lisboa-2 (PORTUGAL)

Comissão de redacção:

J. Moreira de Araújo — Carlos Braga — Carlos Cacho — A. Pires de Carvalho — M. Abreu Faro — J. Gomes Ferreira — F. Bragança Gil — Manuel Laranjeira. Amaro Monteiro — J. Pinto Peixoto — J. da Providência — Lídia Salgueiro — J. de Almeida Santos — José Sarmento — António da Silveira — J. Veiga Simão.

ÍNDICES

MATÉRIAS

MATIÈRES-MATTERS

VOLUME 9

Fasc. 1 (1974)

Molecular approach to the hydrodynamic viscosities of nematic liquid crystals, by ASSIS F. MARTINS 1- 8

Le tenseur d'impulsion-énergie liée et les systèmes relativistes à masse propre variable, par ANTÓNIO C. DE SALES LUÍS 9- 20

Scaling, extended vector meson dominance and the existence of the neutral pion, by R. VILELA MENDES 21- 28

Fasc. 2 (1974)

The influence of the mixing on the Coulomb excitation probabilities of beta and gamma bands, by J. M. DOMINGOS 29- 40

On the divergence of enthalpy and the energetics of the atmosphere, by JOSÉ PINTO PEIXOTO 41- 58

Fasc. 3 (1975)

The field of the divergence of enthalpy of the atmosphere in the Southern Hemisphere, by JOSÉ PINTO PEIXOTO 59- 84

The decay of some $^{27}Al(p,\gamma)^{28}Si$ *resonances,* by J. D. CUNHA, P. M. CORRÊA and C. M. DA SILVA 85- 96

Interference effects in heavy ion elastic and inelastic scattering, by R. DA SILVEIRA and CH. LECLERCQ-WILLAIN 97-116

Fasc. 4 (1975)

Pauli correction to the deuteron folded potential, by A. M. GONÇALVES and F. D. SANTOS 117-128

Simple molecular statistical interpretation of the nematic viscosity γ_1, by A. F. MARTINS and A. C. DIOGO 129-140

La correspondance entre modeles microscopiques et macroscopiques, par E. MATAGNE 141-176

Liste des publications reçues actuellement en échange avec Portugaliae Physica 177

Instructions pour les auteurs 181

AUTORES

AUTEURS — AUTHORS

CORRÊA, P. M. — vd. J. D. CUNHA

CUNHA, J. D., P. M. CORRÊA and C. M. DA SILVA — *The decay of some* $^{27}Al(p,\gamma)^{28}Si$ *resonances* 85

DIOGO, A. C — vd. A. F. MARTINS

DOMINGOS, J. M. — *The influence of the mixing on the Coulomb excitation probabilities of beta and gamma bands* 29

GONÇALVES, A. M. and F. D. SANTOS — *Pauli correction to the deuteron folded potential* 117

LECLERCQ-WILLAIN, CH. — vd. R. DA SILVEIRA

LUÍS, António C. de Sales — *Le tenseur d'impulsion-énergie liée et les systèmes relativistes à masse propre variable* 9

MARTINS, Assis F. — *Molecular approach to the hydrodynamic viscosities of nematic liquid crystals* 1

MARTINS, A. F. and A. C. DIOGO — *Simple molecular statistical interpretation of the nematic viscosity* γ_1 129

MATAGNE, E. — *La correspondance entre modeles microscopiques et macroscopiques* 141

MENDES, R. Vilela — *Scaling, extended vector meson dominance and the existence of the neutral pion* 21

PEIXOTO, José Pinto — *On the divergence of enthalpy and the energetics of the atmosphere* 41

PEIXOTO, José Pinto — *The field of the divergence of enthalpy of the atmosphere in the Southern Hemisphere* 59

SANTOS. F. D. — vd. A. M. GONÇALVES

SILVA, C. M. da — vd. J. D. CUNHA

SILVEIRA, R. da and CH LECLERCQ-WILLAIN — *Interference effects in heavy ion elastic and inelastic scattering* 97

PORTUGALIAE PHYSICA

VOLUME 9
FASCÍCULO 1
1974

INSTITUTO DE ALTA CULTURA
CENTROS DE ESTUDOS DE FÍSICA DAS UNIVERSIDADES PORTUGUESAS

PORTUGALIAE PHYSICA

Fundadores: A. Cyrillo Soares, M. Telles Antunes, A. Marques da Silva, M. Valadares.

VOLUME 9 1974 FASCÍCULO 1

VOLUMES PUBLICADOS:

Vol. 1 — 1943-45 — 326 pp.

Vol. 2 — 1946-47 — 256 pp.

Vol. 3 — 1949-54 — 173 pp.

Vol. 4 — 1965-66 — 304 pp.

Vol. 5 — 1967-70 — 194 pp.

Vol. 6 — 1970-71 — 316 pp.

Vol. 7 — 1971-72 — 210 pp.

Vol. 8 — 1972-73 — 266 pp.

Redacção: Laboratório de Física da Faculdade de Ciências — Lisboa-2 (PORTUGAL)

Comissão de redacção:

J. Moreira de Araújo — Carlos Braga — Carlos Cacho — A. Pires de Carvalho — M. Abreu Faro — J. Gomes Ferreira — F. Bragança Gil — Manuel Laranjeira. Amaro Monteiro — J. Pinto Peixoto — J. da Providência — Lídia Salgueiro — J. de Almeida Santos — José Sarmento — António da Silveira — J. Veiga Simão.

ÍNDICE

(Table des matières)

Molecular approach to the hydrodynamic viscosities of nematic liquid crystals, by ASSIS F. MARTINS 1

Le tenseur d'impulsion-énergie liée et les systèmes relativistes à masse propre variable, par ANTÓNIO C. DE SALES LUÍS 9

Scaling, extended vector meson dominance and the existence of the neutral pion, by R. VILELA MENDES 21

MARTINS, Assis F. — **Molecular approach to the hydrodynamic viscosities of nematic liquid crystals.**

Portgal. Phys. — 9 (1): 1-8, 1974

We discuss the temperature behaviour of the capillary-flow viscosities of nematics and outline a molecular theory of the rotational viscosity γ_1. This theory gives $\gamma_1(T) = \text{const.}\ S^2 \exp(\varepsilon S/kT)$, in good agreement with experimental data. The parameter $\varepsilon = 3A/2mV^2$ comes from the Maier and Saupe's potential and is equal to 0.8795 kcal/mole in the case of *p*-azoxyanisole. From this we get the nearest-neighbor coordination number $m = 6.3$.

LUÍS, António C. de Sales — **Le tenseur d'impulsion énergie liée et les systèmes relativistes à masse propre variable.**

Portgal. Phys. — 9 (1): 9-20, 1974

L'interprétation thermodynamique de l'effect Joule a amené l'auteur à introduire le «tenseur d'impulsion-énergie liée»:

(1) $$S_{\alpha}^{\beta} = \frac{T^0 S^0}{c^2} u^{\alpha} u^{\beta}$$

et le «4-vecteur d'impulsion-entropique»:

(2) $$G_{(s)}^{\alpha} = \frac{T^0 S^0}{c^2} u^{\alpha}.$$

Par conséquent, il faut attribuer à un système relativiste une masse m_s^0

MENDES, R. Vilela — **Scaling, extended vector meson dominance and the existence of the neutral pion.**

Portgal. Phys. — 9 (1): 21-28, 1974

It is shown that in the framework of the extended vector meson dominance model, scaling in electron-positron annihilation is incompatible with the finiteness of the $\pi^0 \to 2\gamma$ decay width.

The implications of the result for the validity of the extended vector dominance idea or for scale breaking are discussed.

telle que:

$$m_s^0 = \frac{T^0 S^0}{c^2} \tag{3}$$

tout à fait d'accord avec les idées d'Einstein. Alors, la masse propre d'un système est la somme de sa masse propre (usuelle) m^0 et de sa masse propre entropique m_s^0:

$$M^0 = m^0 + \frac{T^0 S^0}{c^2}. \tag{4}$$

Toutes les transformations dans la nature sont irréversibles et les phénomènes irréversibles créent effectivement de l'entropie et par conséquent de l'énergie liée. Alors, compte tenu de (4), les systèmes relativistes sont des systèmes à masse propre variable; par l'intermédiaire d'un exemple (collision inélastique) on montre le rôle joué par le 4-vecteur d'impulsion-entropique et la cohérence des idées introduites.

CDU 53 (469) (05)

PORTUGALIAE PHYSICA

VOLUME 9
FASCÍCULO 1
1974

117

MOLECULAR APPROACH TO THE HYDRODYNAMIC VISCOSITIES OF NEMATIC LIQUID CRYSTALS (*)

Assis F. Martins

Instituto de Física e Matemática
Av. Gama Pinto-2, Lisbon-4, Portugal

ABSTRACT — We discuss the temperature behaviour of the capillary-flow viscosities of nematics and outline a molecular theory of the rotational viscosity γ_1. This theory gives $\gamma_1(T) = \text{const.}\ S^2 \exp(\varepsilon S/kT)$, in good agreement with experimental data. The parameter $\varepsilon = 3A/2mV^2$ comes from the Maier and Saupe's potential and is equal to 0.8795 kcal/mole in the case of *p*-azoxyanisole. From this we get the nearest-neighbor coordination number $m = 6.3$.

1 — INTRODUCTION

The rheological properties of nematic liquid crystals have received much attention in the past. In particular Miesowicz clearly defined three independent viscosities to characterize the flow of such anisotropic liquids, and latter Porter and Johnson studied experimentally their temperature dependence. More recently Leslie derived a hydrodynamic theory of nematic liquid crystals according to which the rheological properties of incompressible nematics depend on five coefficients. Three of them can be chosen to be the Miesowicz viscosities but this is not always most convenient. For comparison, it is remembered that incompressible isotropic liquids show a single viscosity.

In this paper, the hydrodynamic viscosities of nematic liquid crystals introduced by Leslie are considered from the point of

(*) Received 2 November 1973.

view of molecular theories, and we try to explain their temperature behaviour. Particular attention is payed to the rotational viscosity $\gamma_1(T)$.

2 — TOPICS ON CONTINUUM THEORY

The viscous properties of *incompressible* nematics may be characterized by the following set of five independent coefficients:

$$(1)\qquad \begin{cases} \mu \equiv \mu_1 = A_1 S^2 \\ \lambda \equiv \mu_4 = 2\,\eta_{iso} - a\,S + A_3 S^2 \\ \dfrac{1}{2}\gamma_1 \equiv \dfrac{1}{2}(\mu_3 - \mu_2) = C_1 S + C_2 S^2 \\ \dfrac{1}{2}\gamma_2 \equiv \dfrac{1}{2}(\mu_3 + \mu_2) = -B_1 S - B_2 S^2 \\ \dfrac{1}{2}\gamma_3 \equiv \dfrac{1}{2}(\mu_6 + \mu_5) = \dfrac{3}{2}a\,S + A_2 S^2 \end{cases}$$

Here, μ_i $(i = 1 \cdots 6)$ are the original viscosities introduced by Leslie in his hydrodynamic theory of nematics [1], S is the order parameter, and η_{iso} is the viscosity estrapolated from the isotropic phase $(S = 0)$. Expansions of the μ's in powers of S have been considered first by Helfrich and Imura and Okano [2] and used in (1). According to Imura and Okano, a, A_i, B_i, and C_i $(i = 1, 2, \cdots)$ are constants «which are expected to depend on temperature very weakly» [2]. The rotational viscosity γ_1 is of fundamental importance in the theory of nuclear spin-lattice relaxation in nematic mesophases [3, 12].

Leslie has shown that γ_1 is always positive. The order parameter is usually positive, but it can, in principle, be negative (metastable state). As γ_1 must vanish and have a minimum at $S = 0$, we have $C_1 = 0$ and $C_2 > 0$ in expression (1), so that:

$$(2)\qquad \gamma_1 = 2\,C_2 S^2$$

This result was first presented by Helfrich [2] who supposed it to be valid only for $|S| \ll 1$. The ratio γ_2/γ_1 is a coupling parameter between molecular orientation and shear flow. There

is evidence [4] that this parameter is continuous across the nematic-isotropic transition, in which case $B_1 = 0$ and consequently:

$$\gamma_2 = -2\,B_2\,S^2 \tag{3}$$

Using the theory of Leslie [1] and equations (1) we may derive expressions for the temperature dependence of the capillary-flow viscosities η_{1M} and η_{2M} as measured by Miesowicz and others [5, 6]. With $C_1 = 0$, but independently of B_1, we find:

$$\begin{cases} \eta_{1M} = \dfrac{1}{4}\,a\,S + \left[A_1 \sin^2\theta_0 \cos^2\theta_0 + \dfrac{1}{2}(A_2 + A_3) \right] S^2 + \eta_{iso} - \dfrac{1}{4}\gamma_1 \\ \eta_{2M} = \dfrac{1}{4}\,a\,S + \dfrac{1}{2}(A_2 + A_3)\,S^2 + \eta_{iso} + \gamma_1 \left(\dfrac{1}{4} + \dfrac{1/2}{\cos 2\theta_0} \right) \end{cases} \tag{4}$$

As a first approximation, we may take $\eta_{1M} \sim \eta_{iso} - (1/4)\gamma_1$ and $\eta_{2M} \sim \eta_{iso} + (3/4)\gamma_1$. These functions reproduce qualitatively the data compiled by Porter and Johnson [6], including the rapid increase of η_{1M} and decrease of η_{2M} just below the transition point to the isotropic state. Near T_c the agreement is quantitative. In the opposite side, near $T - T_c = -15^\circ C$ the difference between this approximation and experimental data is only about 11 % for η_{1M} and 8 % for η_{2M}. We have taken $\eta_{iso} = 2.871 \times 10^{-5}$ exp (2867/T) poise, as calculated from data in ref. [6], extrapolating the experimental curve relative to the isotropic phase.

3 — A MOLECULAR THEORY OF $\gamma_1(T)$

Let us now discuss the viscosity γ_1 from a molecular-statistical point of view. This viscosity concerns only the molecular reorientational motions, which take place against a potential barrier whose height is given by:

$$E = D(\theta)_{max} - D(\theta)_{min} = \frac{3}{2}\,\frac{A}{mV^2}\,S = \varepsilon\,S \tag{5}$$

where $D(\theta)$ is the mean field potential given by the Maier and Saupe's theory of nematics [7]. Expression (5) shows that the

activation energy E is nearly proportional to the order parameter S and so varies strongly with temperature. This behaviour contrasts with what is usual in isotropic liquids, for which E is constant over most practical temperature ranges.

The molecular motion which we have in mind (reorientation) is a rate process and may be treated in a manner similar to the one introduced by Eyring [8] in his study of the shear viscosity η of isotropic liquids. In the case of the *rotational* viscosity γ_1 we must, of course, consider an applied couple-density B and the proportional angular velocity N (flux proportional to force) instead of the velocity difference v and the force-density f. We must further remark that for the reorientation to be possible a local lattice expansion around the reorienting particle must take place. The microscopic volume V_N^* generated in this way can be related to the corresponding volume V_I^* of the isotropic phase by a spherical harmonic expansion. To lowest order, in the mean field approximation, we find:

$$V_N^* \propto V_I^* S^2 . \tag{6}$$

With these results in mind, we may apply the general theory of rate processes to calculate the (statistical) rotational velocity N of the molecules submitted to the applied couple-density B and finally obtain:

$$\gamma_1 = c S^2 \exp(\varepsilon S / k T) \tag{7}$$

where $c \simeq$ constant. Expressions (6) and (7) will be derived in more detail in a forthcoming paper.

By comparing expressions (2) and (7) we see that C_2 varies exponentially with temperature in contrast with the above mentioned expectation of Imura and Okano. Our result is significative because, in expression (2), S^2 is a statistical measure of the order and C_2 must contain the physical nature and have the physical dimensions of a viscosity.

Fig. 1 gives a compilation of the so far reported experimental data on γ_1, for *p*-azoxyanisole (PAA), as a function of temperature. The data have been fitted to equation (7) by the least squares method, giving $c = 0.1767\ \mathrm{g\,cm^{-1}\,s^{-1}}$ ($\equiv$ poise) and $\varepsilon = 0.8795$ kcal/mole. We have used the S values calculated by Chandrasekhar, which have been successfully contrasted with

experience [9]. The agreement between our result and experimental data is very good. The broken line in the figure shows that γ_1 cannot be simply proportional to S^2. An Arrhenius-type law with constant activation energy [10] is contradictory with accepted theories, e. g. ref. [7], and gives a not so good fit. Substituting in expression (5) the foregoing value of ε and the value of A/V^2 given by Maier and Saupe [7] we find $m = 6.3$

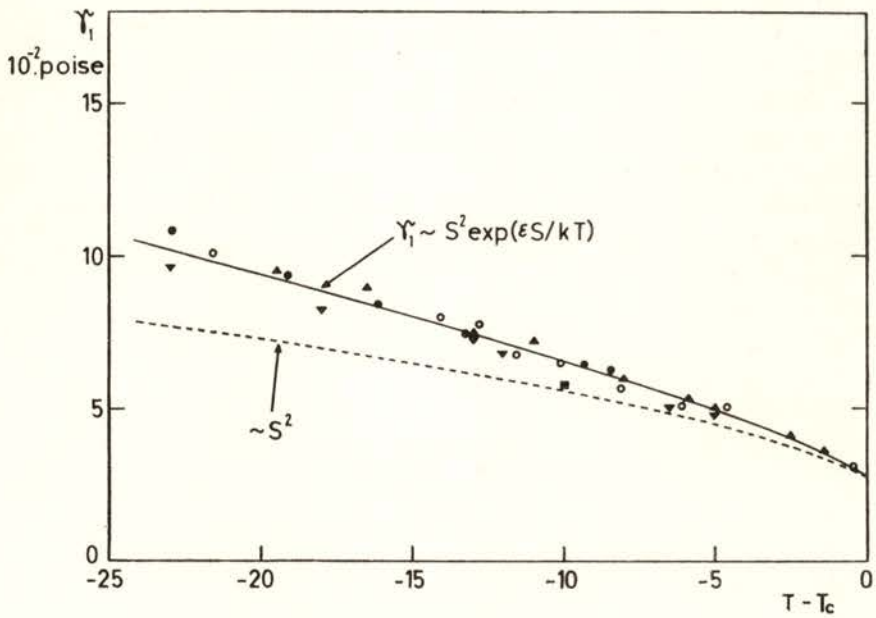

Fig. 1 — Rotational viscosity $\gamma_1(T)$ of PAA. Experimental points: full circles, from ref. [10]; square, from ref. [14]; open circles, from ref. [15]; triangles, from ref. [16].

for the nearest-neighbor coordination number. This is a meaningful result since m is equal to 6 in the Monte Carlo calculation of Lebwohl and Lasher [11] and we expect the real value to be larger, due to incoherent diffusion, but only slightly larger because in PAA the diffusion correlation time is about one order of magnitude greater that the correlation time for reorientation [12]. Note that the ε's definition of Lebwohl and Lasher (ε_{LL}) is not the same as that given by expressions (5) and (7): within the mean field approximation we have $\varepsilon_{LL} =$

$= -\frac{2}{3}\varepsilon$. They give $-\beta\varepsilon_{LL} = 0.77$ (mean field) and we have found from data on γ_1 that $\frac{2}{3}\beta\varepsilon = 0.73$, in good agreement. Another grateful result of the present theory is the value of $\varepsilon S_c = 0.293$ kcal/mole. This is about twice the heat of transition $\Delta Q_c = 0.137$ kcal/mole reported in ref. [13], as expected.

Expression (7) with the above values of c and ε gives $\gamma_1 = 0.0742$ poise at 122° C ($T - T_c = -13°$ C). This, together with the values of the viscosities measured by Miesowicz [5] allows us to compute all the six coefficients introduced by Leslie. Results are displayed in Table 1 for three values of the flow-orientation angle θ_0 (at 122° C) frequently found in the literature. Which of them is the relevant one, if any, remains an unsolved problem. For comparison, the values found by the Orsay Group from light scattering experiments [14] are also displayed in the table.

Results for some other liquid crystals are being prepared and a comparative study should be published soon.

TABLE 1

Leslie's viscosity coefficients for PAA, at 122° C, expressed in poise for three values of the flow-orientation angle

	$\theta_0 = 0°$	$\theta_0 = 9.1°$	$\theta_0 = 19.7°$	Ref. [14]
μ_1	———	0.35	0.17	
μ_2	−0.074	−0.076	−0.085	−0.064
μ_3	−0.000	−0.002	−0.011	−0.006
μ_4	0.068	0.068	0.068	0.083
μ_5	0.042	0.040	0.031	0.025
μ_6	−0.032	−0.038	−0.065	−0.045

REFERENCES

[1] F. M. LESLIE, *Arch. Rational Mech. Anal.* **28** (1968) 265.
The original theory involve six coeficients μ_i $(i = 1 \cdots 6)$ but there is a relation between them, as shown by PARODI, *J. Phys.* **31** (1970) 581.

[2] W. HELFRICH, *J. Chem. Phys.* **56** (1972) 3187;
H. IMURA, K. OKANO, *Jap. J. Appl. Phys.* **11** (1972) 1440.

[3] A. F. MARTINS, *Phys. Rev. Lett.* **28** (1972) 289.

[4] P. C. MARTIN, O. PARODI, P. S. PERSHAN, *Phys. Rev.* **A 6** (1972) 2401.

[5] M. MIESOWICZ, *Nature* **158** (1946) 27.

[6] R. S. PORTER, J. F. JOHNSON, *J. Appl. Phys.* **34** (1963) 51; also in *Rheology,* Vol. 4 Chap. 5, pp. 317-345, ed. by F. R. Eirich (Academic Press, N. Y., 1967).

[7] W. MAIER, A. SAUPE, *Z. Naturforchg.* **14a** (1959) 882; **15a** (1960) 287.

[8] H. EYRING, *J. Chem. Phys.* **4** (1936) 283.

[9] S. CHANDRASEKHAR, N. V. MADHUSUDANA, *Mol. Cryst. Liquid Cryst.* **10** (1970) 151.

[10] S. MEIBOOM, R. C. HEWITT, *Phys. Rev. Lett.* **30** (1973) 261.

[11] P. A. LEBWOHL, G. LASHER, *Phys. Rev.* **A 6** (1972) 426.

[12] A. F. MARTINS, *Portg. Phys.* **8** (1972) 1.

[13] A. SAUPE, *Angew. Chem.* int. ed. **7** (1968) 97.

[14] ORSAY LIQUID CRYSTAL GROUP, *Mol. Cryst. Liquid Cryst.* **13** (1971) 187.

[15] H. GASPAROUX, J. PROST, *J. Physique* **32** (1971) 953.

[16] C. K. YUN, *Phys. Lett.* **43 A** (1973) 369.

LE TENSEUR D'IMPULSION-ÉNERGIE LIÉE ET LES SYSTÈMES RELATIVISTES À MASSE PROPRE VARIABLE (*)

ANTÓNIO C. DE SALES LUIS

Laboratoire de Physique, Instituto Superior Técnico, Lisbonne, Portugal

RÉSUMÉ — L'interprétation thermodynamique de l'effect Joule a amené l'auteur à introduire le «tenseur d'impulsion-énergie liée» :

$$S_{\alpha}^{\beta} = \frac{T^0 S^0}{c^2} u^{\alpha} u^{\beta} \tag{1}$$

et le «4-vecteur d'impulsion-entropique» :

$$G_{(s)}^{\alpha} = \frac{T^0 S^0}{c^2} u^{\alpha}. \tag{2}$$

Par conséquent, il faut attribuer à un système relativiste une masse m_s^0 telle que :

$$m_s^0 = \frac{T^0 S^0}{c^2} \tag{3}$$

tout à fait d'accord avec les idées d'Einstein. Alors, la masse propre d'un système est la somme de sa masse propre (usuelle) m^0 et de sa masse propre entropique m_s^0 :

$$M^0 = m^0 + \frac{T^0 S^0}{c^2}. \tag{4}$$

Toutes les transformations dans la nature sont irréversibles et les phénomènes irréversibles créent effectivement de l'entropie et par conséquent de l'énergie liée. Alors, compte tenu de (4), les systèmes relativistes sont des systèmes à masse propre variable ; par l'intermédiaire d'un exemple (collision inélastique) on montre le rôle joué par le 4-vecteur d'impulsion-entropique et la cohérence des idées introduites.

(*) Reçu le 15 Décembre 1973.

Considérons un corps conducteur, homogène et isotrope, à température uniforme et à composition constante, parcouru par un courant électrique de densité $\vec{J}$. Il se produit un phénomène irréversible, l'effet Joule, (chaleur de Joule) qui, au point de vue de la thermodynamique, se caractérise par une production d'entropie essentiellement positive. On sait [1] que la production d'énergie liée (T S), par unité de temps et de volume s'exprime par la relation:

$$T\sigma = (\vec{J} \cdot \vec{E}) \tag{1}$$

où T est la température de l'élément de volume considéré, σ la production d'entropie par unité de temps et de volume et $\vec{E}$ le champ électrique; remarquons que $T\sigma$ représente la production d'énergie liée par unité de temps et de volume.

Dans la littérature, même contemporaine, on dit que l'effet Joule consiste dans le dégagement de la chaleur, produit par le passage du courant électrique ce qui, a notre avis, n'est pas du tout d'accord avec les deux principes de la thermodynamique. L'équation (1) suggére une interprétation plus cohérente au point de vue thermodynamique. En effet, considérons un corps conducteur en équilibre thermique avec le milieu extérieur; le passage du courant électrique donne lieu à un phénomène irréversible se caracterisant par une production d'entropie positive; cette énergie liée reste dans le système sous la forme d'énergie interne et, par conséquent, la température du conducteur augmente au fur et à mesure que l'électricité y circule. De cette façon, la température du conducteur devient supérieure à celle du milieu extérieur et, d'après le premier principe de la thermodynamique, il y a de la chaleur mise en jeu à travers la frontière du système, si (et seulement si) celui-ci n'est pas isolé. C'est-à-dire, il y a toujours un effet volumique (effet Joule) qui, au point de vue

---

[1] A. Sales Luis, «A expressão Relativista do Segundo Princípio da Termodinâmica», Lisboa (1965).

thermodynamique, se traduit par une production d'entropie au sein du système même; si le système n'est pas isolé, alors, il y aura aussi de la chaleur mise en jeu à travers la frontière du système.

Il nous semble qu'il faut distinguer nettement ce qui est échangé avec le monde extérieur par l'intermédiaire de la frontière de séparation et ce qui est produit au sein du système lui-même; l'effet Joule est un effet volumique relatif à ce qui se passe à l'intérieur du système, n'ayant aucun rapport direct avec la chaleur mise en jeu avec le monde extérieur. Que beaucoup de physiciens, moins avertis de toutes ces nuances thermodynamiques, se sentent quand même portés à regarder l'effet Joule comme «la chaleur», cela est facile à expliquer. D'une part il y a à considérer le poids de la tradiction, soit en regardant la chaleur comme «calorique» (fluide indestructible), soit en la regardant comme une forme d'énergie présente dans le système; d'autre part il est indéniable que c'est le passage du courant électrique qui est la seule cause de l'augmentation de la température du système (en vertu de la production d'entropie, toujours définie positive) et, par conséquent, de cette interaction avec le monde extérieur, dans le cas des systèmes qui ne sont pas isolés. Pourtant, si on coupe, le passage du courant électrique, l'effet Joule cessera tout de suite mais la chaleur mise en jeu (échange d'entropie) persistera jusque la température du système soit égale à celle du monde extérieur.

Considérons, alors, des milieux homogènes et isotropes, sans magnétisation permanente, non-ferro-magnétiques et peu dispersives ($\varepsilon\mu = 1$). En outre, considérons qu'il n'y a pas de champs appliqués et, par conséquent, que la température est toujours uniforme. Dans ces conditions-là, on a [2]

$$\vec{D} = \varepsilon \vec{E} \qquad \vec{B} = \mu \vec{H}$$

dans tous les repères galiléens. Dans un système galiléen quelconque, on peu définir [2], le quadri-vecteur L_α:

$$L_\alpha = \frac{1}{c} F_{\alpha\beta} u^\beta \tag{2}$$

---

(2) M. A. Tonnelat, «Les Principes de la Théorie Electromagnétique et de la Relativité», Masson, 1959, O. Costa de Beauregard, «La Théorie de la Relativité Restreinte», Masson, 1949.

par contraction du tenseur électromagnétique $F_{\alpha\beta}$ avec le quadri-vecteur u^β vitesse d'univers, dont les composantes sont:

$$(3) \qquad L_k = \frac{E_k^*}{\sqrt{1-\frac{u^2}{c^2}}} \qquad L_4 = \frac{i}{c}\,\frac{(\vec{E}^* \cdot \vec{u})}{\sqrt{1-\frac{u^2}{c^2}}}$$

$$(k = x, y, z)$$

et:

$$(4) \qquad \vec{E}^* = \vec{E} + \frac{1}{c}[\vec{u} \wedge \vec{B}].$$

Par contraction du quadri-vecteur L_α avec le quadri-vecteur C^α, densité de courant électrique, on peut former l'invariant relativiste suivant:

$$(5) \qquad L_\alpha C^\alpha = \frac{(\vec{J} \cdot \vec{E}^*)}{\sqrt{1-\frac{u^2}{u^2}}} = (\vec{J}^0 \cdot \vec{E}^0).$$

M. Von Laue [3] a identifié la quantité $(\vec{J} \cdot \vec{E}^*)$ avec la chaleur de Joule et déduit la loi de transformation relativiste de la chaleur

$$Q = Q_0 \sqrt{1-\frac{u^2}{c^2}}$$

ce qui, à notre avis, n'est pas valable, vis-à-vis de l'interprétation thermodynamique de l'effet Joule, que nous venons d'expliciter. Par contre, en tenant compte de (1), on peut écrire:

$$(6) \qquad T\sigma = (\vec{J} \cdot \vec{E}^*) \qquad T^0\sigma^0 = (\vec{J}^0 \cdot \vec{E}^0)$$

ce qui, compte tenu de (5), nous a conduit [1] à la loi de transformation relativiste de la production d'énergie liée, par unité de temps et de volume:

---

[3] M. Von Laue, «La Théorie de la Relativité» (pg. 210), Gauthier-Villars, 1924.

$$T\sigma = T^0\sigma^0\sqrt{1-\frac{u^2}{c^2}} \tag{7}$$

et nous a amené(1) a introduire le tenseur d'impulsion-énergie liée par l'équation:

$$S_\alpha^\beta = \frac{T^0 s^0}{c^2} u_\alpha u^\beta \tag{8}$$

dont les composantes sont:

$$S_\alpha^\beta = \begin{vmatrix} S_{xx} & S_{xy} & S_{xz} & \frac{i}{c}Tsu_x \\ S_{yx} & S_{yy} & S_{yz} & \frac{i}{c}Tsu_y \\ S_{zx} & S_{zy} & S_{zz} & \frac{i}{c}Tsu_z \\ \frac{i}{c}Tsu_x & \frac{i}{c}Tsu_y & \frac{i}{c}Tsu_z & -Ts \end{vmatrix} \tag{9}$$

où:

$$S_{kk} = \frac{Ts}{c^2} u_k u_k \tag{10}$$

$$S_{ki} = \frac{Ts}{c^2} u_k u_1 . \tag{11}$$

Comme il est usuel, u_α et u^β sont les composantes covariantes et contrevariantes du 4-vecteur vitesse d'univers, $u_k (k = x, y, z)$ les composantes du 3-vecteur vitesse, T la température thermodynamique, s la densité d'entropie et Ts la densité d'énergie liée:

$$Ts = \frac{T^0 s^0}{1-\frac{u^2}{c^2}} \tag{12}$$

et par l'indice zéro on désigne que les grandeurs sont rapportées au système de référence propre, c'est-à-dire, celui par rapport

auquel l'impulsion totale mécanique du système est nulle. De (8) résulte que le tenseur d'impulsion-énergie liée est un tenseur symétrique et que sa composante S_4^4 représente, au signe moins près, la densité d'énergie liée, ce qui est bien d'accord avec les idées d'Einstein (4). En outre, la loi de transformation de la composante S_4^4 conduit à l'équation (12).

De ce qui vient d'être dit, on définit naturellement le 3-vecteur densité de courant d'énergie liée par l'équation:

$$\vec{\Sigma}_s = \mathrm{T}\, s\, \vec{u} \tag{13}$$

et le 3-vecteur densité d'impulsion entropique:

$$\vec{g}_s = \frac{\vec{\Sigma}_s}{c^2} = \frac{\mathrm{T}s}{c^2}\,\vec{u}. \tag{14}$$

En outre, la 4e-composante de la divergence du tenseur T_α^β prend la forme:

$$\begin{aligned} \frac{\partial \mathrm{S}_4^\beta}{\partial x^\beta} &= \frac{i}{c}\left(\mathrm{div}\,(\mathrm{T}\, s\, \vec{u}) + \frac{\partial (\mathrm{T}\, s)}{\partial t}\right. \\ &= \frac{i}{c}\,\mathrm{T}\,\sigma. \end{aligned} \tag{15}$$

Considérant que la température thermodynamique est positive, il découle de (15) que:

$$\frac{i}{c}\,\frac{\partial \mathrm{S}_4^\beta}{\partial x^\beta} \leq 0 \tag{16}$$

expression qui traduit, d'une forme tout à fait indépendante du système galiléen consideré, le fait expérimental que la production d'entropie est toujours non-négative.

---

(4) A. Einstein, «The Meaning of Relativity» (pg. 47) Methuen and Co, 1950 («The energy per unit volume has the character of a tensor»).

De plus, on est naturellement amené à introduire le 4-vecteur d'impulsion-entropique, défini par:

$$G_s^\alpha = \frac{T^0 S^0}{c^2} u^\alpha \tag{17}$$

dont les composantes sont:

$$\vec{G}_s = \frac{T S}{c^2} \vec{u} \tag{18}$$

et

$$G_s^4 = \frac{i}{c} T S \tag{19}$$

tenant compte de:

$$T S = \frac{T^0 S^0}{\sqrt{1 - \frac{u^2}{c^2}}} \tag{20}$$

comme résulte de la loi de transformation de la composante G_s^4. On remarquera que la 4e composante du 4-vecteur G_s^α est, à part le facteur $\frac{i}{c}$, l'énergie liée. De cette façon, il faut attribuer à un système thermodynamique une inertie m_s^0 telle que:

$$m_s^0 = \frac{T^0 S^0}{c^2}. \tag{21}$$

C'est-à-dire, la masse propre d'un système thermodynamique est la somme de sa masse propre usuelle (mécanique) m^0 et de sa masse propre correspondant à l'énergie liée:

$$M^0 = m^0 + \frac{T^0 S^0}{c^2}. \tag{22}$$

Le 4-vecteur impulsion du système est, par conséquent, la somme du 4-vecteur impulsion-mécanique et du 4-vecteur impulsion--entropique:

$$G^\alpha = G_m^\alpha + G_s^\alpha. \tag{23}$$

A titre d'exemple, considérons un corps macroscopique de masse propre (mécanique) m_1^0, qui vient heurter, avec la vitesse $u_1 = \beta_1 c$, un autre corps de masse propre m_2^0, primitivement au repos. Supposons que, à la suite du choc, les deux corps restent collés et sont finalement animés de la vitesse commune $u_3 = \beta_3 c$, dans la même direction que u_1. Si nous écrivions l'équation de conservation du 4-vecteur impulsion mécanique, sous la forme qui paraîtrait naturelle:

$$(G_m^\alpha)_1 + (G_m^\alpha)_2 = (G_m^\alpha)_3 \tag{24}$$

dont la 1e composante conduit à.

$$\frac{m_1^0 u_1}{\sqrt{1-\beta_1^2}} = \frac{(m_1^0 + m_2^0) u_3}{\sqrt{1-\beta_3^2}} \tag{24 a}$$

et la 4e composante, à:

$$\frac{m_1^0 c^2}{\sqrt{1-\beta_1^2}} + m_2^0 c^2 = \frac{(m_1^0 + m_2^0) c^2}{\sqrt{1-\beta_3^2}} \tag{24 b}$$

nous serions amenés à un système de deux équations, à une seule inconnue (u_3), qui sont incompatibles. On s'affranchit de cette difficulté en imposant que la masse propre m_3^0 des deux corps une fois collés est supérieure à la masse propre totale $(m_1^0 + m_2^0)$ des deux corps primitifs. Si nous remplaçons, alors, la quantité connue $(m_1^0 + m_2^0)$ par la quantité inconnue m_3^0, nous obtenons le système de deux équations à deux inconnues (m_3^0, u_3) suivant:

$$\frac{m_1^0 u_1}{\sqrt{1-\beta_1^2}} = \frac{m_3^0 u_3}{\sqrt{1-\beta_3^2}} \tag{25 a}$$

$$\frac{m_1^0 c^2}{\sqrt{1-\beta_1^2}} + m_2^0 c^2 = \frac{m_3^0 c^2}{\sqrt{1-\beta_3^2}} \tag{25 b}$$

qui est soluble. Au point de vue qualitatif, on explique le remplacement de $(m_1^0 + m_2^0)$ par m_3^0 en disant que, le choc étant inélastique, il y a «dégagement de chaleur» et, par conséquent, la masse propre m_3^0 est supérieure à $(m_1^0 + m_2^0)$. Somme toute, il nous semble que la considération de la masse m_3^0 résulte, en dernier ressort, d'une raison purement formelle, reposant uniquement sur l'incompatibilité des équations (24 a, b) de conservation de la quantité de mouvement et de l'énergie. Comme nous allons montrer, l'introduction du 4-vecteur impulsion-entropique permet d'expliquer, au point de vue quantitatif, ce problème de collision inélastique d'une façon tout à fait claire et cohérente. Ecrivant, en effet, la conservation du 4-vecteur impulsion (totale), sous la forme:

$$(G_m^\alpha + G_s^\alpha)_1 + (G_m^\alpha + G_s^\alpha)_2 = (G_m^\alpha + G_s^\alpha)_3 \tag{26}$$

on obtient pour la première composante l'équation:

$$\frac{M_1^0 u_1}{\sqrt{1-\beta_1^2}} = \frac{M_3^0 u_3}{\sqrt{1-\beta_3^2}} \tag{27 a}$$

et pour la 4e composante:

$$\frac{M_1^0 c^2}{\sqrt{1-\beta_1^2}} + M_2^0 c^2 = \frac{M_3^0 c^2}{\sqrt{1-\beta_3^2}} \tag{27 b}$$

L'équation (27 b) peut s'écrire:

$$\left(\frac{M_1^0 c^2}{\sqrt{1-\beta_1^2}} - M_1^0 c^2\right) = \left(\frac{M_3^0 c^2}{\sqrt{1-\beta_3^2}} - M_3^0 c^2\right) + \{M_3^0 - (M_1^0 + M_0^2)\} c^2$$

c'est-à-dire:

$$(E_{cin})_1 = (E_{cin})_3 + L' \tag{28}$$

où:

$$L' = \{M_3^0 - (M_1^0 + M_2^0)\} c^2 . \tag{29}$$

En tenant compte de (22):

$$M^0 = m^0 + \frac{T^0 S^0}{c^2}$$

on obtient, à partir de (29):

$$L' = (T^0 S^0)_3 - \{(T^0 S^0)_1 + (T^0 S^0)_2\} \tag{30}$$

en posant, naturellement:

$$m_3^0 = m_1^0 + m_2^0 \tag{31}$$

comme dans le cas des chocs élastiques. L'équation (30) montre que la diminuition de l'énergie cinétique du système est égale à la variation de l'énergie liée du système; la masse propre mécanique m^0 du système est ici conservative (comme elle l'est dans le cas d'un choc élastique) mais la masse propre totale M^0 varie en vertu de la production d'entropie qui caractérise les transformations irréversibles. Cet exemple montre clairement le rôle joué par le 4-vecteur d'impulsion entropique dans les transformations thermodynamiques relativistes pendant lesquelles la masse propre mécanique m^0 reste constante, et met en évidence la nécessité d'associer inertie à l'énergie liée (T S), d'une façon tout à fait cohérente avec l'idée introduite par Einstein dans son génial travail «Does the inertia of a body depend upon its energy-content?» [5]. On remarque, en passant, qu'on arrive naturellement à la proposition d'Einstein que la masse propre d'un corps «chaud» a une valeur supérieure à celle du même corps «froid».

De ce qui vient d'être dit, nous sommes conduits à la conclusion qu'un système thermodynamique est un système à masse propre variable. En utilisant l'équation bien connue de l'électromagnetisme relativiste:

$$f_\alpha = -\frac{\partial T_\alpha^\beta}{\partial x^\beta} \tag{32}$$

---

[5] A. Einstein, Ann. der Physik, 17, 1905 («The Principle of Relativity» (pg. 66), Dover Publ. (1923).

Où f_α est le 4-vecteur densité de force et T_α^β est le tenseur d'impulsion-énergie électromagnétique et considérant l'équation bien connue de la mécanique relativiste à masse propre constante:

$$f_\alpha = \frac{\partial M_\alpha^\beta}{\partial x^\beta} \tag{33}$$

Où M_α^β est le tenseur d'impulsion-énergie mécanique, nous sommes arrivés [1] à écrire l'équation bien connue de la relativité restreinte, valable pour le vide:

$$\frac{\partial (T_\alpha^\beta + M_\alpha^\beta)}{\partial x^\beta} = 0 \tag{34}$$

sous la forme plus générale:

$$\frac{\partial (T_\alpha^\beta + M_\alpha^\beta + S_\alpha^\beta)}{\partial x^\beta} = 0 \tag{35}$$

valable pour les systèmes physiques à masse propre variable. En particulier, la 4e composante prend la forme:

$$\frac{\partial (T_4^\beta + M_4^\beta + S_4^\beta)}{\partial x^\beta} = 0 \tag{36}$$

ce qui, en liaison avec la condition (16), traduit le deuxième principe de la thermodynamique d'une façon tout à fait indépendante du système de coordonnées galiléen considéré.

SCALING, EXTENDED VECTOR MESON DOMINANCE AND THE EXISTENCE OF THE NEUTRAL PION (*)

R. VILELA MENDES

Instituto de Física e Matemática,
Av. Gama Pinto Lisbon-Portugal

ABSTRACT — It is shown that in the framework of the extended vector meson dominance model, scaling in electron-positron annihilation is incompatible with the finiteness of the $\pi^0 \to 2\gamma$ decay width.

The implications of the result for the validity of the extended vector dominance idea or for scale breaking are discussed.

RESUMÉ — On montre que dans le cadre du modèle generalisé de dominance des mesons vectoriels, l'invariance d'échelle dans l'annihilation electron-positron n'est pas compatible avec le charactère fini du taux de déclin $\pi^0 \to 2\gamma$.

On discute les implications du résultat en ce qui concerne la validité du modèle de dominance vectoriel generalisé ou la violation de l'invariance d'échelle.

The purpose of this note is to show that the following three statements cannot simultaneously be true propositions:

1. The $\pi^0 \to 2\gamma$ decay width is finite.
2. The one-photon contribution to $e^+ e^- \to$ hadrons scales as $1/s$ for large s.
3. All photon-hadron couplings, both at low and at high energies, may be approximated by an extended vector meson dominance (EVMD) model.

(*) Received 15 February, 1974.

The first two statements are self explanatory. As for the third, it is meant to state the hypothesis that the virtual photon mass dependence, of the spectral functions of unsubtracted mass dispersion relations associated to photon-hadron vertices, can be approximated by a sum of 1^- pole contributions, ranging over an infinite spectrum (which for simplicity we will take to be discrete).

By «all photon-hadron couplings» it is meant that the EVMD hypothesis should apply both to single and multiple-photon processes. However, to deal with multiphoton processes in the framework of an EVMD model, one needs information on the strengths of vertices involving several vector mesons. Hence, our assignment of a precise meaning to proposition 3 is completed by requiring such couplings to follow the same general pattern as the couplings of excited physical states in the dual resonance model (DRM).

In the Veneziano model or in a relativistic quark model [1] the squared masses of the vector mesons obey a linear mass formula $m^2(n) \sim m_0^2(a_1 + a_2 n)$. Here no such restriction will be made. In fact, proposition 3 only requires the function $m^2(n)$ to be increasing for large n and unbounded, for otherwise the EVMD model would be unable to describe the spectral functions in the asymptotic high energy limit.

The proof of the result goes as follows:

In the framework of the EVMD model, the one photon contribution to the total e^+e^- annihilation cross section into hadrons is:

$$(1) \qquad \sigma(s) = \frac{16\pi^2\alpha^2}{s^{3/2}} \sum_n \frac{m_n^3}{f_n^2} \frac{m_n \Gamma_n}{(s - m_n^2)^2 + m_n^2 \Gamma_n^2}$$

where the sum runs over an infinite spectrum of vector resonances and as in the usual VMD equation, we have neglacted the non-diagonal overlap functions of vector meson amplitudes. The coupling of the n-th resonance to the photon is $e m_n^2/f_n$, and Γ_n is its total width.

Define a function $F(s)$ related to the cross section $\sigma(s)$ by:

$$F(s) = \frac{s^{3/2}\sigma(s)}{16\pi^2\alpha^2}.$$

To study the asymptotic behaviour of $F(s)$ one considers convergence in the mean of the series in Eq. (1) to a smooth function $c/s^{k-3/2}$. For each interval $(m_{n+1}^2 - m_{n-1}^2)/2$ there is a new resonance giving a contribution $2\pi m_n^3/f_n^2$ to the integral of $F(s)$. On the other hand, using the mean value theorem, one writes the integral of $c/s^{k-3/2}$ in the same interval as:

$$\frac{c}{(m(n+\alpha))^{2k-3}} \times \frac{m_{n+1}^2 - m_{n-1}^2}{2} = \frac{c}{(m(n+\alpha))^{2k-3}} \times \frac{\partial}{\partial n} m^2 (n+\alpha') \tag{2}$$

where $|\alpha|, |\alpha'| < 1$.

Equating (2) with the resonance contribution one obtains for large n

$$\frac{1}{f_n^2} \propto \frac{1}{m_n^{2(k-1)}} \frac{\partial}{\partial n} \log m_n^2 \qquad (n > N) \tag{3}$$

If $\sigma(s)$ scales as $1/s$, then $k = 1$ and one has: [2]

$$\frac{1}{f_n^2} \propto \frac{\partial}{\partial n} \log m_n^2 \qquad (n > N) \tag{4}$$

Let us now consider the $\pi^0 \to 2\gamma$ vertex with the pion on the mass shell and general off-shell photon lines

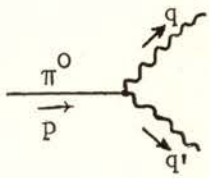

The vertex amplitude is

$$T_{\mu\nu}(q, q') = \varepsilon_{\mu\nu\alpha\beta} q^\alpha q'^\beta T(p^2, q^2, q'^2). \tag{5}$$

In the finite mass dispersion relation (FMDR) approach [3] to the study of $T(p^2, q^2, q'^2)$ one disperses in q^2 with p^2 and q'^2 fixed. Then, the usual assumption is that the low mass region is

dominated by a few resonances whereas the high mass region is light-cone (LC) dominated. In this case only the contributions of a finite number of vector mesons are taken into account and the corrections to VMD should include not only the light cone contribution but also «screening factors» that subtracted from the pole contributions eventually make the particle form factors vanish faster than $1/q'^2$ (so as to preserve LC-dominance of the asymptotic behaviour).

In an EVMD approach (with an infinite number of poles) the point of view should be quite different, for if such a model is to have full merit it should be to the FMDR approach as dual models are to finite energy sum rules (FESR). I. e., the amplitudes should be described exclusively by a sum of infinitely many pole contributions, with all its relevant properties, including the asymptotic behaviour, determined by the rate of variation of the coefficients in such a series. That such an approach does not lead into any obvious contradictions for single-photon processes is clear from our calculation of the $1/f_n^2$ behaviour (Eq. (3)) as well as from recent calculations by other authors [4] on EVMD descriptions of deep annihilation and deep inelastic structure functions. The straightforward generalization of this «dual» EVMD point of view to multiphoton processes is equivalent to an hypothesis of saturation of *unsubtracted* mass dispersion relations by an infinite number of pole contributions. For our results it will not be even necessary that such an approximation be a very good one, in fact, it is enough not to be infinitely bad, i. e not to require infinite corrections.

One then writes:

$$(6) \qquad T(p^2, q^2, q'^2) = \frac{1}{\pi} \int \frac{d\xi}{\xi - q^2 - i\varepsilon} \operatorname{Im} T(p^2, \xi + i\varepsilon, q'^2).$$

In the neighbourhood of the V_n pole

$$\operatorname{Im} T(p^2, \xi + i\varepsilon, q'^2) \simeq \pi \delta(\xi - m_n^2) G_{\pi V_n \gamma}(q'^2) e m_n^2 / f_n .$$

Hence $T(p^2, q^2, q'^2)$ becomes

$$(7) \qquad T(p^2, q^2, q'^2) \simeq \sum_n \frac{e m_{\varrho_n}^2 G_{\pi \varrho_n \gamma}(q'^2)}{f_{\varrho_n}(m_{\varrho_n}^2 - q^2)} + \frac{e m_{\omega_n}^2 G_{\pi \omega_n \gamma}(q'^2)}{f_{\omega_n}(m_{\omega_n}^2 - q^2)} + \cdots$$

where the dots stand for finite width corrections.

Writting now dispersion relations for the $\pi V_n \gamma$ vertices and applying once more the EVMD hypothesis:

$$(8) \qquad T(p^2, q^2, q'^2) \approx 2 \sum_{n,n'} \frac{e^2 m_{\varrho_n}^2 m_{\omega_{n'}}^2 g_{n,n'}}{f_{\varrho_n} f_{\omega_n} (m_{\varrho_n}^2 - q^2)(m_{\omega_{n'}}^2 - q'^2)} + \cdots .$$

The coupling constants $g_{n,n'}$ are the part of the factorized residues of $G_{\pi V_n \gamma}(q'^2)$ at the $m_{V_{n'}}^2$ poles that correspond to the $\pi \omega_n \varrho_{n'}$ vertices. The n-dependence of these coupling constants is a critical point in the present calculation. Let us assume for the moment (see discussion below) that at least the diagonal constants $g_{n,n} \equiv g_n$ do not vanish when $n \to \infty$ {i. e. $g_n \geqslant g$ for almost all $n > N$} [5].

Using Eq. (3) one may now study the convergence properties of the series of Eq. (8). For any fixed q^2 and q'^2 and for n large the remainder of the diagonal ($n = n'$) subseries is

$$(9) \qquad \sum_{n>N} \frac{g}{f_n^2} \propto \sum_{n>N} \frac{1}{m_n^{2(k-1)}} \frac{\partial}{\partial n} \log m_n^2 .$$

For $k = 1$ the r. h. s. of Eq. (9) is greater or equal to

$$\int_N^\infty dn \frac{\partial}{\partial n} \log m_n^2 = \log m_n^2 \Big|_{n=N}^{n \to \infty}$$

and if m_n^2 is unbounded the series will be divergent. On the other hand if $k > 1$ the series will be convergent even for m_n^2 unbounded.

In conclusion: if the proposition 2. is violated (i. e. $k > 1$) the program of simple pole dominance by an infinite number of vector mesons does not run here into any contradictions. On the other hand if one requires both $k = 1$ and m_n^2 unbounded then the pole dominance hypothesis of unsubtracted dispersion relations would predict an infinite $\pi^0 \to 2\gamma$ decay width.

In the derivation above, use was made of the hypothesis that g_n does not vanish when $n \to \infty$. In fact it is hard to understand how it could be otherwise in any dynamical model with an infinite sequence of vector mesons. In a relativistic quark model [1], for example, ω_n and ϱ_n share the same Bethe-Salpeter amplitudes and differ from each other only on their SU(3) pro-

perties which do not depend on n. Then it would be hard to understand how the coupling constant for a virtual transition from a ρ_n to a ω_n with the emission of a space-symmetric state (the pion) could have a strong n-dependence.

To obtain a better quantitative feeling of the pattern of couplings to be expected in a model with an infinite number of resonances I have computed, in the DRM, a vertex involving one scalar ground state particle and two excited transverse physical states with one photon index at the levels N and N′. The coupling strength for such a vertex is:

$$<-\pi, \mathrm{N}, \varepsilon_i | \, v_0(k'', 1) | \, \pi', \mathrm{N}', \varepsilon_{i'} > = (2\pi)^4 \, \delta^4(-\pi - k'' + \pi') \, \mathrm{G}$$

where the states of momentum $-\pi$ and π' are transverse states at the levels N and N′ created from the vacuum by the transverse operator $A_{i,n}$ of Del Giudice, Di Vecchia and Fubini [6] and $v_0(k'', 1)$ is the ground state vertex operator. For the general non-collinear case the result is:

$$\mathrm{G} = \delta_{\mathrm{N},\mathrm{N}'} \, \delta_{i,i'} - \frac{2 \, (\vec{k}'' \cdot \vec{\varepsilon}_i) \, (\vec{k}'' \cdot \vec{\varepsilon}_{i'})}{\sqrt{\mathrm{N}\,\mathrm{N}'}} .$$

One sees that for large N, N′ the diagonal couplings (N=N′) tend to a constant value whereas the non-diagonal couplings become very small. If this is the pattern of couplings that one should expect in a model of extended vector dominance then the critical assumption of non-vanishing of g_n when $n \to \infty$ is justified and the proof goes through in this respect.

On the other hand, if one insists that the high mass vector mesons do decouple after all, then that is the same as to say that something becomes anomalous at the high masses in the EVMD model. This is tantamount to say that the model is necessarily unreliable at high energies for multiple photon processes, i. e., that proposition 3 is not really a true proposition.

Notice that the use of the DRM to compute the mass dependence of strong interaction vertices is quite consistent with proposition 2, for as shown by Greco [7], in a recent paper, in an EVMD description of scaling in e. m. interactions one is quite naturally led to require scaling for the strong interactions and such a behaviour has been shown to hold in dual resonance models [8].

DISCUSSION

Given the experimental validity of proposition 1, we have thus exhibited a clash between scaling and the simplest generalization of the EVMD hypothesis to multiple-photon processes. To find a way out, one might, for example, argue that although unsubracted dispersion relations seem to work well for one-photon processes, when going to multiple photon processes, one should go to subtracted dispersion relations (SDR).

With a once-SDR for example, one finds instead of Eq. (8) a series that is a power of $\frac{1}{m_n^2}$ more convergent. Howeve, because of the subtraction constant, the model can provide non-trivial information on $\frac{d}{dq^2}\mathrm{T}$ but not on $\mathrm{T}(p^2,0,0)$. This is equivalent to saying that the model has nothing to say about the absolute $\pi^0 \to 2\gamma$ decay rate. The EVMD model would then be a rather restricted model providing information on mass extrapolations but not on absolute rates for multi-photon processes.

Presumably, we would then be better off using only a small number of vector mesons to saturate the low mass region and having the high mass region described in some other way, i. e., one might as well abandon the hope of a complete description of hadronic e. m. interactions by a model with infinitely many poles and suggest that a FMDR approach seemed more reasonable.

In the above discussion, I have analyzed the implications of scaling and $\pi^0 \to 2\gamma$ for the prospects of a complete EVMD description of photon-hadron interactions. If, on the other hand, one takes the unpopular view that the storage rings results do not yet prove asymptotic scaling in e^+ e^- and if it turns out that scale is broken after all (for instance at distances of order 10^{-15} cm. as it has been suggested [9]), then the present result leads to the intriguing suggestion that such breaking might somehow be related to the finiteness of the $\pi^0 \to 2\gamma$ width, i. e., to the very existence of an observable neutral pion.

REFERENCES AND FOOTNOTES

[1] M. BÖHM, H. JOOS, M. KRAMER, *Nucl. Phys.* **51 B**, 397 (1973).

[2] In particular for a linear mass formula, Eq. (4) leeds to $m_n^2/f_n^2 \sim$ const (for large n), a result already obtained by A. BRAMON, E. ETIM and M. GRECO, ref. 4.

[3] R. BRANDT, G. PREPARATA, *Phys. Rev. Letters* **25**, 1530 (1970).
G. PREPARATA, *Erice lectures 1972*, ICTP preprint IC/72/151.

[4] J. J. SAKURAI, D. SCHILDKNECHT, *Phys. Lett.* **40 B**, 121; **41 B**, 489; **42 B**, 216 (1972). A. BRAMOM, E. ETIM, M. GRECO, *Phys. Lett.* **41 B**, 609 (1972).

[5] Or at least that g_n vanishes slower than any negative power of n when $n \to \infty$.

[6] E. DEL GIUDICE, P. DI VECCHIA, S. FUBINI, *Ann. Phys.* **70**, 378 (1972).

[7] M. GRECO, CERN preprint TH 1617 (1973).

[8] V. RITTENBERG, H. R. RUBINSTEIN, *Nucl. Phys.* **28 B**, 184 (1971).

[9] M. S. CHANOWITZ, S. D. DRELL, *Phys. Rev. Lett.* **30**, 807 (1973). See also R. V. MENDES, *Phys. Rev.* **D 8**, 3008 (1973).

Composto e impresso na Tip. Matemática, Lda. — R. Diário de Notícias, 134-1.º-Esq. — Lisboa

Toute la correspondance concernant la rédaction de PORTUGALIAE PHYSICA doit être adressée à

PORTUGALIAE PHYSICA
Laboratório de Física da Faculdade de Ciências
LISBOA-2 (Portugal)

Prix de l'abonnement:	250 escudos (US $8.50) par volume
Prix des volumes déjà parus:	300 escudos (US $10)
Prix du fascicule:	75 escudos (US $2.50)

Les membres de la «Sociedade Portuguesa de Química e Física» ont une réduction de 50 % sur les prix indiqués.

Les Universités, les Laboratoires de Physique, les Académies, les Sociétés Scientifiques et les Revues de Physique sont invités à recevoir cette revue en échange de leurs publications.

PORTUGALIAE PHYSICA donnera un compte-rendu detaillé de tous les ouvrages soumis à la rédaction en deux exemplaires.

All mail concerning PORTUGALIAE PHYSICA to be addressed to:

PORTUGALIAE PHYSICA
Laboratório de Física da Faculdade de Ciências
LISBOA-2 (Portugal)

Subscription rates:	250 escudos (US $8.50) per volume
Price of past volumes:	300 escudos (US $10)
Price of copy:	75 escudos (US $2.50)

Members of the «Sociedade Portuguesa de Química e Física» may obtain *Portugaliae Physica* at a reduced price (50 %).

Universities, Physics Laboratories, Academies, Scientific Societies and Physics Publications are invited to receive this review in exchange for their publications.

PORTUGALIAE PHYSICA will give a detailed report of any book if two copies have been submitted.

PORTUGALIAE PHYSICA

VOLUME 9
FASCÍCULO 2
1974

INSTITUTO DE ALTA CULTURA
CENTROS DE ESTUDOS DE FÍSICA DAS UNIVERSIDADES PORTUGUESAS

PORTUGALIAE PHYSICA

Fundadores: A. Cyrillo Soares, M. Telles Antunes, A. Marques da Silva, M. Valadares.

VOLUME 9 1974 FASCÍCULO 2

VOLUMES PUBLICADOS:

Vol. 1 — 1943-45 — 326 pp.

Vol. 2 — 1946-47 — 256 pp.

Vol. 3 — 1949-54 — 173 pp.

Vol. 4 — 1965-66 — 304 pp.

Vol. 5 — 1967-70 — 194 pp.

Vol. 6 — 1970-71 — 316 pp.

Vol. 7 — 1971-72 — 210 pp.

Vol. 8 — 1972-73 — 266 pp.

Redacção: Laboratório de Física da Faculdade de Ciências — Lisboa-2 (PORTUGAL)

Comissão de redacção:

J. Moreira de Araújo — Carlos Braga — Carlos Cacho — A. Pires de Carvalho — M. Abreu Faro — J. Gomes Ferreira — F. Bragança Gil — Manuel Laranjeira. Amaro Monteiro — J. Pinto Peixoto — J. da Providência — Lídia Salgueiro — J. de Almeida Santos — José Sarmento — António da Silveira — J. Veiga Simão.

ÍNDICE

(Table des matières)

The influence of the mixing on the Coulomb excitation probabilities of beta and gamma bands, by J. M. DOMINGOS 29

On the divergence of enthalpy and the energetics of the atmosphere, by JOSÉ PINTO PEIXOTO 41

DOMINGOS, J. M.
Departamento de Física,
Universidade de Coimbra

The influence of the mixing on the Coulomb excitation probabilities of beta and gamma bands.

Portgal. Phys. — 9 (2): 29-40, 1974

The influence of band-mixing on the excitation probabilities for multiple Coulomb excitation with ^{16}O ions for a gamma-band and a beta-band has been studied as a function of the energy of the ^{16}O projectile.

The case of a suggested beta-band in (d, d') work in ^{170}Er is used to show how multiple Coulomb exitation demonstrates the impossibility of that assignment in view of the discrepancy between the measured excitation probabilities and the calculated values.

PEIXOTO, José Pinto
Massachussetts Institute of Technology and the University of Lisbon

On the divergence of enthalpy and the energetics of the atmosphere.

Portgal. Phys. — 9 (2): 41-58, 1974

The role of the divergence of enthalpy in the energetics of the atmosphere is studied and discussed. The heating due to the divergence or the convergence of enthalpy can be regarded in the study of the energetics of the atmosphere as a basic tool in evaluating its energy budget. The analysis of the energy equation applied to the atmosphere shows that the contribution of the term of enthalpy becomes dominant. A balance equation for the enthalpy is established and the physical interpretation and the relative contribution of its various terms are fully discussed. Since the divergence or the convergence of the enthalpy flux reflect the excess or the deficit of diabatic heating, as follows from the balance

equation, the present approach offers an independent way of checking the global energy budget of the Earth and of the atmosphere. The divergence of enthalpy acting in an opposite sense to the adiabative heating offers through its spacial distribution a map of the heat sources and sinks of the system earth-atmosphere, which may be of importance for the mathematical simulation of the general circulation.

CDU 53 (469) (05)

PORTUGALIAE PHYSICA

VOLUME 9
FASCÍCULO 2
1974

THE INFLUENCE OF THE MIXING ON THE COULOMB EXCITATION PROBABILITIES OF BETA AND GAMMA BANDS (*)

J. M. DOMINGOS
Departamento de Física, Universidade de Coimbra

ABSTRACT — The influence of band-mixing on the excitation probabilities for multiple Coulomb excitation with ^{16}O ions for a gamma-band and a beta-band has been studied as a function of the energy of the ^{16}O projectile.

The case of a suggested beta-band in (d, d') work in ^{170}Er is used to show how multiple Coulomb exitation demonstrates the impossibility of that assignment in view of the discrepancy between the measured excitation probabilities and the calculated values.

1 — INTRODUCTION

Coulomb excitation is a time-dependent electromagnetic process of nuclear excitation produced by charged projectiles moving along orbits passing near the nucleus. To minimise the interaction due to nuclear forces there are restrictions on the maximum energy of the incident particle exciting the nucleus [1].

In the semiclassical approximation, the projectile orbit is treated classically, and the interaction with the nucleus quantum-mechanically.

The rapidly varying field, produced by the projectile, results in excitation of the nucleus.

The problem of finding the amplitudes of the excited nuclear states involves solving the time dependent Schrödinger equation [2]

$$(1) \qquad i\hbar \frac{\partial |\psi>}{\partial t} = \{H_N + H_{int}(t)\} |\psi>$$

(*) Received 9 September, 1974.

where H_N is the Hamiltonian of the free nucleus and $H_{int}(t)$ is the Coulomb interaction energy between the nucleus and the projectile [3].

In radiative decay, magnetic transitions can compete with electric ones but not in the excitation process. In Coulomb excitation the magnetic field acting on the nucleus in a collision with the projectile is down by a factor v/c in relation to the electric field [3]. In addition, the magnetic interaction is proportional to the relative orbital angular momentum of the projectile-target system [3], and we shall assume scattering angles close to 180°. In fact we shall have in mind applications to beta and gamma bands in deformed nuclei in the region $150 < A < 190$ excited in experiments with ^{16}O ions back-scattered at an average angle of 160° [4], [5]. Therefore, only electric multipole matrix elements enter in the calculations.

Even if the increasing of multipole order decreases the Coulomb excitation probability much less than it decreases the rate of the inverse transition [3], one might think that most excitations would be of E1 type. In fact this is not so because the reduced matrix elements $< \alpha_f I_f \| \mathfrak{M}(E1) \| \alpha_i I_i >$ are very small and so very few E1 transitions have been observed. The most frequent excitation is of E2 type, and E3 excitations are commonly observed. Recently the effect of E4 moments on the Coulomb excitation of groud-state bands have been studied.

We have then

$$(2) \qquad H_{int}(t) = 4\pi Z_P e \sum_{\lambda=1}^{\infty} \sum_{\mu=-\lambda}^{\lambda} \frac{1}{2\lambda+1} \frac{1}{r_P^{\lambda+1}} Y_{\lambda\mu}(\theta_P, \varphi_P) \mathfrak{M}^*(E\lambda, \mu)$$

with P referring to the projectile and

$$(3) \qquad \mathfrak{M}(E\lambda, \mu) = \int \rho(\vec{r}) r^\lambda Y_{\lambda\mu}(\theta, \varphi) \, d\tau$$

the electric multipole moment of the nucleus.

The dependence of (1) on H_N is removed by passing to the interaction representation using the transformation

$$(4) \qquad |\varphi> = e^{\frac{i}{\hbar} H_N t} |\varphi> .$$

Inserting in (1) one obtains

$$i\hbar \frac{\partial}{\partial t} |\varphi> = \tilde{H}(t) |\varphi> \tag{5}$$

with

$$\tilde{H}(t) = e^{\frac{i}{\hbar} H_N t} H_{int}(t) e^{-\frac{i}{\hbar} H_N t} . \tag{6}$$

The nuclear wave function $|\varphi>$ can be expanded in the complete set of eigenfunctions $|\alpha I M>$ of the undisturbed Hamiltonian H_N whose eigenvalues are $E_{\alpha I}$

$$|\varphi> = \sum_{\alpha I M} a_{\alpha I M}(t) |\alpha I M> \tag{7}$$

with α the remaining quantum numbers necessary to specific the nuclear state.

Substituting (7) in (5) we obtain a set of coupled equations equivalent to (5)

$$i\hbar \dot{a}_{\alpha I M}(t) = \sum_{\alpha' I' M'} e^{\frac{i}{\hbar}(E_{\alpha I} - E_{\alpha' I'}) t} \tag{8}$$

$$<\alpha I M | H_{int}(t) | \alpha' I' M'> a_{\alpha' I' M'}(t)$$

where $a_{\alpha I M}(t)$ are the amplitudes of the nuclear state vector in the set of states of the undisturbed Hamiltonian. The problem is to find $a_{\alpha I M}(t = +\infty)$, integrating (8), with the initial conditions

$$a_{\alpha_i I_i M_i}(t = -\infty) = \delta_{\alpha_i \alpha_0} \delta_{I_i I_0} \delta_{M_i M_0} \tag{9}$$

with $\alpha_0 I_0 M_0$ the quantum numbers of the ground state.

The reduced matrix elements $<\alpha I \| \mathfrak{M}(E\lambda) \| \alpha' I'>$ are introduced in (8) using the Wigner-Eckart theorem.

Once the final amplitudes $a_{\alpha I M}(t = +\infty)$ on the states with spin I and magnetic quantum number M are known, one may easily obtain the probability for Coulomb excitation from the unpolarized

ground-state $|\alpha_0 I_0 M_0>$ to the state $|\alpha I M>$ regardless of the orientation of the initial and final states

$$P_{\alpha I} = \frac{1}{2 I_0 + 1} \sum_{M_0 M} |a_{\alpha I M}|^2 . \tag{10}$$

Therefore, with the use of heavy ions as projectiles, multiple Coulomb excitation of a nuclear state via various intermediate states becomes a very important tool for the study of transition matrix elements in the low energy region. In fact the excitation probabilities (10) through (8) and (2) depend on a set of matrix elements $<\alpha_f I_f || \mathfrak{M}(E\lambda) || \alpha_i I_i>$ between several states.

As we are interested in illustrating the contribution of multiple Coulomb excitation to clarify a consistent description of beta and gamma bands, we shall recall the main principles involved in the rotational model with first order band mixing, and refer to the calculation of reduced matrix elements using this model.

The deviations from the strong-coupling rotational model, in which the zero order Hamiltonian is separable into intrinsic and rotational parts, may be interpreted in terms of coupling between intrinsic motion and rotation. Bohr and Mottelson introduced the higher order terms as a power series in the total angular momentum to be treated by perturbation theory. For an axially symmetric nuclear shape, taking into account hermicity and invariance under time reversal and rotations about the body symmetry axis, one obtains

$$H = H_{rot} + H_{int} + h_0 (I^2 - I_3^2) + h_{+1} I_- + \\ + h_{-1} I_+ + h_{+2} I_-^2 + h_{-2} I_+^2 \tag{11}$$

assuming higher powers of I_+ and I_- negligible to the order of interest. Here H_{rot} is the rotational Hamiltonian, H_{int} is the intrinsic Hamiltonian, I_+ are angular momentum operators in the body-fixed system which lower or raise K by one unit, while h_{+i} are intrinsic operators that change the K of the intrinsic function by i units.

In even-even deformed nuclei we shall only consider the mixing of the ground-state ($K = 0$) band with the beta ($K = 0$) and gamma ($K = 2$) bands. We shall neglect couplings with higher-lying $K = 1$ bands, i. e., we neglect the h_{+1} terms in (11). It is also assumed that

the interaction is weak so that we can treat the coupling terms in (11) by first order perturbation theory.

The wave functions with first order admixtures for states in those bands, and the reduced matrix elements calculated with those wave functions were discussed elsewhere [1], [5], [6].

2 — MULTIPLE COULOMB EXCITATION CALCULATIONS IN THE SUDDEN APPROXIMATION

The presence of the exponential in (8) makes the solution of that set of coupled differential equations very difficult. Lütken and Winther [7] obtained solutions for (8), with model-dependent calculations, and avoided the difficulty of the exponential using the sudden approximation. All the nuclear states are considered as degenerate in this approximation.

The calculations, using the pure rotational model for axially symmetric deformed nuclei, without mixing, were particularly simple for backward scattering and give a qualitative picture of the excitation process. The backward scattering ensures that the magnetic quantum number is conserved during the collision. Lütken and Winther [7] tabulated, in table 4, the relative excitation probability for a level I for a given K band

$$|B^{\lambda}_{I,K}(q)|^2 = \frac{P_{I,K}}{\sum_I P_{I,K}} \tag{12}$$

as a function of a convenient parameter

$$q = 7.624 \frac{A^{\frac{1}{2}} Q_0}{\left(1 + \frac{A_1}{A_2}\right)^2 Z_1 Z_2^2} E^{\frac{3}{2}} \tag{13}$$

where the subscripts 1 and 2 refer, respectively, to projectile and target nucleus, Q_0 is the intrinsic quadrupole moment and E the projectile energy (MeV) in the laboratory system.

3 — A COMPUTER PROGRAM FOR MULTIPLE COULOMB EXCITATION CALCULATIONS

Winther and de Boer [8] wrote a computer program that integrates, on a model-independent way, the set of coupled differential equations (8). The program computes the excitation probabilities for a system consisting of a target nucleus with a finite number of levels and a projectile moving on a classical orbit. The program is independent of any nuclear model and provides a solution subject only to the limitations of the semiclassical approximation.

The imput of this program consists of the nuclear charges and masses, «spins» and energies of the nuclear levels, projectile energy and scattering angle, and the reduced matrix elements between all nuclear levels relevant to the calculations.

The extent of the dependence of the calculated excitation probability of a given level on a particular matrix element connecting any two particular levels may be studied varying this matrix element in the input data.

4 — RESULTS AND DISCUSSION

The values of the relative excitation probabilities for beta and gamma bands as a function of the ^{16}O incident energy are shown in Figs. 1 and 2. The nucleus ^{152}Sm was chosen as a suitable example because of its low-lying beta and gamma bands. However, the behaviour is very similar to the nuclei in the deformed region under consideration in this work.

To calculate the reduced matrix elements for the input data of Winther and the Boer program [8], we considered for the beta band the parameters

$$B(E2, 0_{gs} \rightarrow 2_{gs}) = (3.40 \pm 0.15)\, e^2 b^2$$

$$B(E2, 0_{gs} \rightarrow 2_{\beta}) = (2.28 \pm 0.17) \times 10^{-2}\, e^2 b^2$$

$$Z_0 = 0.08$$

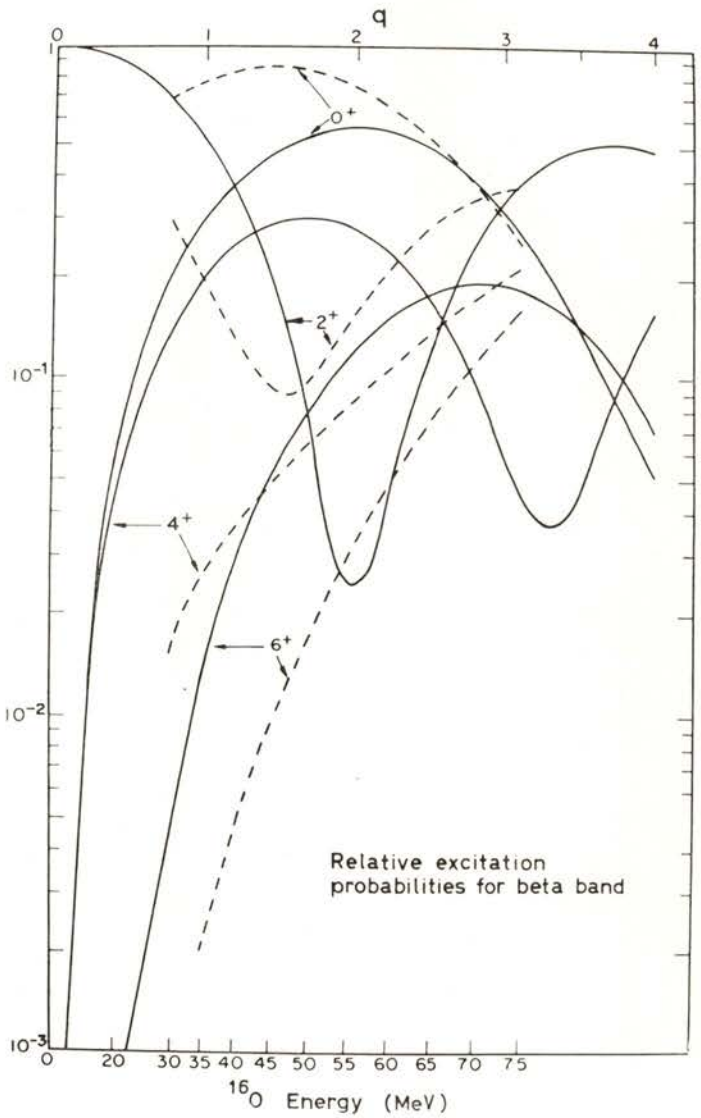

Fig. 1 — Calculated relative excitation probabilities for the 0^+, 2^+, 4^+ and 6^+ states of the beta band, in ^{152}Sm, for multiple Coulomb excitation with ^{16}O ions. The solid curves show the sudden approximation results of Lütken and Winther [7] and the dashed curves show the results of a calculation using the exact level energies and a value of $Z_0 = 0.08$ to acount for the mixing with the ground-state band.

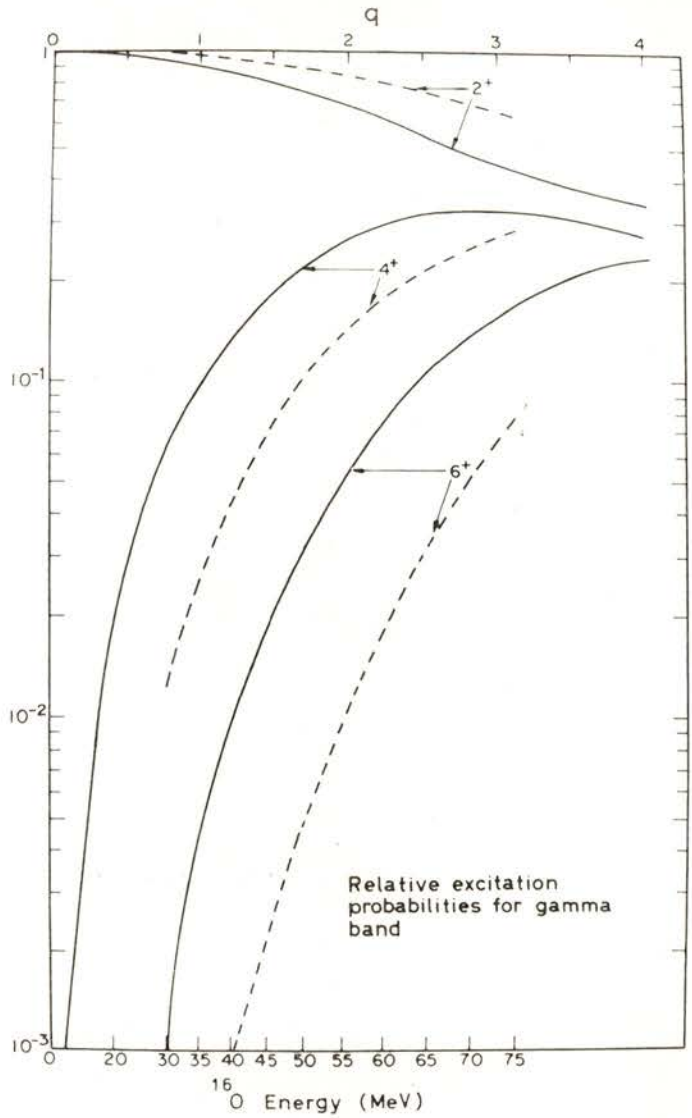

Fig. 2 — Calculated relative excitation probabilities for the 2^+, 4^+ and 6^+ members of the gamma band, in ^{152}Sm, for multiple Coulomb excitation with ^{16}O. The solid curves show the sudden approximation results of Lükten and Winther [7] and the dashed curves show the results of a calculation using the exact level energies and a value of $Z_2 = 0.08$ to account for the mixing with the ground-state band.

and for the gamma band

$$B(E2, 0_{gs} \rightarrow 2_{gs}) = (3.40 \pm 0.15)\, e^2 b^2$$

$$B(E2, 0_{gs} \rightarrow 2_{\gamma}) = (8.13 \pm 0.57) \times 10^{-2}\, e^2 b^2$$

$$Z_2 = 0.08 .$$

The meaning of the mixing parameters Z_0 and Z_2 and the procedure involved in calculating the matrix elements, relevant to these calculations, can be seen in Sec. III and IV of ref. [5].

The 3^+ and 5^+ levels of the gamma band are omitted in Fig. 2 because states of unnatural parity are not excited to any appreciable extent in backward scattering.

For comparison the sudden approximation values, for pure bands, are also shown in Figs. 1 and 2.

It should be noted that in the energy range of interest here, i. e., 40-60 MeV, the excitation of the 2^+ state and higher states in the beta band is predicted to be small compared with that of the 0^+ state.

Tjøm and Elbek [9] studied the nucleus ^{170}Er in inelastic deuteron scattering, and suggested that a 0^+ state at 880 keV and a 4^+ state at 1122 keV together with a 2^+ state at 959 keV could be members of a $K = 0$ beta band. That same nucleus was studied in Coulomb excitation with ^{16}O by J. M. Domingos et. al. [4] and transitions were found that are consistent with a 0^+ state at 889 keV and a 4^+ state at 1124 keV. However they found no evidence for a 2^+ state as proposed by Tjøm and Elbek. If we think in terms of the relative excitation probabilities, as shown in Fig. 1, we might think that the absence of that 2^+ state, in a Coulomb excitation experiment at a ^{16}O effective energy of 53.5 MeV, would not contradict, in principle, their assignment for those states as members of a beta band. A step further could be to assume a ground-state band as shown in ref. [4] and a beta band with 0^+, 2^+ and 4^+ states at 0.889 MeV, 0.959 MeV and 1.124 MeV and an additional 6^+ state at a predictable energy of 1.36 MeV, to perform theoretical calculations with the Winther and de Boer [8] computer program. The comparison of the experimental values with the excitation probabilities

calculated for such a beta band, as shown in Table 1 for no mixing ($Z_0 = 0$) and for a reasonable mixing $Z_0 = 0.04$, clearly excludes that assignment.

ACKNOWLEDGMENTS

This paper is dedicated, as a token of gratitude, to Prof. J. R. de Almeida Santos on his 25th anniversary as Director of the Departamento de Física, Universidade de Coimbra.

I would like to acknowledge a grant from Instituto de Alta Cultura.

TABLE 1. Comparison with experimental results of calculated excitation probabilities P_I for an effective energy of 53.5 MeV ^{16}O ions for a hypothetical beta band in ^{170}Er. Values of the mixing parameter $Z_0=0$ (no mixing) and $Z_0=0.04$ were assumed.

	Calculated values		Experimental values
	$Z_0=0$	$Z_0=0.04$	
P_0+	0.00205	0.00211	0.00030 ± 0.00003
P_2+	0.00005	0.00023	—
P_4+	0.00074	0.00030	0.00049 ± 0.00004
P_6+	0.00029	0.00007	—

REFERENCES

[1] J. M. DOMINGOS, D. Phil. thesis, Nuclear Physics Laboratory, Oxford, **1971** (unpublished).

[2] K. ALDER, and A. WINTHER, *Mat. Fys. Medd. Dan. Vid. Selsk.* **32**, n.º 8 (1960).

[3] K. ALDER, A. BOHR, T. HUUS, B. MOTTELSON, and A. WINTHER, *Rev. Mod. Phys.* **28**, 432 (1956).

[4] J. M. DOMINGOS, G. D. SYMONS, and A. C. DOUGLAS, *Nucl. Phys.* **A180**, 600 (1972).

[5] J. M. DOMINGOS, G. D. SYMONS, and A. C. DOUGLAS, *Phys. Rev. C* **10**, 250 (1974).

[6] E. R. MARSHALEK, *Phys. Rev.* **158**, 993 (1967).

[7] H. LÜTKEN, and WINTHER, *Mat. Fys. Skr. Dan. Selsk.* **2**, n.° 6 (1964).

[8] A. WINTHER, and J. de BOER, in «Coulomb excitation» edited by K. ALDER and A. WINTHER, (*Academic Press*, New York, 1966), p. 303.

[9] P. O. TJØM and B. ELBEK, *Nucl. Phys.* **A107**, 385 (1968).

ON THE DIVERGENCE OF ENTHALPY AND THE ENERGETICS OF THE ATMOSPHERE (*)

by

JOSÉ PINTO PEIXOTO (**)

Massachussetts Institute of Technology
and the University of Lisbon

ABSTRACT — The role of the divergence of enthalpy in the energetics of the atmosphere is studied and discussed. The heating due to the divergence or the convergence of enthalpy can be regarded in the study of the energetics of the atmosphere as a basic tool in evaluating its energy budget. The analysis of the energy equation applied to the atmosphere shows that the contribution of the term of enthalpy becomes dominant. A balance equation for the enthalpy is established and the physical interpretation and the relative contribution of its various terms are fully discussed. Since the divergence or the convergence of the enthalpy flux reflect the excess or the deficit of diabatic heating, as follows from the balance equation, the present approach offers an independent way of checking the global energy budget of the Earth and of the atmosphere. The divergence of enthalpy acting in an opposite sense to the adiabative heating offers through its spacial distribution a map of the heat sources and sinks of the system earth-atmosphere, which may be of importance for the mathematical simulation of the general circulation.

1 — INTRODUCTION

The distribution of the diabatic effects in the earth-atmosphere system is essential for the understanding of the mechanisms of the physical processes which produce and maintain the various scales

---

(*) Received 5 December 1974.

(**) Director of the «Geophysical Institute D. Luís», University of Lisbon.

of motion of the atmosphere and lead to its general circulation (Smagorinsky, 1953).

The general circulation of the atmosphere can be regarded as a generalized convective phenomenon in which the possible regimes of motion depend on the meridional gradient of the temperature of the air between the equator and the poles, on the rate of rotation of the earth and on the nature of the boundary conditions. The nonuniform heating of the atmosphere in the tropical and polar regions and the inhomogeneity of the earth lead to density differences which upset the stable barotropic stratification of the atmosphere and generate *total potential energy* (potential plus internal energy) which is partially *available* for conversion into *kinetic energy* of the motion (Lorenz, 1967).

In a nonrotating Earth, the existing meridional gradient of temperature would produce a direct toroidal circulation, axially symmetric, between the equator and the poles (Hadley regime). However, the Coriolis deflecting force due to the Earth's rotation is strong enough to deform and prevent the purely celular-toroidal regimes of the general circulation of the atmosphere. Under these circumstances, it would seem that the transport of enthalpy, from the regions in which a permanent increase prevails (tropical regions) to those in which a permanent decrease exists (polar and sub-polar regions) would cease and this situation would lead to a steady increase of the latitudinal gradient of temperature. However, beyond a certain critical value of the latitudinal temperature gradient the atmosphere becomes baroclinically unstable, with the formation and selective development of eddies which deform the initially symmetric fields of motion and temperature. Once the dynamic stability is again attained the so called Rossby regime is established. In this regime characterized by large horizontal perturbations, the eddies carry on the excess of enthalpy, accumulated in tropical regions, in a quasi-horizontal macro turbulent processes and set up, simultaneously, the balance of angular momentum, which mantains the westerlies in middle latitudes and the easterlies in tropical regions (Lettau, 1954). The final adjustment of these balances in the Rossby regime can lead to the establishment of a secondary toroidal regime, formed by a tricelular residual circulation with two direct cells one over the equatorial region and another over the polar regions, the Hadley cells, and an indirect one the so called Ferrel cell (Lorenz, 1967).

The continuous dissipation of the kinetic energy of the organized atmospheric motions, due to friction and to turbulent and molecular

viscosity, would in the limit lead the atmosphere, to a state of rest relative to the Earth. As a consequence, the atmosphere would rotate rigidly with the Earth, and no differential rotation could exist. This situation is, of course, against the observed winds and ocean currents, which show the existence of a differentiated and nonstationary character of the atmospheric and oceanographic motions. This implies the existence in the atmosphere of transformations of other forms of energy which will lead to the production of kinetic energy and allow its regeneration against all dissipative processes and guarantee the maintenance of the general circulation. We can thus say that the fundamental problem of atmospheric energetics is the determination of the processes that convert the radiant energy from the sun, which is the primary source of all atmospheric energy, into the kinetic energy of the planetary circulations. The conversion processes of the various forms of energy are not random and the various mechanisms show that otherwise a certain order exists in the sequence of the transformations of the various forms of energy, leading to the concept of an energy cycle in the atmosphere (Peixoto, 1965; Starr, 1968).

A simplified version of this cycle is as follows: the absorption of solar radiation and emission of terrestrial radiation set up a meridional (or latitudinal) gradient of temperature as a result of the non equal heating of the atmosphere in the tropical and polar regions. From a quasi-zonal temperature distribution resulting from the almost axially-symmetric heating, zonal available potential energy is established. Later the distortion of the ideally axially-symmetric fields of motion and of the enthalpy and latent heat leads to a partial conversion of this form of energy into eddy available potential energy, through the meridional transport of enthalpy accomplished by the atmospheric circulations. This latter form of energy is, in turn, converted by baroclinic processes into kinetic energy of the eddies, with ascention of warmer air and the descent of colder air (White and Saltzman, 1956). Finally, by barotropic processes, the eddies feed part of their energy to the mean zonal current (Starr and Wallace, 1964; Starr, 1968). The zonal kinetic energy is mostly dissipated by friction, turbulence and viscosity in a cascade process (Kolmogoroff) into heat. The remainder of this form of energy is converted into total available potential energy by the mean indirect meridional circulations (Ferrel cell). The dissipated energy into heat is finally reradiated to the space as infrared radiation, and thus, closing the cycle.

This is, of course, a very simplied version of the scheme. Actually there are other forms of energy conversion in the atmos-

phere which have to be accounted for in the energy cycle such as those related to the energy released in the transitions of phase of the water vapour (Peixoto, 1965) and those involved in the absorption and emission of radiant energy, etc.

Besides the global aspects of the energetics of the atmosphere in the study of the mechanisms responsible for the maintenance of the general circulation, the geographic-synoptic distribution of the diabatic effects which originate an nonuniform heating of the atmosphere and consequently generate total available potential energy assumes a fundamental importance (Davis, 1963). However, the field of the distribution of diabatic effects can be properly expressed by the field of the divergence of enthalpy in the atmosphere, as we will discuss in the present paper.

In the discussion that follows we will present a theoretical formulation of the general problem of energetics of the atmosphere in the spirit of our previous work, where the importance of the enthalpy fields has been stressed (Peixoto, 1974). However some concepts will be treated with more detail, as required by the present study.

2 — FORMULATION OF THE PROBLEM

2. 1. *Balance equation of the energy*

In the study of the energetics of the atmosphere all the energy forms play a role, but we will restrict ourselves to those which are predominant for the actual study, namely the mechanical, thermal and radiant forms. Under these conditions, the atmosphere can be regarded as an open and nonisolated thermomechanical system. Other forms of energy, such as electric, chemical, nuclear, etc., can be disregarded because their contribution is very small when compared to the forms of radiant, internal, kinetic and potential energies.

The fundamental equation of the energetics of the system earth--atmosphere is obtained by combining the equation of mechanical energy resulting from the equation of motion and the equation of continuity with the first law of thermodynamics (Peixoto, 1965).

Under these conditions the general energy equation of the system earth-atmosphere can be written in the form of a balance equation for the unit volume as follows (Peixoto, 1967)

$$\frac{\partial}{\partial t}\rho(U+K+\Phi)+\operatorname{div}\rho(c_V T+p\alpha+Lq+\Phi+K)\vec{V}-$$

$$-\rho\vec{F}\cdot\vec{V}=\rho\frac{dQ}{dt} \qquad (1)$$

where $\frac{\partial}{\partial t}\rho(U+K+\Phi)=\frac{\partial E}{\partial t}$ represents the local rate of change of the total energy E, ρ the density, U the internal energy, K the kinetic energy; in the divergence term p denotes the atmospheric pressure, α the specific volume of air, L the latent heat of condensation, q the specific humidity of air, $\vec{V}$ the vector field of the wind velocity and $\vec{F}$ the specific frictional force due to small-scale turbulence and the stresses at the boundary.

Finally $\rho\frac{dQ}{dt}$ is the rate of heating or cooling in the atmosphere due to diabatic effects, namely to conduction and friction $\rho\frac{dQ_F}{dt}$, to radiation $\rho\frac{dQ_R}{dt}$ and to condensation $\rho\frac{dQ_L}{dt}$.

Equation (1) has the general form of a balance equation: the local rate of change of energy is associated to a field of energy current density which are the response to the existence of sources or sinks, represented by the dissipation term and by the second member; this, in fact, gives the total rate of production or destruction of energy. The local rate of change of energy is due to:

a) The total flux, represented by the energy current density vector $\vec{J}_E$ which appears in the argument of the divergence term:

$$\vec{J}_E=\rho(c_V T+p\alpha+Lq+\Phi+K)\vec{V}$$

b) the dissipation of the energy of motion due to friction forces represented by the term: $\rho\vec{F}\cdot\vec{V}$, which can produce important tangential stresses, such as those generating ocean currents, etc.

c) The production or destruction of energy by diabatic effects, represented by $\rho\frac{dQ}{dt}$.

In the balance equation the divergence term represents the interaction of the unit volume particle with the surroundings. On the other hand if a physical quantity is an invariant, its rate of production or destruction is zero; therefore any local variation of the quantity due to the interaction with the surroundings is given by the divergence term. If, on the contrary, the particle constitutes a closed system for a given property, its local variation is only due to an internal production or destruction of the property within the particle.

For long periods of time the energy storage rate of change in the atmosphere is probably small and the balance equation (1) reduces to the form:

$$\operatorname{div} \rho (c_p \mathrm{T} + \mathrm{L} q + \Phi + \mathrm{K}) \vec{\mathrm{V}} - \rho \vec{\mathrm{F}} \cdot \vec{\mathrm{V}} = \rho \frac{d\,\mathrm{Q}}{d\,t} . \qquad (2)$$

The kinetic energy of existing motions is at least two orders of magnitude smaller than the other forms of energy and can be disregarded in equations (1) and (2). The enthalpy and the potential energy are, together with latent heat, the major components of the energy transported by the atmosphere to fulfill the balance requirements of the general circulation of the atmosphere. In view of the importance of the enthalpy in the atmosphere in the discussion that follows the balance of the enthalpy is discussed with some detail.

2. 2. *The enthalpy balance equation*

Let $h = c_p \mathrm{T}$ be the specific enthalpy of air, considered a perfect gas, at a given point of the atmosphere where the temperature is T at the instant t. The corresponding value of the absolute enthalpy will be ρh. Under these conditions the general balance equation of enthalpy in a generalized local frame of reference $(0, x^i)$ can be written in the form:

$$\frac{\partial}{\partial t} \rho h + \frac{1}{\sqrt{\mathrm{G}}} \frac{\partial}{\partial x^i} [\sqrt{\mathrm{G}}\, \rho h v^i] = \rho \frac{d h}{d t} = \sigma(h) \qquad (3)$$

where $\mathrm{G} \equiv |g_{ij}|$ is the determinant of the tensor of the metric, v_i is the contravariant component of the air velocity at the point x^i, at a given instant t; $\sigma(h)$ denotes the time rate of production or destruction of enthalpy per unit volume.

Equation (3) shows that the local variation of enthalpy results from the divergence of the transport of enthalpy, and from the production or destruction of enthalpy, $\sigma(h)$.

Let us consider, at a point of the surface of the earth a column of air of unit section, extending from the ground to the top of atmosphere. The balance equation (3) can be integrated along the vertical. The resulting equation is:

$$\frac{\partial}{\partial t}\int_0^\infty \rho h\, dz + \frac{1}{\sqrt{G}}\frac{\partial}{\partial x^i}\int_0^\infty [\sqrt{G}\,\rho h v^i]\, dz = \\ = \int_0^\infty \rho \frac{dh}{dt}\, dz = \Sigma_t(h). \tag{4}$$

Assuming that the atmosphere is in hydrostatic equilibrium, $dp = -\rho g\, dz$ where g is the acceleration of the gravity, this equation can be rewritten in a p-system taking the corresponding boundary conditions ($p = p_0$, when $z = 0$ and $p = 0$ for $z = \infty$).

Let us denote by the total enthalpy of the air column which in the p-system is then given by

$$H = \frac{c_p}{g}\int_0^{p_0} T\, dp. \tag{5}$$

Similarly let us introduce the contravariant component S^i of the total integrated field of transport of enthalpy. In the p-system is then defined by

$$S^i = \frac{c_p}{g}\int_0^{p_0} T v^i\, dp. \tag{6}$$

With these notations equation (4) in the p-system takes the form:

$$\frac{\partial H}{\partial t} + \frac{1}{\sqrt{G}}\frac{\partial}{\partial x^\alpha}\sqrt{G}\, S^\alpha = \frac{1}{g}\int_0^{p_0}\sigma(h)\, dp = \Sigma_t(h) \tag{7}$$

in which $\Sigma_t(h)$ represents the total rate of production or destruction of enthalpy within the column of unit section.

Because of the earth's spherical symmetry it is convenient to take as the reference frame $(0, x^i)$ a system of quasi-lagrangean spherical coordinates (λ, φ, p, t) where λ is the longitude, φ the latitude, p is

taken as vertical coordinate and t the time. In this coordinate system the integrated balance equation can be written as follows:

$$\frac{\partial H}{\partial t} + \frac{1}{a^2 \cos\varphi}\left[\frac{\partial}{\partial \lambda}(S_\lambda a) + \frac{\partial}{\partial \varphi}(S_\varphi a \cos\varphi) + \right.$$

$$\left. + \frac{\partial}{\partial p}(S_p a^2 \cos\varphi)\right] = \Sigma_t(h). \tag{8}$$

In this equation a is the radius of the earth, S_λ, S_φ and S_p are the physical components of the zonal, meridional and vertical transports of enthalpy vertically integrated above a point at the earth's surface given by

$$S_\lambda = \frac{c_p}{g}\int_0^{p_0} u\,T\,dp$$

$$S_\varphi = \frac{c_p}{g}\int_0^{p_0} v\,T\,dp \tag{9}$$

$$S_p = \frac{c_p}{g}\int_0^{p_0} \omega\,T\,dp$$

noting that the wind field $\vec{V}$ is given by

$$\vec{V} = u\vec{i} + v\vec{j} + \omega\vec{k} \tag{10}$$

where u is the zonal component counted positively to the east, v the meridional component taken positive to the north and $\omega = \frac{dp}{dt}$ is the «vertical component» of the wind in the p-system.

The rate of enthalpy generation $\Sigma_t(h)$ due to atmospheric sources or sinks, is given by the term of diabatic effects $\rho\frac{dQ}{dt} = \rho\dot{Q}$ as will be shown. In the p-system the rate of heating or cooling $\frac{dQ}{dt}$ is, according to the first law of thermodynamics, given by

$$\frac{dQ}{dt} = \frac{dh}{dt} - \alpha\frac{dp}{dt} \tag{11}$$

where $\alpha = \frac{1}{\rho}$.

Expanding the term $\frac{dh}{dt}$ and using the continuity equation in the p-system, this equation, noting that $\omega = \frac{dp}{dt}$, becomes

$$\frac{dQ}{dt} = \frac{\partial h}{\partial t} + \mathrm{div}_p\, h\vec{V} + \frac{\partial}{\partial p}(h\omega) - \alpha\omega . \qquad (12)$$

The first term of this equation is as we have mentioned the rate of production due to diabatic effects. In the second member, the term $\frac{\partial h}{\partial t}$ gives the local variation of enthalpy, in the atmosphere; the terms $\mathrm{div}_p\, h\vec{V}$ and $\frac{\partial}{\partial p}(h\omega)$ are the divergence components of enthalpy over and across isobaric surfaces, respectively of the horizontal and of the vertical fluxes. The term $\alpha\omega = \frac{RT}{p}\omega$ represents, as it is well known, the rate of conversion of the total potential energy (internal plus potential) into kinetic energy (Saltzman and White, 1956). This rate of conversion is small compared to the other terms of the R. H. S. Thus we can conclude that the diabatic effects $\frac{dQ}{dt} \equiv \dot{Q}$ constitute practically the rate of production or destruction of the enthalpy in the atmosphere. Or, yet, the field of the divergence of enthalpy constitutes a good representation of the geographical distribution of the heat sources ($\mathrm{div} > 0$) and of the heat sinks ($\mathrm{div} < 0$) for the atmosphere. It gives the spacial distribution of the globe diabatic effects which condition the behaviour of the general circulation of the atmosphere.

3 — ANALYSIS OF THE BALANCE EQUATION OF ENTHALPY

Among the various diabatic effects responsible for the production of enthalpy in a certain region we can enhance the effects due to the absorption of solar (short wave lenghts) and terrestrial radiation (long wave lenghts) jointly represented by $\dot{Q}_R$; the effects due to the conduction of sensible heat from the ground $\dot{Q}_C$, the dissipation due to friction $\dot{Q}_F$ and the effect associated with phase transitions (con-

densation or evaporation) of water $\dot{Q}_L$. Therefore for the total diabatic effects the time rate of change is (Houghton, 1954; London, 1957)

$$\dot{Q} = \dot{Q}_R + \dot{Q}_C + \dot{Q}_F + \dot{Q}_L . \tag{13}$$

Therefore the enthalpy divergence gives the total rate of change of the diabatic effects.

The preceding enthalpy equation becomes more suggestive if it is expressed in terms of temperature and of the transport field of enthalpy $h\vec{V}$. Therefore we can write:

$$\frac{dQ}{dt} = \frac{\partial h}{\partial t} + \operatorname{div} h\vec{V} + C_p \frac{\partial(\omega T)}{\partial p} - \alpha\omega \tag{14}$$

or

$$\frac{\partial T}{\partial t} = \frac{1}{c_p}\frac{dQ}{dt} - \operatorname{div} T\vec{V} - \frac{\partial(T\omega)}{\partial p} + \alpha\omega/c_p . \tag{14a}$$

This equation shows, immediately, that the local variation of temperature $\frac{\partial T}{\partial t}$ is mainly due to the diabatic effects $\frac{dQ}{dt}$ and to the field of divergence of enthalpy, since the other terms give only a very small contribution.

To stress the importance of various diabatic effects we can still put that equation in the form:

$$\dot{Q}_R + \dot{Q}_F + \dot{Q}_C + \dot{Q}_L = c_p \frac{\partial T}{\partial t} + c_p \operatorname{div} T\vec{V} + c_p \frac{\partial(T\omega)}{\partial p} - \alpha\omega . \tag{15}$$

Integrating this equation between the levels p and $p - \Delta p$, and noting that $dp = -\rho g\, dz$, it comes, using the operator $\{\}$ to represent the vertical integration

$$\frac{\Delta p}{g}\Sigma\{\dot{Q}_i\} = \frac{c_p}{g}\Delta p\left\{\frac{\partial T}{\partial t}\right\} + c_p\frac{\Delta p}{g}\{\operatorname{div} T\vec{V}\} +$$

$$+ \frac{1}{g}\{c_p T\omega\}_p - \frac{1}{g}\{c_p T\omega\}_{p-\Delta p} - \frac{\Delta p}{g}\{\alpha\omega\} \tag{16}$$

as it is readily seen by using the theorem of mean value of integral calculus.

This equation shows that the vertical transport of enthalpy $\frac{1}{g}\left\{\frac{\partial}{\partial p} c_p \mathrm{T}\omega\right\}$ given by the difference

$$\frac{1}{g}(c_p \mathrm{T}\omega)_p - \frac{1}{g}(c_p \mathrm{T}\omega)_{p-\Delta p} \tag{17}$$

is very small because the values of ω are very small and the temperature at the two levels are almost equal.

Particularly if the whole atmosphere is taken into account, that is, when the integration is performed between the levels p_0 and $p=0$ that equation can be written in a simple form, since $\omega(0)=0$ and $\omega(p_0)=0$ through the interface earth-atmosphere; under these conditions the equations (14) and (14a) respectively take the forms:

$$\frac{c_p}{g} p_0 \left\{\frac{\partial \mathrm{T}}{\partial t}\right\} + \operatorname{div} \vec{\mathrm{S}} = \Sigma \dot{\mathrm{Q}}_i \tag{18}$$

and

$$\frac{\partial \mathrm{H}}{\partial t} + \operatorname{div} \vec{\mathrm{S}} = \Sigma \{\dot{\mathrm{Q}}_i\} . \tag{19}$$

Equation (19) reveals that the local variation of enthalpy at a given point, represented by the first member, is due to the flux of enthalpy, given by the divergence term and to the production or destruction of enthalpy *in situ* given by the second member.

This equation which is none but a new form of the balance equation, can be written explicitly in the frame (λ, φ, p, t) as follows:

$$\frac{\partial \mathrm{H}}{\partial t} + \frac{1}{a\cos\varphi}\left\{\frac{\partial}{\partial \lambda}\mathrm{S}_\lambda + \frac{\partial}{\partial \varphi}(\mathrm{S}_\varphi \cos\varphi)\right\} = \Sigma \{\dot{\mathrm{Q}}_i\} . \tag{20}$$

For a region of the atmosphere bounded by the earth's surface of area A limited by the contour (c) this equation can be written in the form:

$$\frac{\partial \mathrm{H}}{\partial t} + \frac{1}{\mathrm{A}} \oint_c (\vec{\mathrm{S}} \cdot \vec{n})\, dc = \Sigma \{\dot{\mathrm{Q}}_i\} \tag{21}$$

where $\vec{n}$ is the normal vector to contour (c).

The application of the preceding equation to regions bounded by latitudinal walls, $\Delta\varphi$ degrees apart, leads to a new and more simplified form of the balance equation, as results from the application of the Ostrogradsky-Gauss theorem. It comes:

$$\frac{\partial H}{\partial t} + \frac{1}{a\cos\varphi}\frac{\partial}{\partial\varphi}\oint S_\varphi(\lambda,\varphi)\cos\varphi\, d\lambda = \Sigma\{\dot{Q}_i\} \tag{22}$$

since

$$\oint \frac{\partial S_\lambda}{\partial\lambda} d\lambda = 0\,. \tag{23}$$

In equation (22) only the meridional convergence of enthalpy across the latitudinal walls φ and $\varphi+\Delta\varphi$ appears.

4 — MODES OF DIVERGENCE OF ENTHALPY IN THE ATMOSPHERE

In the atmosphere one can distinguish various types of circulations. When one considers the mean circulations in the space and in time domains the motions can be partitioned in two general categories, namely the mean and the eddy circulations.

Thus the eastward, the northward and the vertical components of the wind u, v and ω and the temperature T may be expressed as the sum of four components

$$\begin{aligned} u &= [\overline{u}] + \overline{u}^* + [u]' + u'^* \\ v &= [\overline{v}] + \overline{v}^* + [v]' + v'^* \\ \omega &= [\overline{\omega}] + \overline{\omega}^* + [\omega]' + \omega'^* \\ T &= [\overline{T}] + \overline{T}^* + [T]' + T'^* \end{aligned} \tag{24}$$

where the bar represents a time average and the prime a deviation from the time average, the brackets a zonal average, the asterisk a deviation from the zonal average.

In the time domain the mean of the products which appear in expressions (9) may be expanded according to the scheme

$$\begin{aligned}\overline{T\,u} &= \overline{T}\,\overline{u} + \overline{T'u'} \\ \overline{T\,v} &= \overline{T}\,\overline{v} + \overline{T'v'} \\ \overline{T\,\omega} &= \overline{T}\,\overline{\omega} + \overline{T'\omega'}.\end{aligned} \tag{25}$$

Averaging zonally around a latitude circle a resolution of these expressions in the mixed space-time domain is obtained using the «bracket-operator»:

$$\begin{aligned}[\overline{T\,u}] &= [\overline{T}][\overline{u}] + [\overline{T}^*\,\overline{u}^*] + [\overline{T'u'}] \\ [\overline{T\,v}] &= [\overline{T}][\overline{v}] + [\overline{T}^*\,\overline{v}^*] + [\overline{T'v'}] \\ [\overline{T\,\omega}] &= [\overline{T}][\overline{\omega}] + [\overline{T}^*\,\overline{\omega}^*] + [\overline{T'\omega'}].\end{aligned} \tag{26}$$

Different schemes for the expansions of the mean total transfer of enthalpy could be used (Starr and White, 1954; Peixoto 1960). However, the type of expansion (26) is the most useful in dealing with general circulation problems. The interpretation of the various terms of expansions (26) is very instructive, since each one corresponds to a mode of enthalpy flux (Peixoto, 1960). In fact the terms $\frac{c_p}{g}[\overline{T}][\overline{u}]$ and $\frac{c_p}{g}[\overline{T}][\overline{v}]$ represent the transport of enthalpy at a given isobaric level by the zonally averaged zonal and meridional wind fields. Particularly the term $\frac{c_p}{g}[\overline{T}][\overline{v}]$ measures the contribution for the total meridional flow of enthalpy of the mean meridional cells. The terms $\frac{c_p}{g}[\overline{T}^*\,\overline{u}^*]$ and $\frac{c_p}{g}[\overline{T}^*\,\overline{v}^*]$ represent the transfer due to spatial covariance between the mean time averaged field departures from zonal symmetry and are associated with the mean standing eddies. Finally the terms $\frac{c_p}{g}[\overline{T'u'}]$ and $\frac{c_p}{g}[\overline{T'v'}]$ arise from the zonally averaged covariances of the instantaneous local values, and represent the local zonal and meridional mean transfers of enthalpy associated with the transient horizontal eddies (Starr and Wallace, 1964). Similar interpretations apply to the various terms of the total mean vertical transports; in particular the term $\frac{c_p}{g}[\overline{T}][\overline{\omega}]$ corresponds to the vertical transport of enthalpy by the ascending and descending branches of the meridional cells, etc.

The integration along the vertical of equations (26) multiplied by C_p/g leads to the corresponding terms of the various modes of transport of enthalpy for all the atmosphere

$$[\vec{\overline{S}}] = \vec{S}_M + \vec{S}^* + \vec{S}' \tag{27}$$

whose components are:

$$\begin{aligned} [\overline{S}_\lambda] &= S_{\lambda M} + S^*_\lambda + S'_\lambda \\ [\overline{S}_\varphi] &= S_{\varphi M} + S^*_\varphi + S'_\varphi \\ [\overline{S}_p] &= S_{pM} + S^*_p + S'_p \,. \end{aligned} \tag{28}$$

Thus

$$\operatorname{div}[\vec{\overline{S}}] = \operatorname{div}\vec{S}_M + \operatorname{div}\vec{S}^* + \operatorname{div}\vec{S}' \tag{29}$$

and the divergence of enthalpy on a global scale is due to the divergence accomplished by the mean meridional circulations, by the standing eddies and by the transient eddies.

The eddies are in general predominantly horizontal, with a meridional and a zonal component, or vertical. The meridional circulations are formed by the so called meridional cells. Due to the uncertainty involved in the evaluation of $[\overline{v}]$ (for the geostrophic approximation it is identically zero), the estimate of the mean meridional transport of enthalpy by the mean meridional circulations is difficult to assess. As the $[\overline{v}]$ values can be significant in the lower levels of the equatorial Hadley cell, the divergence (or convergence) of enthalpy due to this mechanism can be important; the same happens with the divergence or the convergence associated with the vertical branches of the Hadley circulation (Newell, *et al*, 1970).

5 — FINAL COMMENTS

1. As the atmosphere ability for storing enthalpy leads only to small variations we can assume, with a negligible error, that for a sufficiently long interval of time, such as a season, the corresponding local variation of the time mean of enthalpy may be set to zero

$$\frac{\partial \overline{H}}{\partial t} = 0 \,. \tag{30}$$

Therefore, it can be concluded that, on the average, the field of the mean divergence of total enthalpy transport in the atmosphere for any region is balanced by the diabatic effects as results from the time averaged equation (19). Therefore, through the computation of the mean divergence of enthalpy, a dynamic method of verifying the consistency of estimates of the energetic balance of earth and of atmosphere obtained by traditional approach is provided.

2. When we consider a zonal ring of the atmosphere bounded by the latitudes φ and $\varphi + \Delta\varphi$ the mean divergence is reduced to mean meridional components, since

$$\left[\frac{\partial \overline{S}_\lambda}{\partial \lambda}\right] = \frac{1}{2\pi}\int_0^{2\pi} \frac{\partial \overline{S}_\lambda}{\partial \lambda}\, d\lambda = 0 . \tag{31}$$

Under steady state conditions and for a zonal region of the atmosphere, taking into consideration (28), equation (20) reduces to the form

$$\frac{1}{a\cos\varphi}\,\frac{\partial}{\partial \varphi}\{([\overline{S}_{\varphi M}] + S^*_\varphi + S'_\varphi)\cos\varphi\} = \Sigma\{\dot{Q}_i\} . \tag{32}$$

Therefore, from the derivatives of the profiles of the various modes of meridional flux of enthalpy, one can obtain, in principle, the mean zonal distribution of diabatic effects for the system earth--atmosphere.

3. Let us analyse the situation level by level. One method of examining the consistency of the studies of the atmospheric heat balance at a given level is to consider the various factors which control the mean temperature distribution. In a given region, temperature changes are due to diabatic heating or cooling and to heat transport by the various modes of atmospheric motions. These are more explicitly revealed when equation (14a) is averaged zonally and with respect to time. In fact it can be written *in extenso* in spherical coordinates taking into consideration the expressions (26), as follows:

$$\frac{\partial[\overline{T}]}{\partial t} = \frac{1}{c_p}\left[\frac{\overline{dQ}}{dt}\right] + \gamma[\overline{\omega}] - \frac{1}{a\cos\varphi}\,\frac{\partial}{\partial\varphi}[\overline{V'T'} + \overline{V}^*\,\overline{T}^*]\cos\varphi$$

$$-\frac{[\overline{V}]}{a}\,\frac{\partial[\overline{T}]}{\partial\varphi} - \frac{\partial}{\partial p}[\overline{\omega'T'} + \overline{\omega}^*\,\overline{T}^*] + \frac{R}{p\,c_p}[\overline{\omega'T'} + \overline{\omega}^*\,\overline{T}^*] \tag{33}$$

where γ is the static stability factor, given by

$$\gamma = \frac{R}{p\, c_p}[\overline{T}] - \frac{\partial [\overline{T}]}{\partial p}. \tag{34}$$

The terms on the right hand side (R. H. S.) of Eq. (33) can be inferred from the observations with the exception of the vertical heat fluxes.

Let us analyse this equation in detail. The magnitudes of the first three terms on the R. H. S. are of the order of one degree per day, whereas the fourth term, only important in the lower boundary layer, is of the order of 10^{-1} degrees per day. Estimates of the fifth and sixth terms using vertical heat fluxes derived from an 18-level general circulation model were also of the order of 10^{-1} degrees per day (Manabe and Hunt, 1968), although the fifth in the upper troposphere over the middle latitude regions can, at times, approach values of near one degree per day. Since typical values of the time derivative are of the order of 10^{-1} degrees per day the year and the seasonal heat balances can be treated as steady state problems. Thus, as the contributions by the last terms are insignificant, the zonal balance at a given level is governed, to a first approximation, by the three first terms, namely diabatic heating or cooling, adiabatic compression or expansion and meridional eddy convergence (divergence) of enthalpy.

4. In view of the comments already made, and since the heating due to the divergence of enthalpy acts in a sense opposite to the radiative heating, in principle, a map of the mean total divergence of enthalpy, $\operatorname{div}[\vec{\overline{S}}]$, can be regarded as a map of the energy budget of the system earth-atmosphere. Due to the importance that the parameterization of the diabatic effects assumes in the mathematical modelling of the general circulation, such a map can be considered as a first approximation to define the distribution of the «heating function». With this approach it would then be possible from observed quantities to obtain a spacial representation of the heat sources and sinks, that is to say the corresponding distribution of diabatic effects.

Furthermore, the time average physical state of the atmosphere can be regarded as a forced response to the geographically fixed distribution of the mean diabatic effects, topography and to the mean convergence fields of enthalpy, latent heat and momentum associated

to the transient eddies. In particular the forcing F_S due to the enthalpy flux is given by the vertical derivative of the eddy flux of enthalpy

$$F_S = -f \frac{\partial}{\partial p} \left(\frac{1}{\gamma} \operatorname{div} \vec{S}' \right) \tag{35}$$

where $f = 2\omega \operatorname{sen} \varphi$ denotes the Coriolis parameter and γ the static stability. This expression shows how important the bidimensional fields of the eddy transport of enthalpy at various isobaric levels are in studying the dynamics of the general circulation of the atmosphere.

ACKNOWLEDGMENTS

This research was supported by the National Science Foundation, NSF grant GA-36021 and by the «Instituto de Alta Cultura» through Project LF2. Thanks are due to Prof. Victor Starr for valuable discussions and to Lic. João Corte Real for his comments and editorial assistance.

REFERENCES

DAVIS, P. A., Analysis of the Atmospheric heat budget. *Journ. of Atm. Sci.*, **20**, Boston, 1963.

HOUGHTON, H. G. Annual heat balance of the Northern Hemisphere. *Journ. of Meteo.*, **11**, 1-9, 1954.

LETTAU, H., A study of the mass, momentum and energy budget of the atmosphere. *Arch. Mateo. Geophy. Biokl*, A7, 133-157, 1954.

LONDON, J., A study of the atmospheric heat balance. Coll. Eng. Res. Div. Dep. Met. and Oceanog. *NYU Final Rep.* AFC-7R-57-287 OTS, 1957.

LORENZ, E. N. *The Nature and Teory of the General Circulation of the Atmosphere* Tech. Note No. 218, TP115, WMO, Geneva, 1967.

MANABE, S. and B. G. HUNT, Experiments with a stratospheric General Circulation Model I. Radiative and dynamical aspects. *Month. Wea. Review.* **94**, pp 477--502, 1968.

NEWELL, R. E., D. VINCENT, T. G. DOPPLICK, D. FERRUZA and J. W. KIDSON, The energy balance of the global atmosphere; reprinted from the *Global Circulation of the Atmosphere*, London, 1970.

PEIXOTO, J., P. Hemispheric Temperature Conditions during the Year 1950. *Sci. Rept.* 4, Massachussetts Institute of Technology — Dep. of Meteorology, Cambridge, Mass. 1960.

PEIXOTO, J. P., On the role of water vapour in the energetics of general circulation of the atmosphere. *Portugaliae Physica*, **4**, 135, 1965.

PEIXOTO, J. P., Enthalpy Distribution in the Atmosphere over the Southern Hemisphere. *Revista Italiana di Geofisica* (in press); Milano, 1974.

SMAGORINSKY, J., The Dynamical influence of large scale heat sources and sinks on the quasi-stationary mean motions of the atmosphere. *Quart. J. R. Met. Soc.* **79**, 342-366, 1953.

STARR, V. P., *Physics of negative viscosity phenomena.* Mc Graw-Hill, New York, 1968.

STARR, V. P. and R. M. WHITE, Balance requirements of the general circulation. *Final Report*, M. I. T. General Circulation Project, 186-242, 1954.

STARR, V. P. and J. M. WALLACE, Mechanics of Eddy Processes in the tropical troposphere. *Pure and App. Geoph.*, vol. 58 II, 138-149, 1964.

WHITE, R. M., The meridional eddy flux of energy. *Quart. J. R. Met. Soc.*, vol. 75, 1951a.

WHITE, R. M., The meridional flux of sensible heat over the Northern Hemisphere. *Tellus*, vol. 3, 1951b.

WHITE, R. M. and B. SALTZMAN, On conversions between potential and kinetic energy in the atmosphere. *Tellus*, **8**, Stockholm, 1956.

Composto e impresso na Tip. Matemática, L.da — R. Diário de Notícias, 134-1.º-Esq. — Lisboa-2

Toute la correspondance concernant la rédaction de PORTUGALIAE PHYSICA doit être adressée à

PORTUGALIAE PHYSICA
Laboratório de Física da Faculdade de Ciências
LISBOA-2 (Portugal)

Prix de l'abonnement:	250 escudos (US $8.50) par volume
Prix des volumes déjà parus:	300 escudos (US $10)
Prix du fascicule:	75 escudos (US $2.50)

Les membres de la «Sociedade Portuguesa de Química e Física» ont une réduction de 50 % sur les prix indiqués.

Les Universités, les Laboratoires de Physique, les Académies, les Sociétés Scientifiques et les Revues de Physique sont invités à recevoir cette revue en échange de leurs publications.

PORTUGALIAE PHYSICA donnera un compte-rendu detaillé de tous les ouvrages soumis à la rédaction en deux exemplaires.

All mail concerning PORTUGALIAE PHYSICA to be addressed to:

PORTUGALIAE PHYSICA
Laboratório de Física da Faculdade de Ciências
LISBOA-2 (Portugal)

Subscription rates:	250 escudos (US $8.50) per volume
Price of past volumes:	300 escudos (US $10)
Price of copy:	75 escudos (US $2.50)

Members of the «Sociedade Portuguesa de Química e Física» may obtain *Portugaliae Physica* at a reduced price (50 %).

Universities, Physics Laboratories, Academies, Scientific Societies and Physics Publications are invited to receive this review in exchange for their publications.

PORTUGALIAE PHYSICA will give a detailed report of any book if two copies have been submitted.

PORTUGALIAE PHYSICA

VOLUME 9
FASCÍCULO 3
1975

INSTITUTO DE ALTA CULTURA
CENTROS DE ESTUDOS DE FÍSICA DAS UNIVERSIDADES PORTUGUESAS

PORTUGALIAE PHYSICA

Fundadores: A. Cyrillo Soares, M. Telles Antunes, A. Marques da Silva, M. Valadares.

VOLUME 9 1975 FASCÍCULO 3

VOLUMES PUBLICADOS:

Vol. 1 — 1943-45 — 326 pp.

Vol. 2 — 1946-47 — 256 pp.

Vol. 3 — 1949-54 — 173 pp.

Vol. 4 — 1965-66 — 304 pp.

Vol. 5 — 1967-70 — 194 pp.

Vol. 6 — 1970-71 — 316 pp.

Vol. 7 — 1971-72 — 210 pp.

Vol. 8 — 1972-73 — 266 pp.

Redacção: Laboratório de Física da Faculdade de Ciências — Lisboa-2 (PORTUGAL)

Comissão de redacção:

J. Moreira de Araújo — Carlos Braga — Carlos Cacho — A. Pires de Carvalho — M. Abreu Faro — J. Gomes Ferreira — F. Bragança Gil — Manuel Laranjeira. Amaro Monteiro — J. Pinto Peixoto — J. da Providência — Lídia Salgueiro — J. de Almeida Santos — José Sarmento — António da Silveira — J. Veiga Simão.

ÍNDICE

(Table des matières)

The field of the divergence of enthalpy of the atmosphere in the Southern Hemisphere, by José Pinto Peixoto 59

The decay of some $^{27}Al(p,\gamma)^{28}Si$ *resonances,* by J. D. Cunha, P. M. Corrêa and C. M. da Silva 85

Interference effects in heavy ion elastic and inelastic scattering, by R. da Silveira and Ch. Leclercq-Willain 97

PEIXOTO, José Pinto
University of Lisbon and the Massachussetts Institute of Technology

The field of the divergence of enthalpy of the atmosphere in the Southern Hemisphere.

Portgal. Phys. — 9 (3): 59-84, 1975

A study of the mean atmospheric divergence of enthalpy fields on a planetary scale for the Southern Hemisphere during the IGY covering the calendar year 1958 is presented. The fields of divergence of enthalpy integrated along the vertical for yearly and seasonal conditions for the entire hemisphere are analysed and discussed. In order to obtain a view of the distribution of the enthalpy along the vertical, zonally averaged values of the enthalpy at various levels up to 50 mb were also computed. The mean zonal results of the vertically integrated values are shown and the zonal estimates were compared whenever possible with previous results and with climatological data. In particular the

CUNHA, J. D.;
CORRÊA, P. M.
and SILVA, C. M. da
Laboratório de Física e Engenharia Nucleares, Sacavém, Portugal

The decay of some $^{27}Al(p,\gamma)^{28}Si$ resonances.

Portgal. Phys. — 9 (3): 85-96, 1975

The γ-decay of three $^{27}Al(p,\gamma)^{28}Si$ singlet resonances, at $E_p = 1262$, 1457 and 1587 keV, and three doublet resonances, at $E_p = 1363$, 1662 and 1962 keV, was studied with a 30 cm^3 Ge (Li) detector. The doublet character of the last three resonances was confirmed and the decay modes of both members were resolved.

Branching-ratios, total widths, energy spacings and relative intensities of the doublet members are reported. From the measured value of the width, a spin

SILVEIRA, R. da
Institut de Physique Nucléaire Division de Physique Théorique 91406 — Orsay — France

LECLERCQ-WILLAIN, Ch.
Université Libre de Bruxelles Physique Nucléaire Théorique 1050 — Bruxelles — Belgique

Interference effects in heavy ion elastic and inelastic scattering.

Portgal. Phys. — 9 (3): 97-116, 1975

The semi-classical theory is used to describe the different oscillatory behaviours observed in the elastic and inelastic heavy ion scattering cross-sections at incident energies near and above the Coulomb barrier. The theory predicts two different phases rules which are well observed in the analyzed data: elastic and inelastic scattering cross-sections of ^{11}B on ^{208}Pb at EL = 72.2 MeV and of ^{12}C on ^{27}Al at EL = 46.5 MeV.

divergence of the various modes and their partial contribution for the mean total divergence are fully discussed. The structure of these fields is studied and the corresponding implications for the energetics of the atmosphere mainly for the energy budget are discussed. The influence of oceans in establishing the energy balance is mentioned. The consequences for the general circulation are analysed regarding the divergence map as a distribution of the heat sources and sinks on a global scale, as a basis for the analysis of the physical mechanisms which lead to the conversion of the various forms of energy.

$J^{\pi} = 2^{+}$ is assigned to the lower member of the doublet at $E_p = 1662$ keV. Evidence was found for two new bound levels in the ^{28}Si nuclide, at $E_x = 10517 \pm 3$ and 9798 ± 3 keV. A possible broad resonance at $E_p \simeq 1970$ keV, with a width of $\simeq 20$ keV and decaying mainly via the α_1 channel is suggested.

CDU 53 (469) (05)

PORTUGALIAE PHYSICA

VOLUME 9
FASCÍCULO 3
1975

THE FIELD OF THE DIVERGENCE OF ENTHALPY OF THE ATMOSPHERE IN THE SOUTHERN HEMISPHERE (*)

JOSÉ PINTO PEIXOTO (**)
University of Lisbon and the Massachussetts Institute of Technology

SUMMARY — A study of the mean atmospheric divergence of enthalpy fields on a planetary scale for the Southern Hemisphere during the IGY covering the calendar year 1958 is presented. The fields of divergence of enthalpy integrated along the vertical for yearly and seasonal conditions for the entire hemisphere are analysed and discussed. In order to obtain a view of the distribution of the enthalpy along the vertical, zonally averaged values of the enthalpy at various levels up to 50 mb were also computed. The mean zonal results of the vertically integrated values are shown and the zonal estimates were compared whenever possible with previous results and with climatological data. In particular the divergence of the various modes and their partial contribution for the mean total divergence are fully discussed. The structure of these fields is studied and the corresponding implications for the energetics of the atmosphere mainly for the energy budget are discussed. The influence of oceans in establishing the energy balance is mentioned. The consequences for the general circulation are analysed regarding the divergence map as a distribution of the heat sources and sinks on a global scale, as a basis for the analysis of the physical mechanisms which lead to the conversion of the various forms of energy.

1 — INTRODUCTION

The present study may be regarded as an extension and an application of the theory developed in a previous paper by the writer (Peixoto, 1974).

Diabatic heating in the atmosphere occurs as a result of the convergence of radiative flux, of phase changes of water substance

(*) Received 9 April, 1975.

(**) Director of the «Geophysical Institute D. Luís», University of Lisbon and of Project LF/2 (IAC).

and of the heat exchange between the earth and the atmosphere. Solar radiation is the ultimate source of radiative energy, whereas thermal or terrestrial radiation constitutes a sink. The release of latent heat is the predominant diabatic heating effect in the troposphere above the atmospheric boundary layer. The turbulent heat exchange near the earth's surface in the boundary layer is generally from the earth to the atmosphere because the ocean surface is usually warmer than the air above and in addition in the tropical zones and in the summer hemisphere at middle latitude regions the land surfaces are also relatively warmer.

However, south of 60° S, where oceans of near-freezing temperature, and floating ice of melting temperature, cover most of the area, heat must be given off from the atmosphere to the ocean. Much of the heat loss of atmosphere south of the Antarctic Circle may be represented by heat transfer to the melting snow and ice surfaces.

As discussed in the above mentioned paper (Peixoto, 1974) the divergence and convergence of enthalpy in the atmosphere plays a very decisive role in the energetics of the general circulation and the energy balances of the earth as a whole, and of the atmosphere and oceans systems, taken separately.

We must recognize that in studying the energy balance of a given region, the divergence of enthalpy is much more important than the enthalpy flux by itself. In fact, on a long-term basis the energy storage rate of change in the earth-atmosphere system can be assumed not to change substantially. Therefore, in order to keep the long range observed steady state of the atmosphere in regions where there is a net diabatic effect, mainly due to radiation (incoming minus outgoing radiation) release of latent heat, contact heat, etc., an outflow of energy carried by both the atmosphere and the oceans must be observed. On the other hand, whenever a deficit of the heat balance is observed an inflow of energy must take place. The substantial part of the mechanism which provides the necessary compensation is provided by the divergence field of enthalpy of the atmosphere.

On the whole the heating or the cooling due to the convergence or the divergence of enthalpy acts in a sense opposite to the diabatic effects in a given region (Peixoto, 1974).

Regions where the divergence of enthalpy is positive, $(\overline{\text{div}\,\vec{S}} > 0)$, constitute, in the mean, sources of enthalpy. We conclude then, that in these regions there must be a net excess of energy when all the diabatic effects, such as radiation, release of latent heat, heat of contact,

etc., are taken into consideration. This excess is, thus, exported under the form of enthalpy.

Inversely, regions where convergence of enthalpy, $(\overline{\operatorname{div}\vec{S}}<0)$, are predominant, constitute sinks of enthalpy, which determine an inflow of energy into such regions to compensate the observed deficit of energy.

There have been numerous studies concerned with the general circulation and the heat and energy balances of the atmosphere, mainly based on Northern Hemisphere data. Not until the International Geophysical Year (IGY), have sufficient data become available in the Southern Hemisphere because of the poor aerological network, due to vast ocean areas, to undertake this type of study.

Thus, the purpose of the present study is to use the IGY data within the framework of the observational approach to investigate seasonal changes in the divergence field of enthalpy in the atmosphere and its application to the energy budget of the earth, ocean and atmosphere, in the Southern Hemisphere. In previous papers seldom there have been attempts to use observations in the global circulation studies over the Southern Hemisphere and, therefore, no basis for comparing results obtained extensively for the Northern Hemisphere.

2 — FORMULATION OF THE PROBLEM

Since the formulation principles of the problem have been presented in a previous paper (Peixoto, 1974) only the basic equations will be given here.

For a unit column of the atmosphere, which extends from the surface $(p=p_0)$ to the top of the atmosphere $(p=0)$ the balance equation of the total time mean enthalpy, $\overline{H}$, is given by

$$\frac{\overline{\partial H}}{\partial t} + \operatorname{div}\overline{\vec{S}} = \overline{\{\dot{Q}\}} \tag{1}$$

where the bar operator indicates a time average for the time interval τ

$$\overline{(\quad)} = \frac{1}{\tau}\int_{\tau}(\quad)\,dt.$$

Let us discuss the meaning of the symbols. The total enthalpy H is given by

$$H = \frac{C_p}{g} \int_0^{p_0} T \, dp \tag{2}$$

where C_p denotes the specific heat at constant pressure, g the acceleration of gravity, T the temperature and p the pressure.

The transport field of enthalpy $\vec{S}(\lambda, \Phi)$ is a two-dimensional vectorial field represented by

$$\vec{\overline{S}} = \overline{S} \, \vec{i} + \overline{S}_\Phi \vec{j} \tag{3}$$

where $\vec{i}$ and $\vec{j}$ are the unit vectors of the local β-plane and $\overline{S}_\lambda$ and $\overline{S}_\Phi$ the zonal and the meridional components, respectively defined by

$$\begin{aligned} \overline{S}_\lambda &= \frac{C_p}{g} \int_0^{p_0} \overline{u\,T} \, dp \\ \overline{S}_\Phi &= \frac{C_p}{g} \int_0^{p_0} \overline{v\,T} \, dp \end{aligned} \tag{4}$$

where u and v are the zonal and the meridional components of the wind. $\{\dot{Q}\}$ represents the total diabatic effects for all the column; $\{\dot{Q}\}$ is the resultant of the net radiation (solar minus terrestrial), $\{\dot{Q}_R\}$, of the release of latent heat $\{\dot{Q}_L\}$, of the conduction of sensible heat from the ground $\{\dot{Q}_C\}$ and of friction $\{\dot{Q}_F\}$:

$$\{\dot{Q}\} = \{\dot{Q}_R\} + \{\dot{Q}_L\} + \{\dot{Q}_C\} + \{\dot{Q}_F\} . \tag{5}$$

Equation (1) can be written explicitly in a spherical coordinates referencial (λ, Φ, p, t), where Φ and λ are the latitude and the longitude, as follows:

$$\frac{\overline{\partial H}}{\partial t} + \frac{1}{a \cos \Phi} \left\{ \frac{\partial \overline{S_\lambda}}{\partial \lambda} + \frac{\partial}{\partial \Phi} (\overline{S}_\Phi \cos \Phi) \right\} = \{\overline{\dot{Q}}\} \tag{6}$$

a is the mean radius of the earth.

The application of the Ostrogradsky-Gauss theorem to equation (1) leads to the equivalent equation

$$\overline{\frac{\partial H}{\partial t}} + \frac{1}{A}\oint (\overline{\vec{S}} \cdot \vec{n})\, d c = \{\overline{\dot{Q}}\} \tag{7}$$

when an area A is bounded by a contour c, with a normal vector $\vec{n}$. For an area bounded by the latitudes Φ and $\Phi + \Delta\Phi$ this equation transforms into

$$\overline{\frac{\partial H}{\partial t}} + \frac{1}{a\cos\Phi}\,\frac{\partial}{\partial \Phi}\oint \overline{S}_\Phi(\lambda, \Phi)\cos\Phi\, d\lambda = \{\overline{\dot{Q}}\} \tag{8}$$

where only the meridional convergence of enthalpy appears, since

$$\oint \frac{\partial S_\lambda}{\partial \lambda}\, d\lambda = 0\,.$$

Expressions (4) can be expanded in the space-time domain using the bar and the «bracket-operator» [ ], given by:

$$[\ ] = \frac{1}{2\pi}\oint (\ )\, d\lambda$$

as follows:

$$\begin{aligned}
[\overline{S}_\lambda] &= \frac{C_p}{g}\left\{\int_0^{F_0} [\overline{u}][\overline{T}]\, dp + \int_0^{F_0} [\overline{u'T'}]\, dp + \int_0^{F_0} [\overline{u^*}\,\overline{T^*}]\, dp\right\} \\
[\overline{S}_\Phi] &= \frac{C_p}{g}\left\{\int_0^{F_0} [\overline{v}][\overline{T}]\, dp + \int_0^{F_0} [\overline{v'T'}]\, dp + \int_0^{F_0} [\overline{v^*}\,\overline{T^*}]\, dp\right\}.
\end{aligned} \tag{9}$$

Symbolically we have then:

$$\begin{aligned}
[\overline{S}_\lambda] &= \overline{S}_{\lambda M} + \overline{S}'_\lambda + \overline{S}^*_\lambda \\
[\overline{S}_\Phi] &= \overline{S}_{\Phi M} + \overline{S}'_\Phi + \overline{S}^*_\Phi\,.
\end{aligned} \tag{9a}$$

These expressions show that the total mean fluxes of enthalpy are carried by the mean zonally averaged motion (mean circulations) $\overline{\vec{S}}_M$, by the transient eddies $\overline{\vec{S}}'$, and by the standing eddies $\overline{\vec{S}}^*$.

In a global scale the mean divergence of enthalpy is given by:

$$\operatorname{div}[\bar{\vec{S}}] = \operatorname{div}\bar{\vec{S}}_M + \operatorname{div}\bar{\vec{S}}' + \operatorname{div}\bar{\vec{S}}^* . \tag{9b}$$

The first term of R. H. S. of equations (9) or (9a) is the advection of mean temperature field due to the mean zonally averaged wind field. The second term associated with the zonal average along a latitude circle of the time correlation of winds and temperatures at individual points measures the transport associated with the transient horizontal eddies (baroclinic perturbations, cyclones, etc.).

The last term measures the zonally averaged flux associated with the standing eddies (semi-permanent lows, anticyclones, etc.).

For a long period of time the local rate of change of storage of enthalpy in the atmosphere is negligible and in the balance equations we may set it at zero:

$$\overline{\frac{\partial H}{\partial t}} = 0 . \tag{10}$$

From equation (1) under steady state conditions the divergence of enthalpy equals the diabatic effects in such a way that there is compensation of cooling $\{\bar{Q}\} < 0$ by convergence of enthalpy, $\overline{\operatorname{div}\vec{S}} < 0$, and excess of warming $\{\bar{Q}\} > 0$ by export of enthalpy, $\overline{\operatorname{div}\vec{S}} > 0$. The sources of enthalpy are associated in the mean with the warming due to diabatic effects, and the sinks with the corresponding cooling of the atmosphere.

Let us focus our attention on expressions (9) and (9a). For the global budget of energy of the system oceans-atmosphere the meridional transport is more relevant than the zonal transport. So we will analyse with some more detail the various components of $[\bar{S}_\Phi]$. The flux of enthalpy by the mean meridional circulation, $\bar{S}_{\Phi M}$, is given by:

$$\bar{S}_{\Phi M} = \frac{C_p}{g} \int_0^{p_0} [\bar{v}][\bar{T}]\, dp . \tag{11}$$

As it is well known it is very difficult to estimate mainly due to the uncertainty and lack of precision involved in the evaluation of the mean meridional circulation $[\bar{v}]$. If the winds were geostrophic the mean zonal value of $[\bar{v}_{gs}]$ would vanish identically.

However, with actual winds $\overline{S}_{\Phi M}$ has not to be zero. The corresponding values are associated with the transport of enthalpy by the mean meridional circulations. This transport may be important in the tropical regions where the Hadley cell predominates, whereas the mean meridional eddy transports are more important in middle and high latitudes, the transient eddies being more predominant. This point will be taken again, later.

3 — DATA AND PROCEDURES

The data used in this study are the values of $\overline{S}'_{\lambda}$ and $\overline{S}'_{\Phi}$ at grid points with 5° latitudinal and longitudinal increments over the Southern Hemisphere between 0° and 80° S. These values were read from maps with the analyses of $\overline{S}'_{\lambda}$ and $\overline{S}'_{\Phi}$ fields (Peixoto, 1973) obtained from directly observed values of u, v and T at various isobaric levels during the IGY for 125 upper-air stations which form the basic aerological network. The maps were analysed for the winter season (April-Sept), for the summer season (Oct-March) and for the whole year.

The bidimensional continuum (λ, Φ) is substituted by a discretum (λ_j, Φ_j) in which the dimensions of the fundamental grid are $\partial \Phi_j = \partial \lambda_j = \frac{\pi}{36}$ and $\lambda_j = j\frac{\pi}{36}$, $\Phi_j = j\frac{\pi}{36}$ where j is an integer number varying from 0 to 72 for the longitude λ and from 0 to 16 for the latitude Φ.

In a generic point (λ_k, Φ_k) of the discretum the expression of mean bidimensional (lateral) divergence of enthalpy is:

$$\operatorname{div} \overline{\vec{S}}' = \frac{1}{a \cos \Phi_{k+\frac{1}{2}}} \left[\frac{\partial \overline{S}'_{\lambda_k}}{\partial \lambda_k} + \frac{\partial (\overline{S}'_{\Phi_k} \cos \Phi_k)}{\partial \Phi_k} \right]. \qquad (12)$$

Using centered differences we arrive at the expression in finite differences:

$$\operatorname{div} \overline{\vec{S}}' = \frac{1}{a \cos \Phi_{k+\frac{1}{2}}} \frac{36}{\pi} [\partial \overline{S}'_{\lambda_k} + \partial \overline{S}'_{\Phi_k} \cos \Phi_k]. \qquad (13)$$

The centered differences $\partial \overline{S}'_{\lambda_k}$ and $\partial \overline{S}'_{\Phi_k} \cos \Phi_k$ using current notation are given by

$$\partial \overline{S}'_{\lambda_k} = \overline{S}'_{\lambda_{k+\frac{1}{2}}} - \overline{S}'_{\lambda_{k-\frac{1}{2}}}$$

$$\partial \overline{S}'_{\Phi_k} \cos \Phi_k = \overline{S}'_{\Phi_{k+\frac{1}{2}}} \cos \Phi_{k+\frac{1}{2}} - \overline{S}'_{\Phi_{k-\frac{1}{2}}} \cos \Phi_{k-\frac{1}{2}} . \tag{14}$$

Numerical computation of divergence in a region bounded by a contour c becomes much simplified when the contour c is formed by segments of meridians and paralels, because disposing of all the grid points values of the discretum the boundary values are immediately available.

If, for instance, the contour c is formed by two segments of paralels $\Phi_1 = \text{const.}$ and $\Phi_2 = \text{const.}$ of amplitude $n\,\partial\lambda = \lambda_2 - \lambda_1$ and by two segments of meridians $\lambda_1 = \text{const.}$ and $\lambda_2 = \text{const.}$ of amplitude $m\,\partial\Phi = \Phi_2 - \Phi_1$ where m and n are integer numbers, the arithmetic expression of the total enthalpy flux across c is:

$$\oint (\vec{\overline{S}}' \cdot \vec{n})\, dc = a \frac{\partial \Phi}{2} \left\{ (\overline{S}'_{\lambda_{2,0}} - \overline{S}'_{\lambda_{1,0}}) + 2 \sum_{\alpha=1}^{m-1} [\overline{S}'_{\lambda_{2,\alpha}} - \overline{S}'_{\lambda_{1,\alpha}}] + \right.$$

$$\left. + (\overline{S}'_{\lambda_{2,m}} - \overline{S}'_{\lambda_{1,m}}) \right\} + a \frac{\partial \lambda}{2} \left\{ (\overline{S}_{0,\Phi_2} \cos \Phi_2 - \overline{S}'_{0,\Phi_1} \cos \Phi_1) + \right. \tag{15}$$

$$\left. + 2 \sum_{\beta=1}^{n-1} [\overline{S}'_{\beta,\Phi_2} \cos \Phi_2 - \overline{S}'_{\beta,\Phi_1}] + (\overline{S}'_{n,\Phi_2} \cos \Phi_2 - \overline{S}'_{n,\Phi_1}) \right\}.$$

If the contour c bounds a nonsimply connected spherical zone, limited by two paralels $\Phi_1 = \text{const.}$ and $\Phi_2 = \text{const.}$, the first term of the second member of the preceding expression is zero and, taking into consideration the dimensions of the grid (for the entire paralel $n = 72$), the final expression for computational purposes becomes:

$$\oint (\vec{\overline{S}}' \cdot \vec{n})\, dc = a\, \partial\lambda \sum_{\beta=1}^{72} [\overline{S}'_{\beta,\Phi_2} \cos \Phi_2 - \overline{S}'_{\beta,\Phi_1} \cos \Phi_1] . \tag{16}$$

The area A bounded by the contour c is now given by $A = 72\, a^2 \cos \Phi_{1+\frac{1}{2}}\, \partial\lambda\, \partial\Phi$ and the corresponding mean value of divergence is:

$$\operatorname{div} \bar{\bar{S}}' = \frac{1}{A} \oint \bar{\bar{S}}' \cdot \vec{n}\, dc = \tag{17}$$

$$= \frac{1}{a \cos \Phi_{1+\frac{1}{2}}\, \partial\Phi} \sum_{\beta=1}^{72} [\bar{S}'_{\beta,1_2} \cos \Phi_2 - \bar{S}'_{\beta,1_1} \cos \Phi_1] .$$

The mathematical treatment for the computation of the field of divergence of enthalpy and the processing of the basic data was done with the help and cooperation of the M. I. T. Planetary Circulations Project and with the Numerical Weather Prediction Unit of the National Meteorological Service of Portugal.

With the computed values of the mean horizontal divergence of enthalpy, $\overline{\operatorname{div} \vec{S}'}$, in approximately 648 points, for the year, summer and winter semesters, hemispheric charts were prepared with the mean values of divergence referred to the centers of each element of the grid of the discretum. An analysis of the divergence of enthalpy field was then performed for the mentioned periods, using the scalar analysis methodology by the drawing of isopleths.

4 — ANALYSIS AND INTERPRETATION OF RESULTS

4. 1. *Analysis of the hemispheric fields of divergence*

The maps with the analysis of the field of mean divergence of the vertically integrated transient eddy flux of enthalpy relative to the year and to the winter and summer semesters, for the Southern Hemisphere are represented in figures 1, 2 and 3.

The isopleths are in units of 10^{-3} cal/(cm^2 · min) that is, approximately 1,44 langley/day (ly/day). The isopleths of positive divergence are drawn as continuous lines while those for convergence are dashed lines.

The exam of the spacial distribution of the divergence field shows that in any of three maps the regions of convergence and those of divergence are not formed by isolated centers. The analysis present an almost continuous zonal distribution with some sort of polar

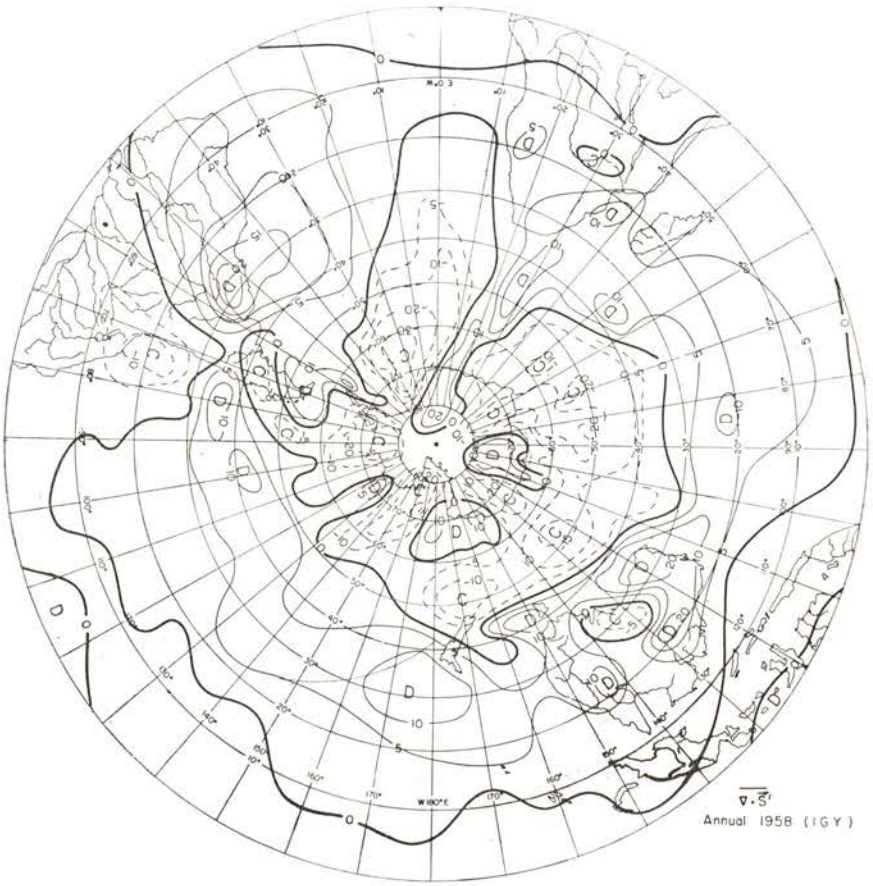

Fig. 1 — Mean annual distribution of the horizontal divergence of the vertically integrated transient eddy flux of enthalpy in 10^{-3} calories per square centimeter per minute.

symmetry although with some variable longitudinal intensities. It is apparent that, in middle latitudes, most part of oceans, are zones of divergence (lost of enthalpy), distributed in centers of greater intensity mainly in the zone between 20° and 45° S. On the other hand zones

of convergence predominate south of the latitude circle of 50° S. There is also slight convergence in some equatorial regions.

The analysis of the map relative to the year shows that in Southern Hemisphere the areas of regions of convergence and the

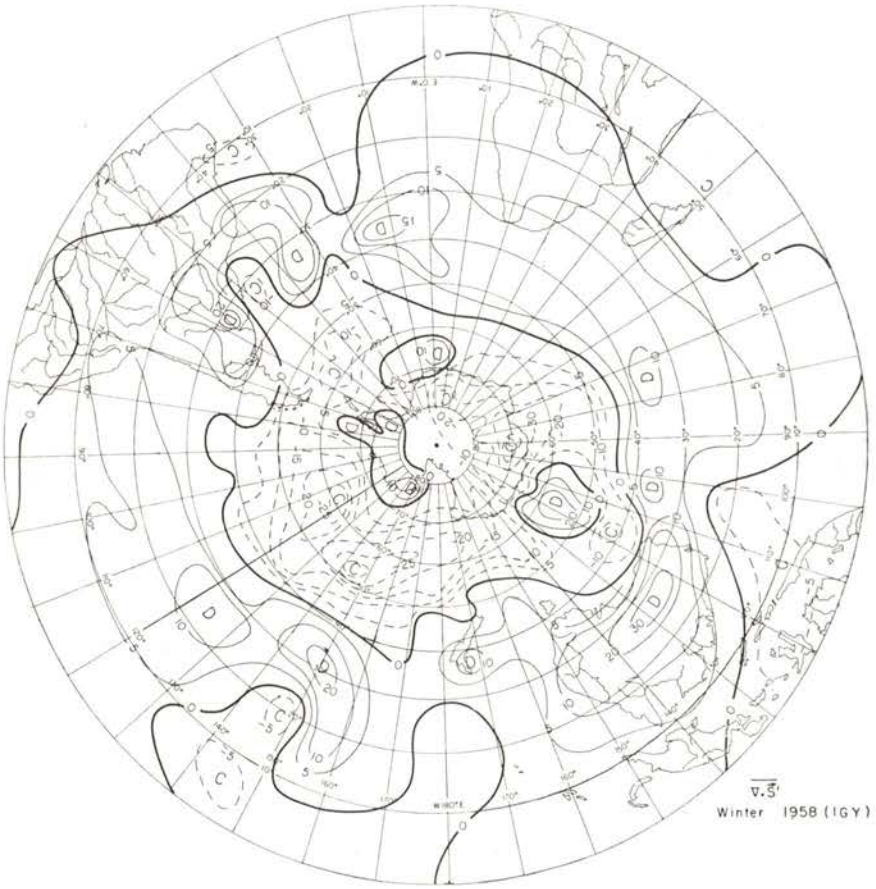

Fig. 2 — Mean winter distribution of the horizontal divergence of the vertically integrated transient eddy flux of enthalpy in 10^{-3} calories per square centimeter per minute.

areas of divergence of enthalpy associated to the eddies almost balance themselves. This is due to the fact that the net mean annual eddy flux of enthalpy across the equator is almost zero. This aspect will be discussed later with more detail.

Consequently for the interval of a year, regions where there is an excess of energy must, on the average, balance those where a deficit is observed.



Fig. 3 – Mean summer distribution of the horizontal divergence of the vertically integrated transient eddy flux of enthalpy in 10^{-3} calories per square centimeter per minute.

Thus, for a sufficiently long interval of time the storage power of atmosphere for the enthalpy cannot suffer an appreciable variation. This leads to the conclusion that the annual variation of the enthalpy stored in the atmosphere is very small.

The centers of convergence are located in the equatorial regions

and in middle and high latitudes, south of the latitude 50° S, with the exception of small centers of divergence in the polar regions.

Centers of divergence are located in the east position of Brasil and Argentina extending over most of the South Atlantic Ocean, over South Africa and over Australia. However the most important centers of divergence are located over the oceans. The more intense are observed over the Atlantic near the South America Coast over a large belt covering all the central Pacific and another belt over the Indian Ocean. It is interesting to point out that the regions where divergence is most intense are located in the latitudes where the circulation of the atmosphere is associated with the large semi-permanent subtropical anticyclones.

The most predominant centers of divergence, over the Continents coincide with arid or desertic regions such as happens with Australia. Therefore, the regions of large subtropical anticyclones which are related to the location of desertic regions, are sources of enthalpy for the atmosphere. This is to be expected, since the subtropical oceanic zones are regions of formation of tropical maritime air masses (Tm), caracterized by high temperature and humidity. Furthermore it is interesting to see that the dynamics of climate plays a predominant role in the modelation of the crust and in the physiography of the globe.

The existence of divergence of enthalpy over the ocean agrees with the fact that oceans constitute sources of heat for the atmosphere due to its large capacity of storing enthalpy and to the small fluctuations of the mean temperature of water. Also, in the region of divergence, the evaporation is stronger, which is corroborated by the higher values of the salinity in that regions. It is also interesting to stress that in the Southern Hemisphere the Continental zones, in spite of some isolated centers of convergence, show, on the average, a net divergence of enthalpy during all the year.

The maps with the seasonal analyses of the divergence of enthalpy (figs. 2 and 3) show that the global configurations of the corresponding seasonal fields don't differ substantially from the annual distribution.

Let us consider the winter analysis (fig. 2). The intensities of the divergence and convergence centers are, in general, much higher and the convergence extends deeper to lower latitudes. In fact, two large zonal belts of convergence alternating with zones of divergence may be observed. In middle latitudes the transition from divergence to convergence regions, $\operatorname{div} \vec{\bar{S}}' = 0$, is now much better defined. Australia,

South Africa, and most of South America are under the influence of a much more intense divergence than it is revealed by the annual map. Furthermore, the isolated centers of convergence shown in the yearly analyses almost disappeared. The centers of divergence over the South Pacific, over the Indian and over the Atlantic Oceans are more intense in the winter than in the year. However, relatively to the continents they are now much less intense.

The analysis relative to the summer semester (fig. 3) shows the same general features, but the intensities of the centers are much weaker than in the preceding cases, as was to be expected. The intensities of the field over the oceans and over the continents are now reversed as regards to the winter distribution. Now the divergence is slightly higher over the oceans. The influence of the continents is very striking when the seasonal distribution over Australia, South America and Africa are compared. Although there is divergence in summer and winter, the values of the latter are much more intense. This is, however, the general rule, even for the convergence, as can be seen in comparing both distributions in the high latitude belt of convergence.

In the study of the energetic balance of an oceanic region and in the global study of the flux of energy, it cannot be forgotten the important role played by oceans in the storing of enthalpy which is much higher than that of the atmosphere and in its distribution and transport effected as well as by surface currents, as by internal currents of oceans. The flux of energy is considerable and can reach relatively high values.

The analysis demonstrate two other features of this eddy heating. Firstly note the area of intense heating in polar regions during the winter months. This is to be expected since during the summer, the polar regions are receiving much more solar radiation than in the winter months when they are in continual darkness. It should also be noticed that the relative areas of heating and cooling display more seasonal dependence in midlle to high latitudes than in the tropics. This is also commensurate with radiation results.

From the inspection of the maps, it is seen there, that there is a net heating in the equatorial regions. This is not, however, as questionable a result as might be thought. Equatorial heat transports in the high equatorial troposphere have been noted by Peixoto (1960a), Starr and Wallace (1964), and Gilman (1964). In view of this the actual results seem quite plausible.

The existence, in the mean, of an inflow of enthalpy through the

equator leads to the existence of an excess in the energy balance of northern hemisphere. This result agrees with the values obtained by Budyko according to which northern hemisphere receives in the mean more energy, i. e. 479 cal/(cm². year) as compared with 467 cal/(cm². year) received by the southern hemisphere.

4. 2. *Vertical distribution of the mean meridional divergence of enthalpy*

Vertical distributions of the zonally averaged values of the divergence of total eddy flux of enthalpy (transient plus standing eddy) at various isobaric levels are presented in figs. 4, 5 and 6. The values

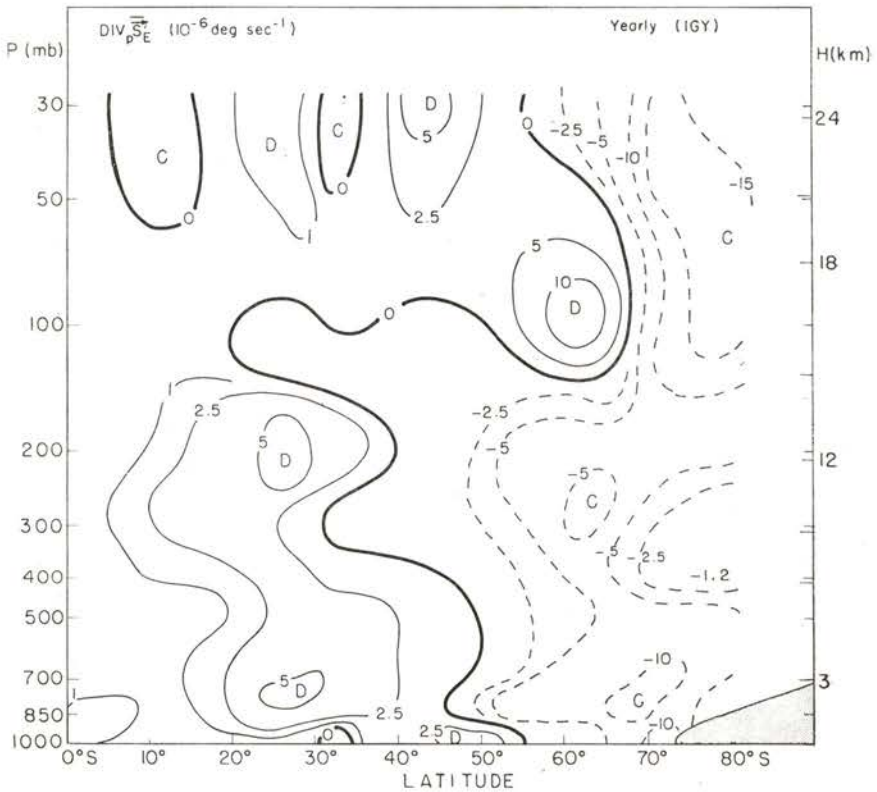

Fig. 4 — Vertical meridional cross-section through the atmosphere showing the distribution of the mean meridional eddy divergence of enthalpy for yearly data. The units are 10^{-6} deg sec^{-1}.

were computed from the mean total eddy fluxes at various levels ($\vec{\bar{S}}_E = \vec{\bar{S}}' + \vec{\bar{S}}^*$) published in a previous paper (Peixoto, 1974).

The values of $\operatorname{div} \vec{\bar{S}}_E = \operatorname{div} \vec{\bar{S}}' + \operatorname{div} \vec{\bar{S}}^*$ were computed for the zone bounded by latitude Φ_1 and Φ_2 through the variant of expression (17)

$$\operatorname{div} \vec{\bar{S}}_E = \frac{1}{2\pi (\sin \Phi_2 - \sin \Phi_1)} \oint \{[\bar{S}_{E,\Phi} \cos \Phi]_{\Phi_2} - [\bar{S}_{E,\Phi} \cos \Phi]_{\Phi_1}\} d\lambda . \tag{18}$$

These cross-sections give the main characteristics of the distribution of the divergence of enthalpy along the vertical. By and large,

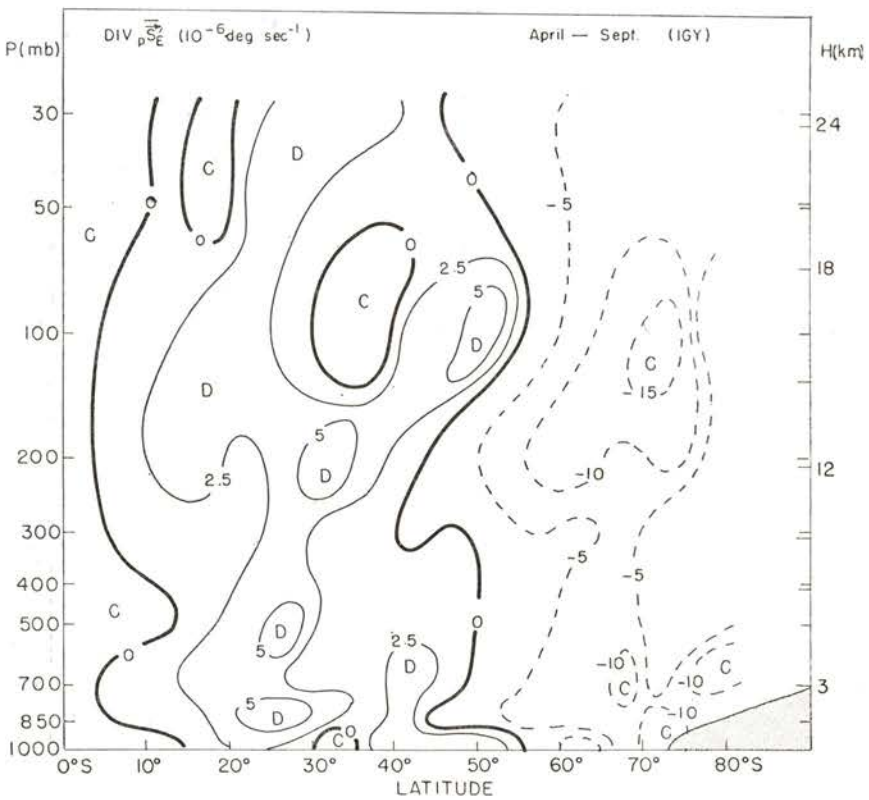

Fig. 5 — Vertical meridional cross-section through the atmosphere showing the distribution of the mean meridional eddy divergence of enthalpy for winter data. The units are 10^{-6} deg sec^{-1}.

divergence predominates north of 50° S at all levels with two main centers in the lower and upper troposphere. South of 50° S, convergence prevails, and is much more intense in the stratosphere. In the equatorial region there is also a slight convergence. In winter, both the divergence and convergence centers are more intense in the

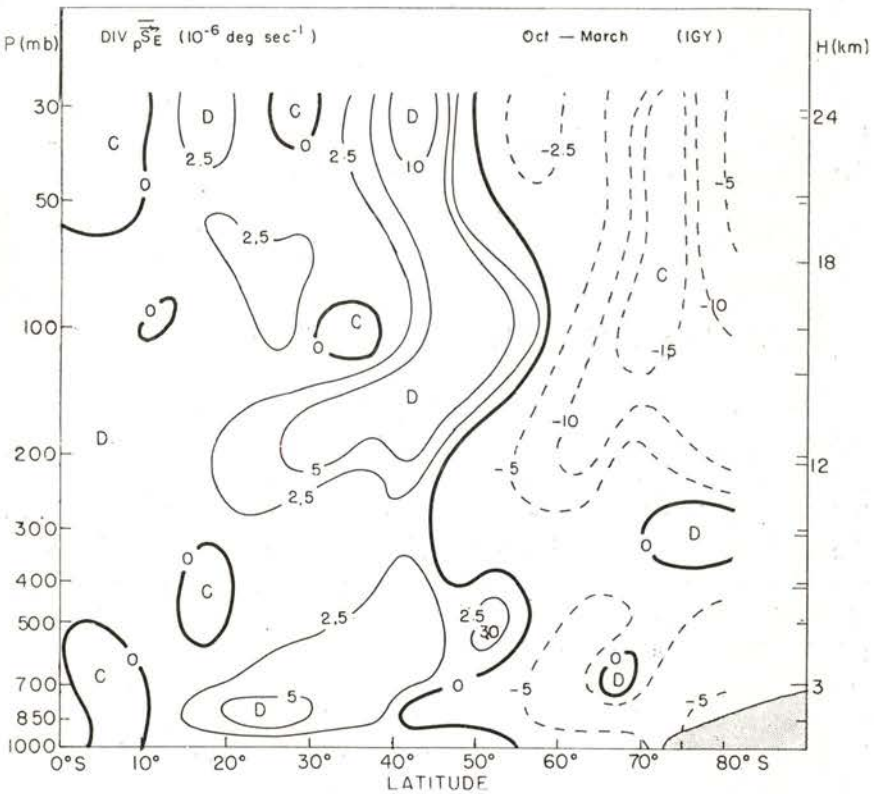

Fig. 6 — Vertical meridional cross-section through the atmosphere showing the distribution of the mean meridional eddy divergence of enthalpy for summer data. The units are 10^{-6} deg sec^{-1}.

troposphere than they are in summer. The intense convergence observed in the high to subpolar latitudes at all levels in the stratosphere during the winter are associated with the cooling caused by polar night. The centers in the lower troposphere are associated with the transient perturbations along the polar front and with the semi-permanent lows which prevail in high latitude levels.

On the other hand the main divergence centers observed in the upper levels are associated with the warming due to the net radiation excess, solar minus terrestrial, observed in the low latitudes whereas those observed in the lower troposphere are associated with the semi-permanent anticyclones belt centered over the subtropical latitudes.

The centers of divergence and of convergence in the lower troposphere suggest that the effects of winter cooling and summer warming due to the presence of the globe do not penetrate much above 500 mb. The similarity of the two seasonal distributions in the lower layers must be due to the existence of large oceanic expanses in the Southern Hemisphere. However, longitudinal cross-sections, for example, along the latitude circle of 20° S, would show for both seasons significant differences over the continents as compared with the oceans.

4. 3. *Mean meridional divergence of enthalpy*

In the studies of the global heat budget of the earth or of the subsystems globe and atmosphere, it is convenient to use the mean meridional profiles of the various components of the budget at given latitudes. This procedure gives a general view of the importance of the various components in achieving the required energy balance and provides some insight on the mechanisms which run the general circulation of the atmosphere. Moreover, it makes the analysis of the relative influence of the various forms of energy in the global process easier.

Since the enthalpy is one of the main components of the heat budget through its divergence or convergence, the corresponding vertically integrated values of the mean meridional divergence of the transient and stationary modes, as well as the total eddy divergence up to 50 mb, was evaluated at various latitudes. The values for yearly, winter and summer seasons are presented in Table 1 in units of watt/m^2 and in degree/day. The corresponding meridional profiles with the latitudinal distributions of the various modes of divergence are also shown in Fig. 7. The abscissa axis is graduated in degrees of latitude proportional to $\sin\Phi$, so that areas bounded by the profile curves are comparable with each other.

The results were obtained using the values of the total mean stationary and transient eddy transports already published (Peixoto, 1974) applying the formulation expressed by (18). The convergence

TABLE 1. *Zonally averaged divergence of the total eddy flux of enthalpy of the atmosphere in the Southern Hemisphere in units of watt/m² and in degree/day between brackets* (1 watt $m^{-2} = 1.435 \times 10^{-3}$ cal cm^{-2} $min^{-1} = 0{,}754$ kilolangleys $year^{-1}$).

Lat (S)	Annual			Winter			Summer		
	$\overline{\text{div } \vec{S'}}$	$\overline{\text{div } \vec{S^*}}$	$\overline{\text{div } \vec{S}_E}$	$\overline{\text{div } \vec{S'}}$	$\overline{\text{div } \vec{S^*}}$	$\overline{\text{div } \vec{S}_E}$	$\overline{\text{div } \vec{S'}}$	$\overline{\text{div } \vec{S^*}}$	$\overline{\text{div } \vec{S}_E}$
0–10°	14,84	13,06	27,90	—5,93	19,00	13,06	0,59	27,32	27,91
	(0,13)	(0,15)	(0,24)	(—5,27)	(0,16)	(0,11)	(52,71)	(0,24)	(0,24)
10–20	77,79	—4,90	72,90	52,07	29,40	81,47	53,90	—13,47	40,43
	(0,68)	(—4,34)	(0,65)	(0,46)	(0,26)	(0,72)	(0,47)	(—0,11)	(0,35)
20–30	168,44	16,32	184,80	190,64	17,62	208,27	146,89	8,48	155,38
	(1,49)	(0,41)	(1,63)	(1,69)	(0,15)	(1,84)	(1,30)	(7,53)	(1,37)
30–40	161,80	—35,40	126,41	251,62	—104,74	110,51	164,69	—38,28	126,41
	(1,43)	(—0,31)	(1,12)	(1,91)	(—0,92)	(0,98)	(1,46)	(—0,33)	(1,12)
40–50	24,26	2,51	26,78	46,86	51,04	97,90	66,94	20,28	87,02
	(0,12)	(2,22)	(0,23)	(0,41)	(0,45)	(0,86)	(0,59)	(0,17)	(0,77)
50–60	244,49	57,77	186,72	—267,19	53,64	—213,54	—202,19	63,96	138,23
	(2,17)	(0,51)	(—1,65)	(—2,37)	(0,47)	(—1,89)	(—1,79)	(0,56)	(—1,22)
60–70	385,03	37,80	347,72	—441,03	—9,80	—450,83	—358,42	36,40	—322,02
	(3,41)	(0,33)	(—3,08)	(—3,91)	(—8,69)	(—4,00)	(—3,18)	(0,32)	(—2,85)
70–80	267,48	—116,59	384,04	—260,62	—86,87	—347,50	—210,33	—93,73	—304,46
	(2,37)	(—1,03)	(—3,40)	(—0,23)	(—0,77)	(—3,08)	(—1,86)	(—0,83)	(—2,69)

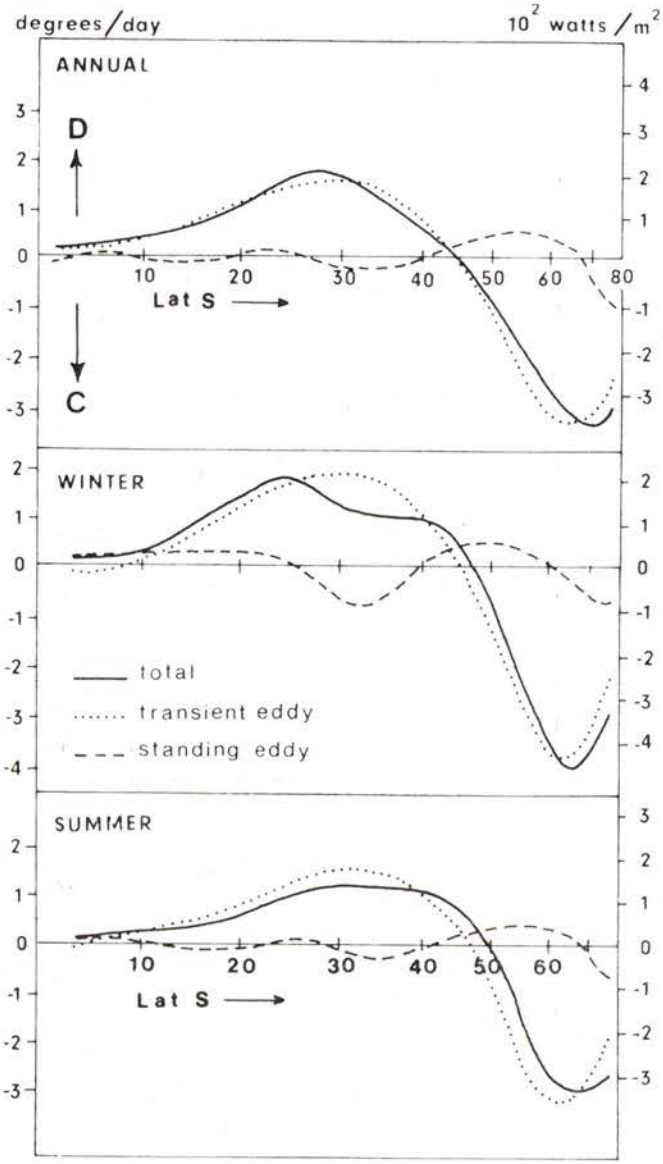

Fig. 7 — Profile of the mean meridional divergence of total eddy flux of enthalpy in units of cal/(cm^2. min), watt m^2 and ^0K/day, for yearly, winter and summer data.

or divergence of enthalpy was also evaluated in degrees per day of uniform warming or cooling of the atmosphere within a ten-degree latitude zone, for a depth of the atmosphere from 1000 to 50 mb.

The mean zonal values of the divergence of transient eddy flux of enthalpy, $[\overline{\text{div}\,\vec{S}'}]$, constitute a synthesis of the maps previously discussed. The mean annual profile shows that there is divergence in low and middle latitudes, ($\Phi \leq 45^{\circ}$ S), and convergence polewards of 45° S and near the equator, although slight. The divergence predominates over the tropical to middle latitudes regions.

The marked convergence of enthalpy observed in high and subpolar latitudes with an extreme of $-0.58 \times 10^{+3}$ watt/m² (+3,4 degrees/day) near 65° S, is associated with the flux due to the transient perturbations predominating in those regions. This convergence is going to compensate the intense cooling due to the radiative deficit observed in the subpolar latitudes.

The weak convergence observed in the vicinity of the equator is mainly due to the perturbations along the intertropical convergence zone (ITCZ) and to its latitudinal shift during the year.

The divergence observed over the tropics and middle latitudes is generated by the heating due to the surplus of the radiation existing in this extense region. It presents a maximum of the order of $0{,}17 \times 10^{3}$ watt/m² which is equivalent to a cooling rate of 1,5 degree/day. This export of enthalpy by the eddy circulations of the atmosphere plays a decisive role in the overall balance of heat and energy of the earth system as a whole, as well as of the atmosphere and of the oceans, since it prevents a continuous accumulation of heat in these regions.

The profiles relative to the divergence of stationary eddy fluxes $\overline{\text{div}\,\vec{S}^{*}}$ are in general much less intense than those due to the transient eddy transport. The values of $\overline{\text{div}\,\vec{S}^{*}}$ show alternating zones of divergence and of convergence. As the profiles show, there is slight convergence in the tropical, middle and subpolar latitudes and mean divergence in the high latitudes. It is noteworthy to point out the high values of the divergence in the high latitudes and the systematic convergence observed in the subpolar regions. As expected, these features are associated with the fluxes due to the predominance of the semi-permanent perturbations of the general circulation of the atmosphere, namely the tropical anticyclones and the semi-permanent lows in the high latitudes.

The profiles of the total eddy divergence $\overline{\text{div}\,\vec{S}_E}$ combined the divergence of both eddy components, as can be seen from the inspection of values of Table 1 and from the meridional curves in figures 7, 8 and 9.

In analysing the winter and summer values and in comparing them with the corresponding annual results, if we discount the larger values in the winter season, it is apparent the similarity of all the distribution. This is due to the homogeneity of the interface conditions in the Southern Hemisphere.

A comparison of the results just discussed, with those for the Northern Hemisphere, (Peixoto, 1967), shows by and large a good similarity. The Southern Hemisphere values are, as a rule, smaller than those in the Northern Hemisphere. This is particularly true when one considers the divergence of stationary eddy flux, which must be related to the difference in the geography, since the standing eddies are affected directly by the surface inhomogeneities.

As regards to the interannual and seasonal variations of the various modes of divergence of enthalpy, they are much less pronounced in the Southern Hemisphere than in the Northern Hemisphere, as expected.

5 — FINAL COMMENTS

a) In this study not all the modes of divergence of enthalpy were considered, namely those associated with the mean meridional circulations ($\text{div}\,\overline{\vec{S}}_M$). For the toroidal circulation the value of $\overline{S}_{M\Phi}$ is given by

$$\overline{S}_{M\Phi} = \frac{C_p}{g} \int [\overline{v}]\,[\overline{T}]\,dp$$

noting that by continuity considerations in the long term $\int [\overline{v}]\,dp = 0$.

The computation of $\overline{S}_{M\Phi}$ involves the evaluation of the mean meridional component of the wind $[\overline{v}]$ from the actual observations and the estimates of $[\overline{v}]$ involve a very high degree of uncertainty (the geostrophic winds at any isobaric level are such that: $[\overline{v}_{gs}] = 0$). It is expected that the divergence of enthalpy by the mean meridional

circulations becomes important in the tropics, mainly due to the effect of the Hadley cell.

It must be pointed out, however, that this form of divergence of enthalpy should not be taken independently from the equivalent divergence of potential energy because the meridional transports of both forms of energy by the toroidal circulations are intimately connected. In fact, the toroidal circulations are efficient in transporting enthalpy in the tropics toward the equator in the low levels and potential energy away from the equator in the upper levels leading to a relative net cooling near the equator and heating in the subtropical latitudes. Furthermore, it is well known that in an adiabatic atmosphere the mean meridional flux of enthalpy should be compensated exactly by a flux of potential energy in the opposite sense $[\overline{g\,dz + C_p\,dT}][\bar{v}] = 0$.

This point deserves further study.

b) It should be noted that in the present study only one part of the total flux of the global energy was treated, namely that associated with the enthalpy transport. In evaluating the heat balance by the dynamic method through the divergence of total energy fluxes as was mentioned, the enthalpy and the potential energy ($\Phi = g\,z$) transports must be taken together, simultaneously. The divergence of the flux of the kinetic energy can be neglected since it is very small when compared with the divergence of the other mentioned forms of energy.

Nevertheless the actual results already point out in the right direction. The heating or the cooling due to the convergence or to the divergence of enthalpy act in a sense opposite to the radiative heating as required by previous radiative studies (London, 1971). This is particularly true in the subtropical and intermediate latitude regions, where most of the divergence is due to the presence of transient eddies. It so happens that for this mechanism the influence of the potential energy is negligible, since the time and space covariances of T and v are much larger than those of Z and v, as it is known from synoptic experience. Therefore the divergence of the eddy flux of potential energy does not count for the heat balance. In the low and polar latitudes the situation may become somewhat different.

c) With the IGY homogeneous sets of data it was possible to elaborate a consistent study of the various forms of energy transports in the Southern Hemisphere. It is then possible to assess now the balance of energy, on a global scale, by the dynamic method, using the fluxes of potential energy, enthalpy and latent heat, combined with

the radiation data. This results from the consideration of condition (5) when applied to equation (1) in a steady regime. From scale analysis considerations it is obvious that $\{\dot{Q}_F\}$ can be disregarded in comparison with the others terms. This shows that the high latitude heating by flux convergence is compensated by net loss of heat, and the cooling in low latitudes by net gain of heat by the atmosphere through the following processes: (1) convergence, or divergence, of enthalpy flux in the atmosphere maintained by mean meridional or eddy circulations of permanent or intermitent kind, (2) net gain, or loss, of heat by radiation, (3) net gain, or loss, by conduction of sensible heat through the interface with the ocean and the solid ground, and (4) net gain of heat of condensation by the precipitation of rain or snow.

d) In discussing the energy balance of the earth, the oceans and the atmosphere must be taken as a single system, since both carry and store energy. The vectorial field $\vec{S}(\lambda, \Phi)$ must then be formed by the superposition of the oceanic and atmospheric transport fields $\vec{S}_0(\lambda, \Phi)$ and $\vec{S}_a(\lambda, \Phi)$, respectively:

$$\vec{S}(\lambda, \Phi) = \vec{S}_a(\lambda, \Phi) + \vec{S}_0(\lambda, \Phi).$$

Separate budgets for each subsystem, the atmosphere, or the oceans, can be determined when the exchange of energy across its interface is known.

The enthalpy balance for a polar cap south of Φ^o S which includes the atmosphere, the oceans and cryosphere can then be written symbolically, assuming that the change of energy storage can be disregarded as follows:

$$\operatorname{div} \vec{S}_a + \operatorname{div} \vec{S}_0 = \{\dot{Q}_R\} + \{\dot{Q}_L\} + \{\dot{Q}_C\}.$$

The values of the atmospheric flux $\vec{S}_a$ can be estimated rather accurately from the radiosonde network. On the contrary the transports by ocean currents $\vec{S}_0$ are not well known, since the available estimates are obtained indirectly.

Reliable estimates of the radiation flux $\{\dot{Q}_R\}$ have recently become available from satellite data (Von der Haar and Suomi, 1971).

The values of $\{\dot{Q}_L\}$ can also be estimated from aerological data, since for the system oceans-atmosphere

$$\{\dot{Q}_L\} = \{L \operatorname{div} \vec{Q}\} = L(E - P).$$

Where $\vec{Q}$ is the water vapour transport in the atmosphere, L the latent heat, E the evaporation and P the precipitation (Peixoto, 1972).

For this system $\{\dot{Q}_C\}$ need not to be considered. Thus, one obvious method of estimating the ocean enthalpy flux, is from previous equation as a residual. Robinson (1970) in a preliminary study of the heat flux by the oceans in the Southern Hemisphere came to the conclusion that it seems to be of the same order as the values of the atmospheric energy flux.

This point requires further study and should be investigated using a more homogeneous set of data now available for the Southern Hemisphere. Using the dynamic approach it will be possible to infer the role played by the oceans in the energy and heat balances and to compare them with previous estimates (Sellers, 1965; Emig 1967, Newton, 1972, etc.).

ACKNOWLEDGEMENTS

The author wishes to express his thanks to Prof. Victor P. Starr for many stimulating discussions of the various problems and to Prof. Reginald Newell for allowing the use of data for the Tropical General Circulation Project (AEC) and finally to Mrs. Rachel Morton and Lic. J. Corte Real for aiding the computations, to Miss Isabel Kole for drafting the figures, and to Mrs. Fernanda Dias for editorial assistance.

This study was supported by the «Instituto de Alta Cultura» through Project LF/2 and by the M. I. T. Department of Meteorology under the NSF grant GA — 36021.

REFERENCES

DAVIS, P. A., Analysis of the Atmospheric Heat Budget. *J. Atmos. Sci,* **20,** Boston, 1963.

EMIG, M., Heat transport by ocean currents. *J. Geophys. Res,* **72,** 2519-2529, 1967.

LONDON, J. and T. SASAMORI, Radiative energy budget of the atmosphere. *Space Research XI,* Berlim, Akademie-Verlag, 639-649, 1971.

NEWTON, C. W., Southern Hemisphere General Circulation in relation to global energy and momentum balance requirements in *Meteorology of the Southern Hemisphere*, Mete. Monographs, vol. 13, Boston, 1972.

OORT, A. H., The Observed Annual Cycle in the meridional transport of Atmospheric Energy. *J. Atmos. Sci.* **28**, Boston, 1971.

PEIXOTO, J. P., A divergência da Entalpia na Atmosfera (The divergence of enthalpy in the atmosphere). Publ. n.º 8, Geophysical Institute D. Luís (Univ. Lisbon), 1968.

PEIXOTO, J. P., Pole-to-Pole water balance for the IGY from aerological data. *Nordic Hydrology*, **3**, 22-43 Copenhagen, 1972.

PEIXOTO, J. P., Temperature Conditions in the Southern Hemisphere during the IGY. Publ. n.º 12, Geophysical Institute D. Luís (Univ. Lisbon), 1973.

PEIXOTO, J. P., Enthalpy Distribution in the Atmosphere over the Southern Hemisphere *Rivista Italiana Di Geofísica*, vol. XXIII, 3/4, Milano, 1974

PEIXOTO, J. P., On the Divergence of Enthalpy and the Energetics of the Atmosphere *Portug. Physica*, **9**, 41-58, 1974.

RASOOL, S. I. and C. PRABBAKARA, Heat budget of the Southern Hemisphere, reprinted from *Problems in Atmospheric Circulation*. Eds Garcia and Malone Washington D. C., 1966.

ROBINSON, I. B., Meridional Eddy flux of Enthalpy in the Southern Hemisphere during the IGY, *Pure and App. Geoph.*, vol. 80, 319-334, Basel, 1970.

RUBIN, M. J., Antarctic Weather and Climate, reprinted from *Research in Geophysics*, MIT Press Cambridge Mass, 1964.

RUBIN, M. J. and W. S. WEYANT, The mass and heat budget of the Antarctic Atmosphere. *Mont. Wea. Review*, 487-493, 1963.

SELLERS, W. D., Physical Climatology. The University of Chicago Press, 272 pp, Chicago, 1965.

VONDER HAAR, T. H. and V. E. SUOMI, Measurements of the earth's radiation budget from satellites during a five year period, *J. Atmos. Sci.*, **28**, 305-314, 1971.

THE DECAY OF SOME $^{27}Al(p,\gamma)^{28}Si$ RESONANCES (*)

J. D. Cunha, P. M. Corrêa and C. M. da Silva (**)
Laboratório de Física e Engenharia Nucleares, Sacavém, Portugal

ABSTRACT — The γ-decay of three $^{27}Al(p,\gamma)^{28}Si$ singlet resonances, at $E_p = 1262$, 1457 and 1587 keV, and three doublet resonances, at $E_p = 1363$, 1662 and 1962 keV, was studied with a 30 cm^3 Ge(Li) detector. The doublet character of the last three resonances was confirmed and the decay modes of both members were resolved.

Branching-ratios, total widths, energy spacings and relative intensities of the doublet members are reported. From the measured value of the width, a spin $J^\pi = 2^+$ is assigned to the lower member of the doublet at $E_p = 1662$ keV. Evidence was found for two new bound levels in the ^{28}Si nuclide, at $E_x = 10517 \pm 3$ and 9798 ± 3 keV. A possible broad resonance at $E_p \simeq 1970$ keV, with a width of $\simeq 20$ keV and decaying mainly via the α_1 channel is suggested.

1 — INTRODUCTION

The doublet resonances at $E_p = 1363$, 1662 and 1962 keV (†) were studied with Ge(Li) detectors by Meyer *et al.* [1] without resolving the decay modes of both members of each doublet. Nordhagen and Tveter [2] tentatively resolved the doublet at $E_p = 1363$ keV using a NaI(Tl) gamma spectrometer. Recent data by Tveter [3] indicate that the γ-decay of the doublet at $E_p = 1662$ keV is from the lower member only. Summaries of earlier work are found in these references and in Endt and van der Leun [4].

(*) Received 9 April, 1975.

(**) Present address: Universidade Nova de Lisboa, Lisboa, Portugal.

(†) Doublets are identified by the energy of the lower member, as measured in this work.

In the present work an attempt was made to separate the decay modes of the doublet members. The resonances at $E_p = 1262$, 1457 and 1587 keV were also studied in the light of some discrepancies noted in recent data on their gamma transitions.

Total widths were measured for all resonances mentioned above, together with the energy spacing of doublet members.

2 — EXPERIMENTAL PROCEDURE

The present experiment was performed with the proton beam of the LFEN 2 MeV Van de Graaff accelerator. Over a long run, the standard deviation of the beam energy distribution was typically 600 eV. The absolute beam energy was determined to within 2 keV, using an electrostatic voltmeter associated to a precision Wheatstone bridge, and this was considered sufficient for resonance identification. The targets, made from 99.999 % pure ^{27}Al evaporated onto thick gold backings, were water cooled and replaced as soon as any significant carbon deposition was observed. Beam currents between 2 and 6 μA were used.

In order to obtain resonance yield curves, a sinusoidal voltage (50 Hz) with a peak to peak amplitude up to 18 kV was applied to the target, thus modulating the proton energy ([5]). Every time a selected pulse was detected, a sample was drawn from the applied voltage and its amplitude analysed and stored. The yield curve of the channel corresponding to the selected pulses was automatically obtained, but a correction was needed to account for the non-linear time dependence of the applied voltage. (A small fraction ($\simeq 1$ keV) of the energy window was still disregarded at each end of the spectrum, to account for the strong local non-linearity.) This was made using a radioactive source to produce a random spectrum. This system is faster than the step by step method and more reliable since it is not affected by the errors in the energy and beam current measurements, is independent of target evaporation and provides a permanent check on carbon deposition. The calibration of the amplitude in energy units was made using the well known $^{27}Al(p,\gamma)^{28}Si$ doublet resonance at $E_p = 1381$ keV. The data for the $E_p = 1962$ keV doublet, however, had to be taken step by step over an energy range of about 30 keV.

Two gamma-ray detectors were used in the experiment. The singles spectra were taken with a 30 cm^3 Ge(Li) detector supplied by Ortec, with a FWHM resolution of 2.5 keV at $E_\gamma = 1$ MeV and 10 keV at $E_\gamma = 10$ MeV, which was placed at 55 degrees to the beam direction. To obtain the excitation functions, a 7.5 cm × 7.5 cm NaI(Tl) detector was generally used. However, for resonances decaying via a particle channel the Ge(Li) detector was used. In the case of the $E_p = 1662$ keV doublet the excitation function was measured also in the α_0-channel, using a silicon surface-barrier detector. Ortec spectroscopy amplifiers model 452 and a dual Northern Scientific 4096 channel ADC were used. Full gain stabilization was better than 2/4000 during data acquisition.

The relative efficiency of the Ge(Li) detector was measured in the energy range 1-13 MeV using a ^{56}Co source (6) and some resonances in the $^{27}Al(p,\gamma)^{28}Si$ and $^{23}Na(p,\gamma)^{24}Mg$ reactions (7).

The singles spectra were stored in a PDP-15 on-line computer in two buffers of 4096 channels each, one containing the full spectrum up to 14 MeV and the other gamma-rays up to 7 MeV.

The yield curves were generally stored in a routed DIDAC multichannel analyser, selecting the appropriate γ-rays in single-channel analysers. The particle (p_1, p_2 and α_1) and gamma channels were studied via the associated γ-rays at $E_\gamma = 847$, 1013, 1369 and $E_\gamma > 1500$ keV, respectively. In the case of the $E_p = 1662$ keV doublet, the PDP-15 computer was used and the single-channel analysers were replaced by digital windows placed on the γ-ray Ge(Li) spectrum. Background corrections were made, using the information from windows at left and right of the γ-ray of interest.

3. METHOD OF ANALYSIS

As it was impossible to populate separately the individual members, several measurements were made in each doublet, using different bombarding energies and targets of different thickness, thus allowing a change in the relative population of the doublet members. If there are N decay modes and M experiments, the branching-ratios can be obtained from a system of $NM + 2$ equations, provided that $M \geqq 2(N-1)/(N-2)$ (12). Three experiments were enough to resolve each doublet studied, since $N \geqq 4$ for all of them. The experimental

conditions were chosen in such a way that the resulting population ratios of the doublet members were sufficiently different to avoid ambiguities in the calculation of the system solution.

Using a non-linear least squares technique, experimental yield curves were fitted to an expression derived [12] under the assumptions of a gaussian beam energy spread [8], continuous energy loss [9] and negligible thermal vibrations. Since energy resolution tends to deteriorate in long runs, the corresponding parameter was adjustable in the fits, together with resonance widths and spacing.

The standard deviations of the resonance widths and doublet spacings were obtained using basically the method proposed by James *et al.* (ref. [10]; see also ref. [11]). Some changes had to be made and are described elsewhere [12].

4. RESULTS AND DISCUSSION

A typical γ-ray spectrum is shown in fig. 1. The γ-decay modes obtained for the singlets at $E_p = 1262$, 1457 and 1587 keV are in good agreement with previous work [1, 13, 14, 15], except for a few weak transitions as discussed below. The resonances at $E_p = 1363$, 1662 and 1962 keV exhibit a doublet character. In the present work the decay modes of these doublets were resolved as indicated in section 3. The observed γ-spectra show that some of the resonances decay by proton and or alpha emission. The relative (p,α_1), (p,p_1) and (p,p_2) strengths were estimated from the intensities of the 1.369, 0.847 and 1.013 MeV γ-rays from these reactions and from the total γ-ray intensity of the corresponding (p,γ) resonances. Corrections were made for the small contribution from the p_2 deexcitation channel to the 0.847 MeV γ-ray intensity.

The data obtaind for the γ-decay of the known bound levels populated in the present experiment are in good agreement with previous work [1, 13-16].

Excitation functions were obtained in the vicinity of all resonances as described in section 2, and the measured widths are shown in table 2.

The existence of transitions from the $E_p = 1262$ keV resonance to states at $E_x = 6.89$, 10.91 and 11.08 MeV, unsucessfully searched for by Meyer *et al.* [1], has been confirmed. However, the present

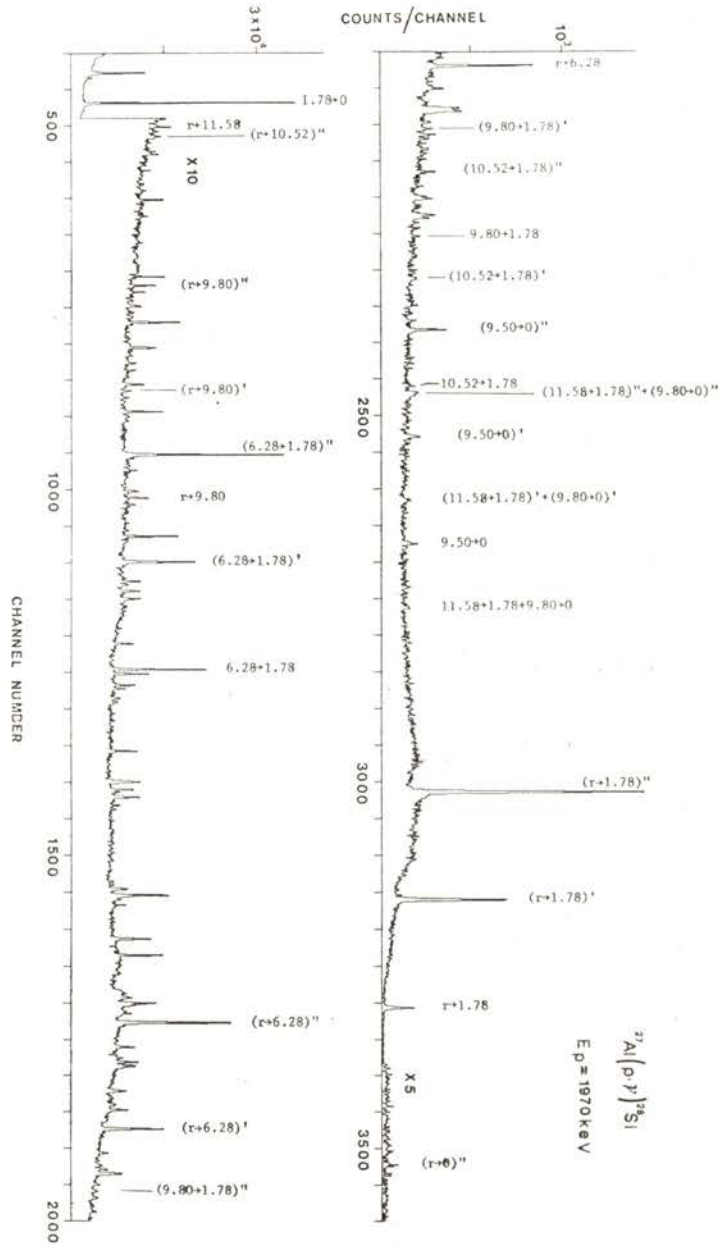

Fig. 1 — Gamma-ray spectrum taken at $E_p = 1970$ keV. The labelled peaks are those relevant to the discussion of section 4 and also some prominent lines used in the calibration procedure.

data do not support the presence of 0.5 % transitions to the levels at $E_x = 7.94$ and 9.42 MeV, reported respectively by Gibson *et al.* [13] and by Meyer *et al.* [1]; an upper limit of 0.3 % could be put on these branches. This resonance was seen to decay by α-emission to the first excited state of ^{24}Mg with a relative intensity $\Gamma_{\alpha_1}/\Gamma_\gamma$ of the order of 0.03.

The results obtained for the $E_p = 1457$ keV resonance are in good agreement with those of Forsblom [14], confirming [1] that the transition $r \rightarrow 1.78$ MeV is much weaker than reported by Gibson *et al.* [13]. This resonance was seen to decay via the p_1 channel with a relative intensity of $\Gamma_{p_1}/\Gamma_\gamma \simeq 0.14$, which is significantly greater than reported by Meyer *et al.* [1].

The present data for the singlet at $E_p = 1587$ keV are in quite good agreement with Meyer *et al.* [1], except for a 1 % transition $r \rightarrow 8.59$ MeV, seen in this work. Several weak transitions, reported by Gibson *et al.* [13], Forsblom [14] and Gonidec [15], were also not observed. The width of this resonance was measured to be 90^{+60}_{-30} eV.

4.1. *The $E_p = 1363$ keV doublet*

The lower member has an intensity in the γ-channel that is approximately twice that of the upper member, as can be inferred from the measured excitation function (fig. 3) and from the fitted populations to the observed γ-spectra at the three bombarding energies used. This observation contradicts clearly the suggestion by Nordhagen and Tveter [2] that the upper member would have a γ-strength 50 times smaller. The analysis shows that the γ-decay of both members is very similar (table 1) in contrast with the scheme suggested by Nordhagen and Tveter [2]. Several weak transitions are reported wich were not observed by those authors and by Meyer *et al.* [1]. A significant feature of this doublet is the strong α-decay of the upper member [2,3]. From the interpretation of the γ-spectra discussed above, we have measured a relative intensity $\Gamma_{\alpha_1}/\Gamma_\gamma \simeq 0.44$ for the upper member. A very weak proton decay was observed ($\Gamma_{p_1}/\Gamma_\gamma \simeq 0.007$), with an yield curve following that of the 1.369 MeV γ-ray and has been interpreted as due only to the upper member.

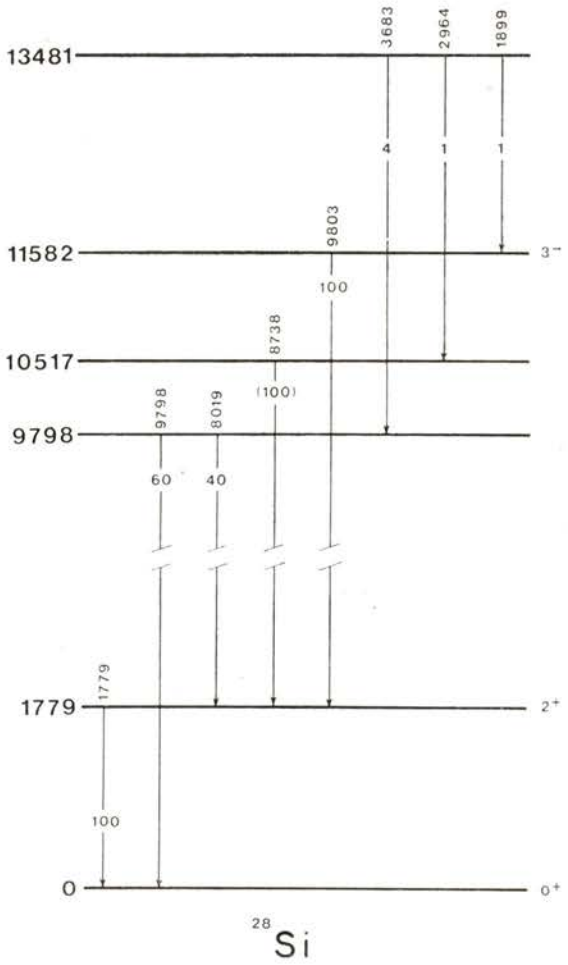

Fig. 2 — Partial level diagram for the γ-decay of the upper member of the $E_p = 1962$ keV doublet, showing the observed transitions involving new levels in ^{28}Si (see subsection 4.3).

4.2. *The $E_p = 1662$ keV doublet*

The γ-decay of this doublet was found to be essentially due to the lower member, while only the upper memper has p_1 and p_2-decays, in agreement with Tveter [3]. A very weak α_0-decay was observed for the lower member, confirming the result quoted by Tveter [3] and suggesting that this $T=1$ state must have a $T=0$ contamination. The measured branching-ratios for the γ-decay agree well with those given by Meyer *et al.* [1] for the unresolved doublet; however, a 0.4% transition to ground state was observed in this work. The total widths were measured to be 1700 ± 110 and 690 ± 60 eV, respectively for the lower and upper members. Tveter [3] studied the lower member by elastic proton scattering and obtained acceptable fits for the spins $J^\pi = 2^+$ or 3^+ with widths respectively 1650 ± 100 and 970 ± 100 eV. Thus, the width measured in this work allows a spin assignment $J^\pi = 2^+$ for this member.

4.3. *The $E_p = 1962$ keV doublet*

Excitation functions were measured in the region $E_p = 1949$ to 1978 keV for the p_1, p_2 (fig. 3), γ and α_1 channels. The yield curve for α_1-decay appears to originate mainly in a very wide resonance ($\Gamma \simeq 20$ keV) at a bombarding energy somewhat above the second member of the doublet. Unfortunately, it was not possible to extend the measurements any further. However, the present yield curve suggests that the lower member at $E_p = 1962$ keV also decays via the α_1-channel and this is compatible with the intensities of the 1369 keV γ-ray, observed at the three bombarding energies where γ-ray spectra were taken. The remaining channels do not show any evidence for the presence of the wide resonance and are compatible with a doublet having an energy spacing of 5.6 ± 0.5 keV. The lower member, at $E_p = 1962$ keV, has a width of 6.9 ± 0.6 keV and decays strongly via proton emission ($\Gamma_{p_1}/\Gamma_\gamma \simeq 75$ and $\Gamma_{p_2}/\Gamma_\gamma \simeq 60$); the upper one, at $E_p = 1967$ keV, has a width of 2180 ± 100 eV and relative proton intensities $\Gamma_{p_1}/\Gamma_\gamma \simeq 5$ and $\Gamma_{p_2}/\Gamma_\gamma \simeq 120$.

The γ-spectra were analysed in terms of the decay of the two members referred above, which were seen to have similar intensity. Several weak γ-transitions were seen, that were not reported by

TABLE 1. Gamma-decay of $^{27}Al(p,\gamma)^{28}Si$ résonances from spectra taken at 55°.

Final levels		E_p (keV)																											
E_x (MeV)	J^π a)	1262			1363		1365		Unr.	1457			1587				1662	1664	Unr.	1962	1967	Unres.	
		b)	c)	d)	b)	e)	b)	e)	c)	b)	c)	d)	b)	c)	d)	f)	b)	b)	c)	b)	b)	c)	d)
0	0^+				—	—	$5 \leqslant 30$		—								0.4		—	—	0.3	—	—
1.78	2^+	43	43	43	24	35	32	20	25	6	3	15	45	45	45	48	79		82	47	28	40	41
4.62	4^+	5	5	6	11	12	8	—	10	11	13	11	21	22	22	22				2	2	—	—
6.28	3^+	1	1	1.6	41	35	23	—	42	2	1	2	3	3	3.2	3.2	3		3	15	19	17	21
6.88	3^-	37	41	32						2	4	—	4	6	6	1.6				3	8	10	14
6.89	4^+	1	—	1.8	10	9	6	—	15				< 0.4	—	—	1.8							
7.38	2^+												8	9	7	7.2	4		5	1	5	4	4
7.42	2^+	6	6	7	—	—	2	—	—				3	2	1.7	1.6				—	5	5	4
7 80	3^+				5	—	4	—	—	8	9	8	< 0.3	—	1.0	1	3		2	3	—	—	—
7.94	2^+	$< 0\ 3$	—	0.5	—	—	1	—	—				< 0.2	—	—	0.5	3		2	5	4	4	2
8 26	2^+												2	1	1.6	1.5	2		1				
8.33	1^+																			—	3	1	—
8.41	4^-	2	2	1.8	—	—	1	—	—	5	5	3	4	3	2.4	2.6							
8.59	3^+				3	—	2	—	2	9	8	12	1	—	0 8	0.8				3	6	7	6
8.90	1^-				—	1.5	—	—	—														
8 94	$\pi =$ nat.				2	—	—	—	—														
9.16	$(2^+, 3^-, 4^+)$												4	3	3.4	2.9				—	< 0.5	—	4
9.32	3^+	1	0.5	1.3	3	5	6	—	3	56	57	49	< 0.4	—	0.9	—				11	3	3	< 3
9.38	2^+	2	1	0.7	1	—	10	50	3											7	—	2	—
9.42	$(2^+, 3^-, 4^+)$	< 0.3	0.5	—																			
9.50	$(1,2)^+$																6		5	1	4	4	—
9.76													< 0.2	—	—	0.3				1	1	—	—
(9.80)																				—	4	—	—
10.21	$(2^+, 3, 4^+)$												5	6	5	4.7				1	4	3	4
(10.52)																				—	3	—	—
10.54										1	—	< 0.5											
10.59	1^+				—	2.5	—	—	—														
10.91	$\pi =$ nat.	1	—	1.4																			
11.08		1	—	2.9																			
11.58	3^-																			—	1	—	—

This member of the doublet does not have any appreciable γ-decay

Branching-ratios given in %. Typical errors are of the order of 50 % of the value given for values less than 2, 20 % for values between 2 and 10 and 10 % for values greater than 10.

a) Ref. (4). b) Present work. c) Ref. (1). d) Ref. (13). e) Ref. (2). f) Ref. (14).

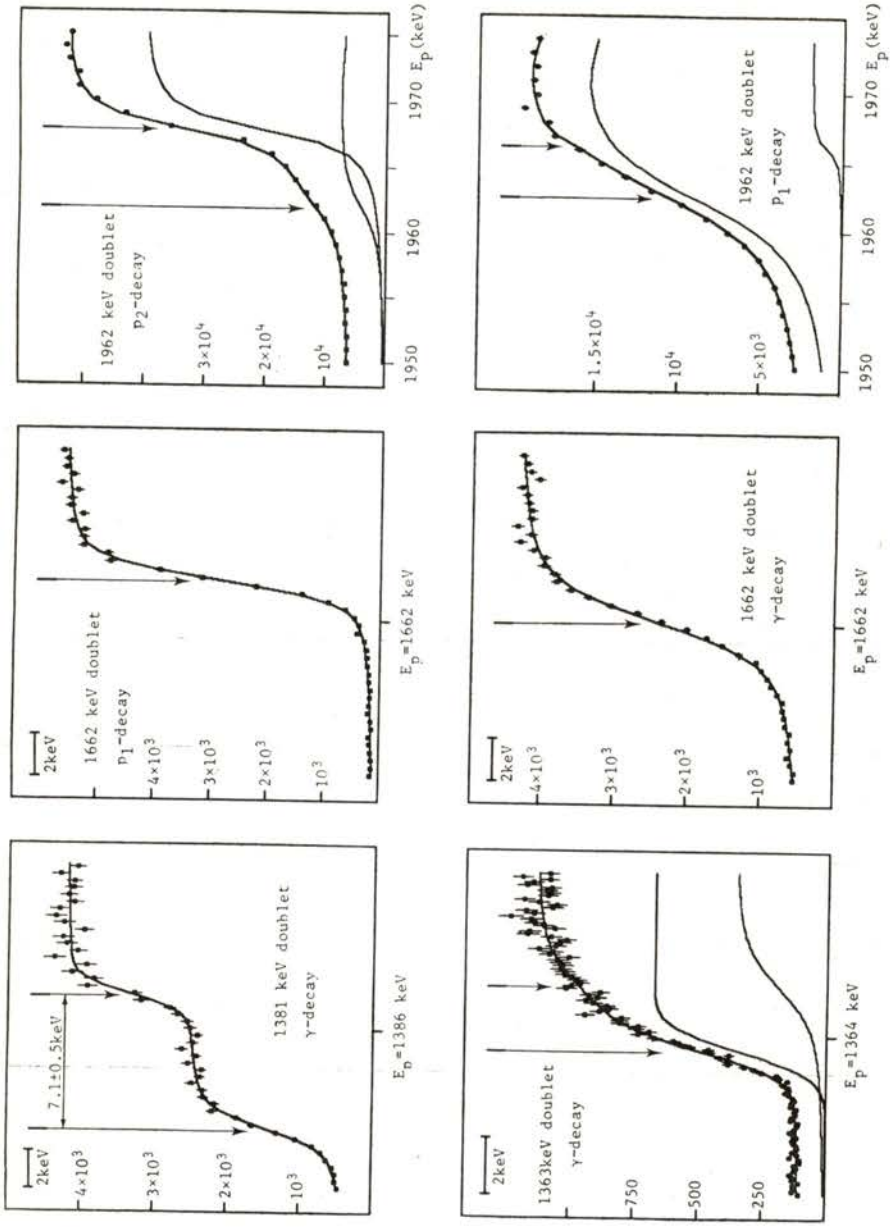

Fig. 3 — Excitation functions taken over the doublet resonances studied. The doublet at $E_p = 1381$ keV, used in the energy calibration of the modulator, is also shown. Experimental points are represented with error bars and the solid line is the best fit obtained, as explained in section 3. The shape of each doublet member, as found by the computer, is also drawn. The excitation functions labelled p_1-decay include a small contamination from the p_2-channel, as referred in the text.

TABLE 2. Resonance widths and energy gaps of doublet members

E_p (keV)	$J\pi$	Γ (eV) Present	Γ (eV) Previous	Energy gap (keV) Present	Energy gap (keV) Previous
Sing. 1262	3^- a)	<50 (γ ch.)	100±40 a)		
1363	(4⁺) a, b)	<100 (γ ch.)	70±40 a)		
Doub.					
1365	2^+ a, b, c)	1630±220 (γ ch.)	1100 a, b) 2000±500 a) 1400±200 c)	2.0±0.3	1.1±0.6 a)
Sing. 1457	3^- c)	2200±600 (γ ch.)	3000 d) 2000±100 c)		
Sing. 1587	$(2^+, 3^-, 4^+)$ e)	90^{+60}_{-30} (γ ch.)	<1000 a)		
1662	2^+ c, f)	1700±110 (γ ch.)	2000 d) 1650±100 c)		
Doub.			or 970±100 c)	1.67±0.15	1.8±0.9 c)
1664		690±60 (p_1, p_2 chs.)			
1962		6900±600 (p_1, p_2 chs.)	12000 d)		
Doub.				5.6±0.5	2 d)
1967		2180±100 (p_1, p_2 chs.)	<2000 d)		

a) Ref. (4). b) Ref. (2).
c) Ref. (3). d) Ref. (17).
e) Ref. (1). f) Present work.

Gibson *et al.* [15] and Meyer *et al.* [1]. A weak transition was observed to the level at $E_x = 11.58$ MeV which lies at the proton separation energy. This level had already been observed as an (α,γ) resonance by Smulders and Endt [18] and the present data support the previously indicated 100 % decay to the first excited state.

The observed intensity of the 9.803 MeV γ-ray is about three times that of the 1 % transition $r \rightarrow 11.582$ MeV and can not correspond only to the reported [18] 100 % decay of this level to the first excited state. The remaining is accounted for (fig. 2) assuming a previously unreported level at $E_x = 9798 \pm 3$ keV, decaying to the ground state and this is supported by the observation of the 4 % transition $r \rightarrow 9.798$ MeV, followed by the 9.798 MeV → g. s. transition referred above and by the clear transition 9.798 MeV → 1.779 MeV. The intensities of the γ-rays involved agree quite well.

Two other γ-rays are seen in the spectrum, which can not be explained by transitions between known levels. Their energies together with that of the first excited state sum quite well to the energy of the upper member, at $E_p = 1967$ keV. Also the observed intensities are of the same magnitude and this suggests the presence of a new level at $E_x = 10517 \pm 3$ keV.

We wish to express our special gratitude to Mr. L. A. Cunha for his assistance during the experiment and in the analysis of single spectra.

REFERENCES

(1) M. A. MEYER, N. S. WOLMARANS and D. REITMAN, *Nucl. Phys.* A**144**, 261 (1970).

(2) R. NORDHAGEN and A. TVETER, *Nucl. Phys.* **56**, 337 (1964).

(3) A. TVETER, *Nucl. Phys.* A**185**, 433 (1972).

(4) P. M. ENDT and C. VAN DER LEUN, *Nucl. Phys.* A**214**, 194 (1973).

(5) L. CRANBERG *et al.*, *The Rev. of Scient. Instr.* **28**, 84 (1957).

(6) D. C. CAMP and G. L. MEREDITH, *Nucl. Phys.* A**166**, 349 (1971).

(7) B. P. SINGH and H. C. EVANS, *Nucl. Instr. and Meth.* **97**, 475 (1971).

(8) A. W. BORGI and O. LÖNSJÖ, *Nucl. Instr. and Meth.* **17**, 31 (1962).

(9) J. M. DONHOWE *et al.*, *Nucl. Phys.* A**102**, 383 (1967); W. G. MOURAD, K. E. NIELSEN and M. PETRILAK JR., *Nucl. Phys.* A**102**, 406 (1967).

(10) A. N. JAMES, P. J. TWIN and P. A. BUTLER, *Nucl. Instr. and Meth.* **115**, 105 (1974).

(11) W. C. HAMILTON, *Statistics in Physical Science*, (New York: The Ronald Press Company, 1964), ch. 4.

(12) P. M. CORRÊA and J. D. CUNHA, *L. F. E. N. Report* (1975), to be published.

(13) E. F. GIBSON, K. BATTLESON and D. K. MCDANIELS, *Phys. Rev.* **172**, 1004 (1968).

(14) I. FORSBLOM, *Comment. Phys. Math.* **40**, 65 (1970).

(15) J. P. GONIDEC, *Thesis* (1972), Louis Pasteur University, Strasbourg.

(16) M. A. MEYER and N. S. WOLMARANS, *Nucl. Phys.* A **136**, 663 (1969).

(17) P. B. LYONS, J. W. TOEVS and D. G. SARGOOD, *Nucl. Phys.* A **130**, 1 (1969).

(18) P. J. M. SMULDERS and P. M. ENDT, *Physica* **28**, 1093 (1962).

INTERFERENCE EFFECTS IN HEAVY ION ELASTIC AND INELASTIC SCATTERING (*)

R. DA SILVEIRA

Institut de Physique Nucléaire
Division de Physique Théorique (**)
91406 — Orsay — France

and

CH. LECLERCQ-WILLAIN (***)

Université Libre de Bruxelles
Physique Nucléaire Théorique
1050 — Bruxelles — Belgique

ABSTRACT — The semi-classical theory is used to describe the different oscillatory behaviours observed in the elastic and inelastic heavy ion scattering cross-sections at incident energies near and above the Coulomb barrier. The theory predicts two different phases rules which are well observed in the analyzed data: elastic and inelastic scattering cross-sections of ^{11}B on ^{208}Pb at EL = 72.2 MeV and of ^{12}C on ^{27}Al at EL = 46.5 MeV.

1 — INTRODUCTION

In heavy ion reactions, the structure of the elastic and inelastic scattering cross-sections strongly depends on the scattering angle region and on the incident energy. At energies below or just near the Coulomb barrier, the nuclear potential can be treated as a small perturbation to the Coulomb one and the classical deflection function is nearly of Coulomb form. The agreement of semi-classical theory to describe such process is well known [1]-[5] [17].

(*) Received 14 April, 1975.
(**) Laboratoire associé au C. N. R. S.
(***) Maître de Recherches au F. N. R. S.

At higher energies [6]-[9] (above the Coulomb barrier), there exist a scattering angle θ_r close to the angle of grazing collision for which the deflection function is stationary. On one side $\theta > \theta_r$ the elastic and inelastic scattering cross-sections drop rapidly to very low values, on the other side $\theta < \theta_r$ they present «out of phase» oscillations irrespective of the parity of the transition [14] [16].

In the lit region $\theta < \theta_r$ the observed phase rule results from the quantal interference effect between two classical trajectories which contribute to the cross-sections at each scattering angle, and to the fact that the one, with high impact parameter is mainly described by the Coulomb forces whereas the other, with low impact parameter is mainly described by the nuclear forces. The contribution of the negative branch of the deflection function can be neglected (Section 2. 2).

In the dark region $\theta > \theta_r$ the scattering is essentially described by the rainbow process and drops exponentially to very low values. When the incident energy increases [15], the elastic and inelastic cross-sections present in the lit region the previously mentioned «out of phase» oscillations structure. On the dark side of θ_r, the fall-off is corrected by oscillations. This oscillations structure observed for $\theta > \theta_r$ can be interpreted as the interference between the rainbow scattering (decreasing fastly) and that defined by the negative branch of the classical deflection function whose relative contribution increases with the incident energy (Section 2. 3). In the inelastic cross-sections, the theory predicts oscillations which are «in phase», or «out of phase» with the elastic one according as the transition is even or odd. This result his exactly the inverse of the well-known Blair phase rule [26].

The forms of the ion-ion potentials and the resulting classical deflection functions are discussed in Section 3. The theory outlined in Section 2 is used to describe:

- the elastic scattering and inelastic 3^- (2.61 MeV), 5^- (3.20 MeV), 2^+ (4.10 MeV) and 4^+ (4.31 MeV) transitions in ^{208}Pb in the collision with ^{11}B at laboratory incident energy of 72.2 MeV
- the elastic scattering and inelastic 2^+ (4.43 MeV) transition in ^{12}C in the collision of ^{12}C on ^{27}Al at laboratory energy of 46.5 MeV.

The experimental data [9] [15] and the theoretical results are presented in Section 4.

2 — INELASTIC SCATTERING

2. 1. *Outline of the theory*

The semi-classical formulation of the inelastic cross-section is developed by use of mathematical approximations analogous to those defined in the description of the elastic scattering [10]-[13].

In order to discuss correctly the approach to the classical limit, it is most expedient to start from the scattering amplitude in the form usually defined in quantum theory for a central interaction [16].

$$\frac{d\sigma}{d\Omega} = \frac{\mu_i \mu_f}{(2\pi\hbar^2)^2} \frac{k_f}{k_i} \frac{2I_f+1}{2I_i+1} \sum_{L\,M} \delta(l, I_i, I_f) \frac{|\beta_{L\,M}|^2}{2L+1} \qquad (2.1)$$

$$\beta_{L\,M} = (4\pi)^2 \sum_s \sum_{l_i m_i} \sum_{l_f m_f} i^{l_i + l_f - l} Y^*_{l_i m_i}(\hat{k}_i)\, Y^*_{l_f m_f}(-\hat{k}_f)$$

$$\exp\left(i(\eta_{l_i} + \eta_{l_f})\right) < l_i\, m_i\, l_f\, m_f \mid L\, M > < l_i \circ l_f \circ \mid L \circ >$$

$$\frac{\hat{l}_i\, \hat{l}_f}{(4\pi)^{1/2}\, \hat{L}} A^s_L\, I^s_{l_i l_f}(L) \qquad (2.2)$$

where

$$I^s_{l_i l_f}(L) = \frac{1}{k_i k_f} \int_0^\infty dr\, u_{l_i}(k_i r)\, u_{l_f}(k_f r)\, F^s_L(r)\,. \qquad (2.3)$$

For the incoming waves $u_{l_i, l_f}(kr)$, we assume the form defined outside the nuclear region

$$u^-_l(kr) = \cos\delta_l\, F_l(kr) + \sin\delta_l\, G^-_l(kr) \qquad (2.4)$$

where F_l, G_l are the regular and irregular Coulomb wave functions and δ_l is the nuclear phase shift of the l-partial wave.

In (2. 2) and (2. 3), L defines the multipolarity of the transition, A^s_L and F^s_L are respectively the spectroscopic factor and the form factor of the Coulomb or nuclear excitation forces used to describe the interaction of the ions. Their explicit forms are defined in the framework of a collective model (vibrational or rotational) of the target

nucleus [1] [16]. In (2. 1), (2. 2), (2. 3), μ_{if}, k_{if}, η_{if} are respectively the reduced masses, the wave numbers and the total (Coulomb + nuclear) phase shifts in the incomming (i) and outgoing (f) channels.

In near classical conditions, many partial waves contribute to the sum in (2. 2) and we may introduce some approximations. We take the variables (L, M) fixed and let the angular momentum l_i, l_f become infinite with the difference $\mu = l_f - l_i$ finite. The classical limit of the radial integrals (2. 3) have already been discussed [17]

$$I^s_{l_i, l_f}(L) \sim \frac{1}{2k^2} a \cos(\delta_{l_i} - \delta_{l_f}) \int_{-\infty}^{+\infty} dw \exp(i\xi(\varepsilon \sin h w + w))$$

$$\frac{(\varepsilon + \cos h w + i \sin h w (\varepsilon^2 - 1)^{1/2})^{\mu}}{(\varepsilon \cos h w + 1)^{\mu - 1}} F^s_L(r(w))$$

$$= I^s(l, \mu, L). \tag{2. 5}$$

The use of the variable «w» is the usual parametrization defined for the radial variable in semi-classical Coulomb theory

$$r = a(\varepsilon \cos h w + 1) \tag{2. 6}$$

where $a = \eta^c / k$ for the Coulomb trajectory.

η^c is the Sommerfeld number and

$$\varepsilon = \frac{(\eta_c^2 + (l + 1/2)^2)^{1/2}}{\eta^c}. \tag{2. 7}$$

In order to improve the semi-classical results, we use some average values between the initial and final ones for η^c, k and l:

$$\eta^c = (\eta_i^c \eta_f^c)^{1/2} \quad k = (k_i k_f)^{1/2} \quad l = \frac{l_i + l_f}{2} \tag{2. 8}$$

To proceed further, we replace the sums $\sum_{l_i} \sum_{l_f}$ by $\sum_{\mu} \int_0^{\infty} dl$ and we require the asymptotic forms for the spherical harmonics, the total phase shift and the Wigner coefficients [18]

$$Y_{lm}(\theta, \varphi) \sim \frac{1}{\pi} e^{im\varphi} \frac{1}{(\sin\theta)^{1/2}} \cos\left((l + 1/2)\theta + (m - 1/2)\frac{\pi}{2}\right)$$

valid for

$$\frac{1}{l} \leqq \theta \leqq \pi - \frac{1}{l}$$

$$\eta_{l_i, l_f} \sim \overset{\text{W. K. B}}{\eta}(l) = \frac{1}{\hbar}\left(\frac{\pi}{2}\hbar(l+1/2) - \int_{r_m}^{\infty} dr\, r\, d_r \mathrm{F}^{1/2}(r)\right)$$

where

$$\mathrm{F}(r) = 2m\left(\mathrm{E} - v(r) - \frac{\hbar^2(l+1/2)^2}{r^2}\right)$$

$$<l_i o l_f \mathrm{M} \mid \mathrm{L}\,\mathrm{M}> \sim (-)^{l_i + \mathrm{L} + \mathrm{M}} \left(\frac{2\,\mathrm{L}+1}{2\,l_f+1}\right)^{1/2} \mathrm{D}^{\mathrm{L}}_{l_f - l_i, \mathrm{M}}\left(0, \frac{\pi}{2}, 0\right). \quad (2.9)$$

The classical expression of the scattering coefficient (2. 2) is:

$$\beta^{c}_{\mathrm{L}\,\mathrm{M}} = 4 \sum_{s} \sum_{\mu} \frac{(4\pi)^{1/2}}{2\,\mathrm{L}+1} \frac{i^{-\mathrm{L}}}{(\sin\theta)^{1/2}} \mathrm{Y}_{\mathrm{L}\,\mu}\left(\frac{\pi}{2}, 0\right) d^{\mathrm{L}}_{\mathrm{M}, -\mu}(\pi/2)$$

$$e^{-i\,\mathrm{M}(\varphi+\pi)}\, e^{i\mu\frac{\pi}{2}}\, \mathrm{A}^{s}_{\mathrm{L}}(\mathrm{I}^{+}_{\mathrm{L}\,\mu\,s} + \mathrm{I}^{-}_{\mathrm{L}\,\mu\,s}) \quad (2.10)$$

where

$$\mathrm{I}^{\pm}_{\mathrm{L}\,\mu\,s} = \frac{1}{\sqrt{2}} e^{\pm i\frac{\pi}{4}}\, e^{\mp i\,\mathrm{M}\frac{\pi}{2}} \int d\,l\, \mathrm{I}^{s}(\mathrm{L}, \mu, l)\, l^{1/2}\, e^{i(2\eta(l) \mp l\theta)} \quad (2.11)$$

To obtain an accurate evaluation of the semi-classical expression (2. 10) we must examinate the various approximations available to evaluate the integrals $\mathrm{I}^{\pm}_{\mathrm{L}\,\mu\,s}$ (2. 11). The classical deflection functions $\Theta(l)$ we consider to describe heavy ions collision will be explicitly defined in Section 3.

2. 2. *Analysis in the lit region of* ϑ_r

In the lit region $\theta < \theta_r$, the most important contributions to the scattering come from Coulomb and nuclear surface trajectories defined by $\theta = +\Theta(l)$. So, in (2, 10), we only retain the $\mathrm{I}^{+}_{\mathrm{L}\,\mu\,s}$ terms. In

order to calculate the amplitude integral (2. 11), let us define the new variable [12]:

$$\varphi^{+}(l) = 2\eta(l) - l\theta = \xi(\theta)\, x + \frac{x^3}{3} + \mathrm{A}(\theta) \qquad (2.\ 12)$$

such that

$$\mathrm{I}^{+}_{\mathrm{L}\,\mu\,s} = e^{-i\mathrm{M}\frac{\pi}{2} + i\frac{\pi}{4}}\, e^{i\,\mathrm{A}(\theta)}$$

$$\frac{1}{\sqrt{2}} \int_0^{\infty} \lambda^{1/2}(x)\, \frac{d\lambda(x)}{dx}\, \mathrm{I}^{s}(\mathrm{L}, \mu, \lambda(x))\, e^{i(\xi(\theta)x + x^3/3)}\, dx\,. \qquad (2.\ 13)$$

Only the stationary points regions at $x = \pm i\xi^{1/2}(\theta)$ are considered to contribute to the integral, and we stipulate the correspondence to be

$$\begin{aligned} l = l_1 &\longleftrightarrow x = -i\xi^{1/2}(\theta) \\ l = l_2 &\longleftrightarrow x = +i\xi^{1/2}(\theta) \end{aligned} \qquad (2.\ 14)$$

When alternatively inserted in (2. 12), these relations yield the values of $\mathrm{A}(\theta)$ and $\xi(\theta)$. For $\theta < \theta_r$, l_1 and l_2 are real values and $\xi(\theta)$ will be real and negative: $\xi(\theta) = -|\xi(\theta)|$. In order to evaluate (2. 13) we introduce the serie:

$$\lambda^{1/2}(x)\, \frac{d\lambda(x)}{dx}\, \mathrm{I}^{s}(\mathrm{L}\,\mu\,\lambda(x)) = \sum_{m=0}^{\infty} (x^2 + \xi(\theta))^m\, (p_m + q_m x)\,. \qquad (2.\ 15)$$

The stationary phase approximation in (2. 13) defined for $\xi(\theta) + x^2 = 0$, corresponds to the lowest order $m = 0$ approximation (2. 15). Using the relations (2. 14), p_0 and q_0 are defined by

$$p_0 = \frac{1}{2}(i_1 + i_2) \qquad q_0 = \frac{1}{2\, i\, \xi^{1/2}}(i_2 - i_1) \qquad (2.\ 16)$$

with

$$i_{\substack{1\\2}} = \lambda_1^{1/2} \left[\frac{2\, i\, \xi^{1/2}}{|\Theta'(l)|_{l_{1,2}}} \right]^{1/2} \mathrm{I}^{s}(\mathrm{L}\,\mu\,\lambda_{\substack{1\\2}})\,. \qquad (2.\ 17)$$

In these expressions (2. 17) the derivative is supposed to be negative for $l = l_1$ and positive for $l = l_2$ (Fig. 1-2). By inserting (2. 15)-

(2. 17) into (2. 13) and integrating, the inelastic scattering integral is approximated by:

$$I^{+}_{L\mu s} = \pi\, e^{-iM\frac{\pi}{2}+i\frac{\pi}{4}}\, e^{iA(0)}\,.$$

$$\left\{(-\xi)^{1/4}\,A\,i\,(\xi)\left[\left(\frac{l_1+1/2}{|\Theta'(l)|_{l_1}}\right)^{1/2} I^{s}(L\,\mu\,l_1)+\left(\frac{l_2+1/2}{|\Theta'(l)|_{l_2}}\right)^{1/2} I^{s}(L\,\mu\,l_2)\right]\right.$$

$$\left.-\frac{i}{(-\xi)^{1/4}}\,A'i(\xi)\left[\left(\frac{l_2+1/2}{|\Theta'(l)|_{l_2}}\right)^{1/2} I^{s}_{(L,\mu,l_2)}-\left(\frac{l_1+1/2}{|\Theta'(l)|_{l_1}}\right)^{1/2} I^{s}_{(L,\mu,l_1)}\right]\right\} \quad (2.\ 18)$$

It we describe the excitation of a vibrational even-even nucleus from its fondamental 0^+ to a state $I^{(-)^I}$, the expression for the cross-sections is:

$$\frac{d\sigma^{0,I}}{d\Omega} = \eta^{c^2}\,\pi\,(1-\tau)^{1/2}\sum_{\mu}\left|Y_{I\mu}\left(\frac{\pi}{2},0\right)\right|^2 \cdot$$

$$|\xi|^{1/2}\,A^2\,i\,(-|\xi|)\cdot[\sigma^{c}_{(1)}\,|\,a_{0I,\mu}(l_1)\,|^2+\sigma^{c}_{(2)}\,|\,a_{0I,\mu}(l_2)\,|^2$$

$$+(\sigma^{c}_{(1)}\,\sigma^{c}_{(2)})^{1/2}\,(a_{0I,\mu}(l_1)\,a^{*}_{0I,\mu}(l_2)+a^{*}_{0I,\mu}(l_1)\,a_{0I,\mu}(l_2))]$$

$$+\frac{1}{|\xi|^{1/2}}\,A'^{2}\,i\,(-|\xi|)\cdot[\sigma^{c}_{(1)}\,|\,a_{0I,\mu}(l_1)\,|^2+\sigma^{c}_{(2)}\,|\,a_{0I,\mu}(l_2)\,|^2$$

$$-(\sigma^{c}_{(1)}\,\sigma^{c}_{(2)})^{1/2}\,(a_{0I,\mu}(l_1)\,a^{*}_{0I,\mu}(l_2)+a^{*}_{0I,\mu}(l_1)\,a_{0I,\mu}(l_2)]$$

$$+2\,i\,A\,i\,(-|\xi|)\,A'i\,(-|\xi|)\,(\sigma^{c}_{(1)}\,\sigma^{c}_{(2)})^{1/2}$$

$$\cdot[a_{0I,\mu}(l_1)\,a^{*}_{0I,\mu}(l_2)-a^{*}_{0I,\mu}(l_1)\,a_{0I,\mu}(l_2)]\}\qquad (2.\ 19)$$

with

$$|\xi| = \left[\frac{3}{4}\,\partial(\theta)\right]^{2/3} \qquad (2.\ 20)$$

$\sigma^{c}_{(i)}$ and $\partial(\theta)$ are respectively the classical elastic cross-section and the phase difference [10]-[13]

$$\sigma^{c}_{(i)} = \frac{l_i+1/2}{k^2\sin\theta\,|\,\Theta'(l)\,|_{l_i}} \qquad (2.\ 21)$$

$$\delta(\theta) = \int_{l_2(\theta)}^{l_1(\theta)} |(\Theta)(l) - \theta| \, dl = 2\eta(l_1) - l_1\theta - 2\eta(l_2) + l_2\theta \,. \qquad (2.\ 22)$$

The coefficient $(1-\tau)^{1/2}$ where $\tau = \dfrac{\Delta E_{0,I}(A_T + A_P)}{A_T \cdot E_L}$ results from the use of the symmetrized form (2. 8) for the impulse parameter k.

The inelastic amplitudes $a_{0I,\mu}(l_i)$ have been explicitly defined in references [1] [16].

Far from θ_r ($\theta \ll \theta_r$), $|\xi(\theta)|$ is large; the Airy functions and their derivatives may be replaced by their asymptotic expressions [19] and (2. 19) reduces to the form

$$\frac{d\sigma^{0I}}{d\Omega} = \eta^{c^2}(1-\tau)^{1/2} \sum_{\mu} |Y_{I\mu}\left(\frac{\pi}{2}, 0\right)^2 \cdot$$

$$\{\sigma^c_{(1)} |a_{0I,\mu}(l_1)|^2 + \sigma^c_{(2)} |a_{0I,\mu}(l_2)|^2$$

$$+ \sin\delta\,(\sigma^c_{(1)}\sigma^c_{(2)})^{1/2}[a_{0I,\mu}(l_1)\, a^*_{0I,\mu}(l_2) + a^*_{0I,\mu}(l_1)\, a_{0I,\mu}(l_2)]$$

$$- i\cos\delta\,(\sigma^c_{(1)}\sigma^c_{(2)})^{1/2}[a_{0I,\mu}(l_1)\, a^*_{0I,\mu}(l_2) - a^*_{0I,\mu}(l_1)\, a_{0I,\mu}(l_2)]\} \,. \qquad (2.\ 23)$$

This expression is exactly the form deduced when evaluating the inelastic integral (2. 11) by the method of stationary phase [14] [16].

At each scattering angle, the contributions of the two branchs of the deflection function (Figs. 1-2) are required; branch (1) is essentially defined by the Coulomb interaction, branch (2) by the nuclear one. The inelastic amplitudes being of opposite signs on these two branchs, the interference terms in the expressions of the elastic [16] and inelastic scattering cross-sections (2. 23) have opposite signs. So, these expressions reproduce quite well the out of phase rule observed for $\theta < \theta_r$ in the experimental results (Section 4) and its independence on the parity of the transition.

2. 3. *Analysis of the dark region of* θ_r

In the dark side of θ_r, the structure of the elastic and inelastic scattering cross-sections strongly depends on the incident energy. In experiments performed at energies about 1. 5 times the Coulomb barrier [6]-[9], the elastic and inelastic scattering drop rapidly to very low values [10]-[13]. The scattering cross-section is derived from the

same formulation (2. 19) with complex conjugate values of l_1, l_2 and of $\Theta'(l_1)$, $\Theta'(l_2)$. Near θ_r, l_1 and l_2 are both nearly real and equal to the rainbow l value l_r. So, using this value and the cubic approximation of $\eta(l)$ near $l = l_r$ [10], (2. 11) reduces to the Airy approximation:

$$I^{+(r)}_{L\mu s} = e^{-i M \frac{\pi}{2}} e^{i\frac{\pi}{4}} e^{i(2\eta(l_r) - \theta l_r)} \sqrt{2}\,\pi\, l_r^{1/2}$$

$$q^{-1/3}\, A\, i(q^{-1/3}(\theta - \theta_r))\, I^s(l_r\, \mu\, L) \qquad (2.\ 24)$$

The rainbow scattering being the main process, the rapid fall-off of the elastic and inelastic cross-sections in the dark region is described by the behaviour of the Airy function for $\theta > \theta_r$. The inelastic cross-section for $\theta > \theta_r$ can be defined by the expression:

$$\frac{d\sigma^{I_i, I_f}}{d\Omega} = \frac{a^2(1-\tau)^{1/2}}{\sin\theta}\, \frac{2I_f + 1}{2I_i + 1}\, 2\pi\, l_r\, q^{-2/3}\, A^2\, i(q^{-1/3}(\theta - \theta_r))$$

$$\sum_{\mu} \left| Y_{L\mu}\left(\frac{\pi}{2}, 0\right)\right|^2 |\, a_{L\mu}(l_r)\,|^2\, \frac{\partial(l\, I_i\, I_f)}{2L + 1} \qquad (2.\ 25)$$

At higher incident energies [15] — about 2. 7 times the Coulomb barrier —, one observes well defined oscillations in the elastic and inelastic cross-sections. In this case, the contribution of the negative branch of the deflection function (Fig. 2) is no more negligibly small in front of the rainbow amplitude. So, in (2. 10) we have:

$$I^{+}_{L\mu s} + I^{-}_{L\mu s} \cong I^{+(r)}_{L\mu s} + I^{-}_{L\mu s}(l_3) \qquad (2.\ 26)$$

where $I^{+(r)}_{L\mu s}$ is the rainbow amplitude defined in (2. 24) and $I^{-}_{L\mu s}(l_3)$, defined with the stationary phase approximation, is

$$I^{-}_{L\mu s}(l_3) = e^{i M \frac{\pi}{2}} e^{-i\frac{\pi}{4}} \left[\frac{\pi\, l_3}{|\,\Theta'(l)\,|_{l_3}}\right]^{1/2} e^{i\left(2\eta(l_3) + \theta l_3 + \frac{\pi}{4}\right)}$$

$$\cdot\, I^s(l_3, \mu, L)\,. \qquad (2.\ 27)$$

With the scattering integrals (2. 26) and the approximations (2. 24) and

(2. 27), the explicit expression of the scattering amplitude (2. 10) is:

$$\beta^{c}_{\mathrm{L\,M}}(\theta > \theta_r) = 4 \sum_{s} \frac{\sqrt{4\pi}}{2\,\mathrm{L}+1} \frac{i^{-\mathrm{L}+1}}{(\sin\theta)^{1/2}} e^{-i\,\mathrm{M}\left(\varphi + \frac{3\pi}{2}\right)} \cdot \mathrm{A}^{s}_{\mathrm{L}}$$

$$\sum_{\mu} \mathrm{Y}_{\mathrm{L}\,\mu}\left(\frac{\pi}{2}, 0\right) d^{\mathrm{L}}_{\mathrm{M},-\mu}\left(\frac{\pi}{2}\right) e^{i\,\mu\,\frac{\pi}{2}} \cdot (a_r\, e^{i\,\delta_r} - (-)^{\mathrm{M}}\, a_3\, e^{i\,\delta_3}) \qquad (2.\ 28)$$

where we define:

$$a_r = 2\,\pi\, l_r^{1/2}\, q^{-1/3}\, \mathrm{A}\, i\,(q^{-1/3}(\theta - \theta_r))\, \mathrm{I}^{s}_{\mathrm{L}\,\mu}(l_r)$$

$$a_3 = \left[\frac{2\,\pi\, l_3}{|\,\Theta'(l)\,|_{l_3}}\right]^{1/2} \mathrm{I}^{s}_{\mathrm{L}\,\mu}(l_3)$$

$$\delta_r = 2\,\eta(l_r) - \theta\, l_r - \frac{\pi}{4}$$

$$\delta_3 = 2\,\eta(l_3) + \theta\, l_3 - \frac{\pi}{2}. \qquad (2.\ 29)$$

In this case, the inelastic cross-section for $\theta > \theta_r$ will be given by the approximated form:

$$\frac{d\,\sigma^{\mathrm{I}_i \mathrm{I}_f}}{d\,\Omega} = \frac{a^2\,(1-\tau)^{1/2}}{\sin\theta} \frac{2\,\mathrm{I}_f + 1}{2\,\mathrm{I}_i + 1} \sum_{\mathrm{L}} \delta\,(\mathrm{L}\,\mathrm{I}_i\,\mathrm{I}_f) \frac{\mathrm{A}^2_{\mathrm{L}}}{2\,\mathrm{L}+1}$$

$$\sum_{\mu} \left| \mathrm{Y}_{\mathrm{L}\,\mu}\left(\frac{\pi}{2}, 0\right) \right|^2 \cdot \{2\,\pi\, l_r\, q^{-2/3}\, \mathrm{A}^2\, i\,(q^{-1/3}(\theta - \theta_r))\,|\,\mathrm{I}_{\mathrm{L}\,\mu}(l_r)\,|^2$$

$$+ \frac{l_3}{|\,\Theta'(l)\,|_{l_3}}\,|\,\mathrm{I}_{\mathrm{L}\,\mu}(l_3)\,|^2$$

$$- 2\,(-)^{\mathrm{L}} \cos(\delta_r - \delta_3) \left[\frac{2\,\pi\, l_r\, l_3}{|\,\Theta'(l)\,|_{l_3}}\right]^{1/2} q^{-1/3}\, \mathrm{A}\, i\,(q^{-1/3}(\theta - \theta_r))$$

$$\cdot\, \mathrm{I}_{\mathrm{L}\,\mu}(l_3)\, \mathrm{I}_{\mathrm{L}\,\mu}(l_r)\}. \qquad (2.\ 30)$$

For $\theta > \theta_r$, the oscillations observed in the elastic and inelastic scattering cross-sections can be described by the quantal interference effects of the rainbow scattering at each angle θ with the semi-

classical scattering defined for $\Theta(l) = -\theta$. From the $(-)^L$ phase factor of the interference term in the expression (2. 30) it results that the inelastic scattering cross-sections of even and odd parity transitions present oscillations that are out of phase. If we now compare the inelastic expression (2. 20) to the elastic one:

$$\frac{d\sigma}{d\Omega}(\theta > \theta_r) = \frac{1}{k^2 \sin\theta}\{2\pi l_r q^{-2/3} A^2 i(q^{-1/3}(\theta - \theta_r)) \quad (2.\ 31)$$

$$+ \frac{l_3}{|\Theta'(l)|_{l_3}} - 2\cos(\delta_r - \delta_r)\left[\frac{2\pi l_3 l_3}{|\Theta'(l)|_{l_3}}\right]^{1/2} \cdot q^{-1/3} A\, i(q^{-1/3}(\theta - \theta_r))\}$$

we conclude that they predict oscillations which are in phase or out of phase according as the inelastic transition is even or odd. This phase rule between the elastic and inelastic cross-sections is just the inverse of the well known Blair phase rule [26] which applies in high energy diffractional like scattering. A typical example of the Blair phase rule in heavy ion is given by the scattering of ^{12}C on ^{16}O at 168 MeV [21].

3 — SCATERING POTENTIAL AND DEFLECTION FUNCTION

To describe heavy ion scattering, we use a central potential defined as the Coulomb potential superposed to a Saxon-Woods shape nuclear one

$$v(r) = \frac{Z_p Z_T e^2}{r} + \frac{-V_0}{1 + \exp\dfrac{r - R_0}{\sigma}}. \quad (3.\ 1)$$

The deflection function is obtained by numerical evaluation of the integral:

$$\Theta(l) = \pi - 2\int_{r_m}^{\infty} \frac{\dfrac{(l+1/2)\hbar}{r^2}}{\left[2m(E - v(r) - \dfrac{(l+1/2)^2\hbar^2}{r^2}\right]^{1/2}} dr \quad (3.\ 2)$$

the parameters $V_0, R_0 = r_0(A_1^{1/3} + A_p^{1/3})$ and σ of the nuclear potential being defined by a best fit of the elastic scatering cross-section. The calculations being greatly simplified by using for $\Theta(l)$ an analytic expression, we fit the deflection function obtained numerically with the parametrization form proposed by Ford and Wheeler [10]

$$\Theta(l) = \theta_r - \varrho\, l^2\, n \frac{l - l_a}{l_r - l_a} \tag{3.3}$$

with $\varrho = q(l_r - l_a)^2$ where

$$q = \frac{1}{2}\left[\frac{d^2\Theta(l)}{dl^2}\right]_{l_r} \tag{3.4}$$

defines the curvature of $\Theta(l)$ at $l = l_r$.

In Fig. 1, we give the exact (3.2) and parametrized forms of the deflection function $\Theta(l)$ used for ^{11}B on ^{208}Pb scattering at $E_{lab} = 72.2$ MeV.

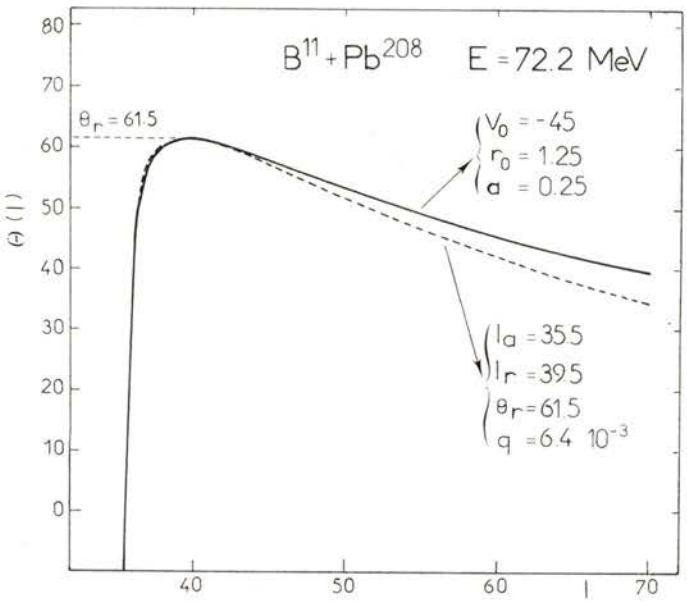

Fig. 1 — Classical deflection function used in the description of the elastic and inelastic scattering of ^{11}B on ^{208}Pb at EL = 72.2 MeV. Full curve: numerical evaluation (3.2); parametrized form (3.3).

For $l > l_r$, the decrease of the parametrized form is much too rapid with respect to the one defined by pure Coulomb field. To palliate this defect, we use in the expressions of elastic and inelastic scattering cross-sections, the Coulomb classical result $\sigma^R = \frac{\eta^2}{4\,k^2 \sin^4 \theta/2}$ for $l > l_r$ i. e. on the right branch (branch 1) of the deflection function.

The deflection function used to describe the scattering of ^{12}C on ^{27}Al is defined on Fig. 2.

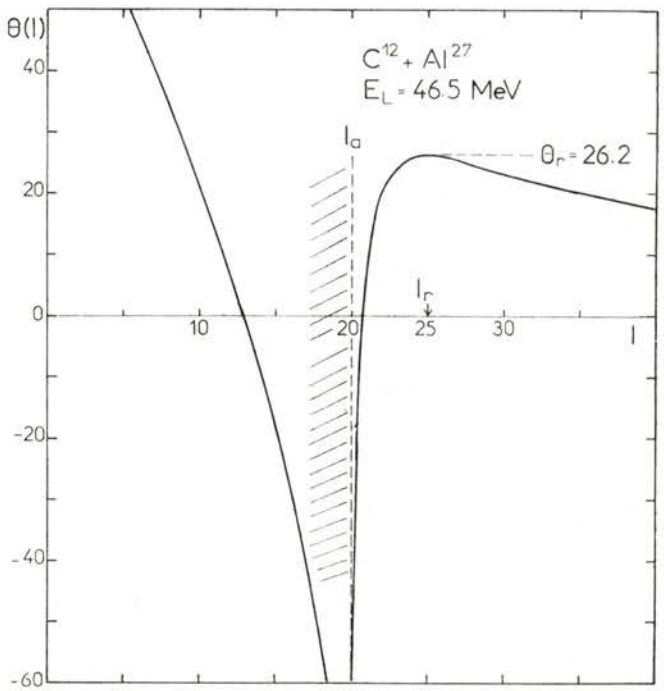

Fig. 2 — Classical deflection function used in the description of the elastic and inelastic scattering of ^{12}C on ^{27}Al at El = 46.5 MeV.

In such a case, the contribution from the negative branch $\Theta(l) = -\theta$ is no more negligeable against the contributions from the positive branch $\Theta(l) = +\theta$, especially in the dark region, owing to the decrease for $\theta > \theta_r$ of the contributions from $\Theta(l) = +\theta$.

4 — RESULTS

The theory outlined in Section 2 is applied to describe some experimental results in elastic and inelastic scattering of heavy ions at incident energies above the Coulomb barrier [9]—[15].

The analyzed data are:

— the elastic scattering and inelastic 3^- (2.61 MeV), 5^- (3.20 MeV), 2^+ (4.10 MeV) and 4^+ (4.31 MeV) excitations of ^{208}Pb in the collision with ^{11}B at laboratory incident energy of 72.2 MeV

— the elastic scattering and inelastic 2^+ (4.43 MeV) transition in ^{12}C in the collision of ^{12}C on ^{27}Al at laboratory energy of 46.5 MeV.

The inelastic scattering cross-sections of ^{11}B on ^{208}Pb at 72.2 MeV laboratory energy reported on Figs. 3-4 are obtained in absolute scale with formulation (2.19); the elastic cross-sections reported are deduced from the associated expression ((2.20) in ref. [16]). The «out of phase» oscillations defined for $\theta < \theta_r$ in the elastic and inelastic scattering cross-sections are well reproduced. The observed phase rule does not depend on the parity of the inelastic transition.

The elastic and inelastic ($L = 2$) scattering cross sections of ^{12}C on ^{27}Al at 46.5 MeV laboratory energy ((2.7) times the Coulomb barrier) (Fig. 5) are obtained in absolute scale with the formulation (2.30) and (2.31) respectively. The «in phase» oscilations observed are quite well reproduced. In this case, the analysis has not been done for $\theta < \theta_r$; the behaviour of the Airy approximation used in (2.30) and (2.31) failing, badly in the lit region even when $(\theta - \theta_r)$ is only a few degrees.

Choice of parameters

The nuclear potential parameters (V_0, r_0, σ) and the parameters (θ_r, l_r, l_a, q) of the parametrized deflection function $\Theta(l)$ are obtained by best fit of the elastic cross-sections. Table I gives the values used in the present analysis. The parameter $R_c = r_c A^{1/3}$ defines the spherical distribution of charges chosen as equilibrium state for the

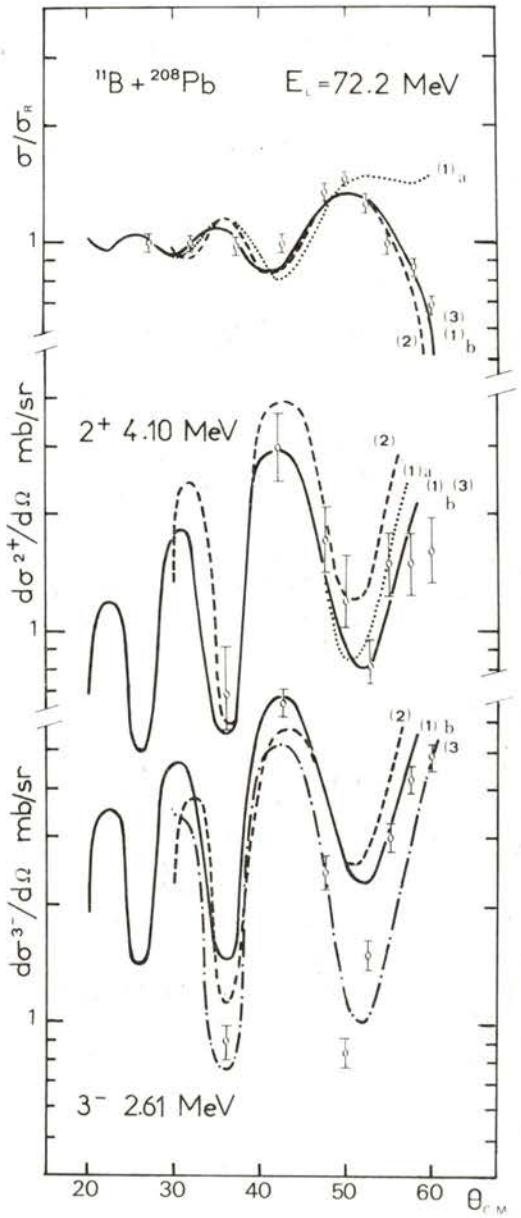

Fig. 3 — Cross-sections of the elastic and inelastic 2^+ (4.10 MeV) and 3^- (2.61 MeV) excitation of ^{208}Pb in scattering of ^{11}B on ^{208}Pb at EL = 72.2 MeV. Potentials (1) and (2) give similar fits to the data; potential (3) gives a better agreement with the experimental results [9] for the 3^- excitation. The uniform approximation (b) for the elastic and inelastic 2^+ cross-sections are compared to the asymptotic expressions (a)

target ion. (a) is the distance of closest approach of the ions on their trajectories [16]. As it is well known, a variation of the potential shape does not really affect the elastic scattering results but introduces sensitive perturbations in the inelastic one, the form factor being proportional to the derivative of the nuclear potential. The variation of the nuclear potential parameters induces variation in the relative

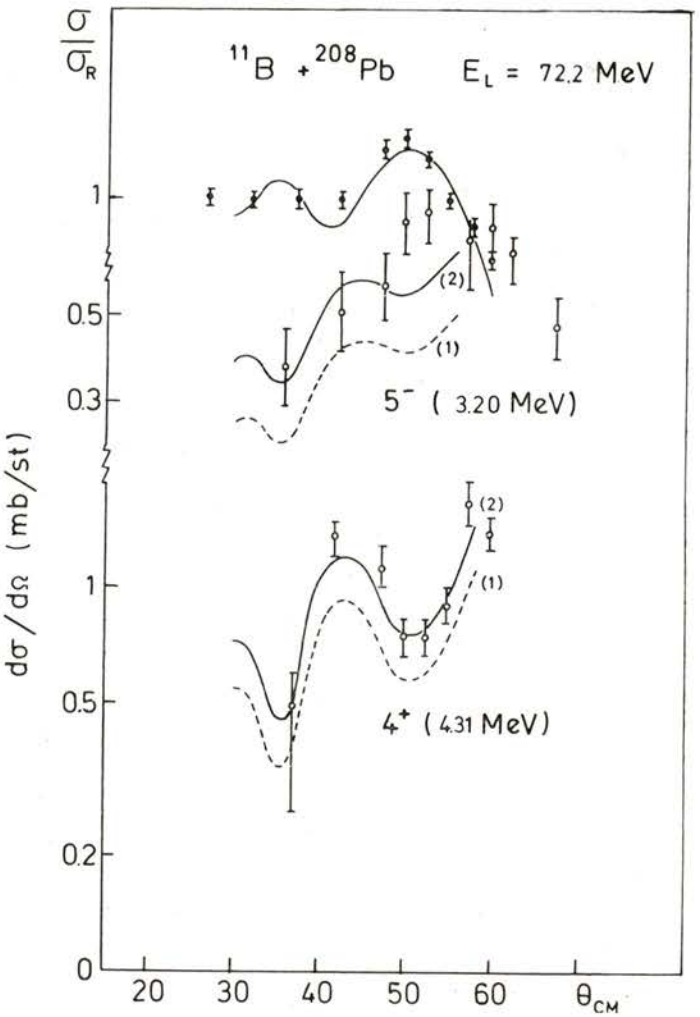

Fig. 4 – Cross-sections of elastic and inelastic 5^- (3.20 MeV) and 3^+ (4.31 MeV) excitation of ^{208}Pb in scattering of ^{11}B on ^{208}Pb at EL = 72.2 MeV. Potentials (1) and (2) are the same of Figure 3.

amplitudes of the oscillations and in the absolute scale of the inelastic results. The interference structure is very sensitive to the diffuseness of the nuclear potential and to the distance parameter (a) whose value depends on the form of the nuclear potential.

In the scattering of ^{11}B on ^{208}Pb, three potentials have been used. For set (2) the last minimum ($\theta < \theta_r$) in the inelastic cross-section is not deep enough for the 2^+ as well as for the 3^- state excitation. This choice defines too small values of the deformation parameters β_L^T (Table II) for $L = 2$ and $L = 3$.

In direct process formalism, the interference of Coulomb and nuclear excitation terms in describing the inelastic cross-section to higher multipolarity is a more drastic test to define accurate choice of the nuclear potential paramenters.

The deformation parameters β_L defined by the inelastic result only acts as a scale factor to adjust the absolute values of the inelastic cross-section. In electron and light ions inelastic scattering, the deformation of the interaction potential can be expected to be nearly the same as the charge or mass deformation of the target ion. This is not expected to be the case when the projectile size is large as it

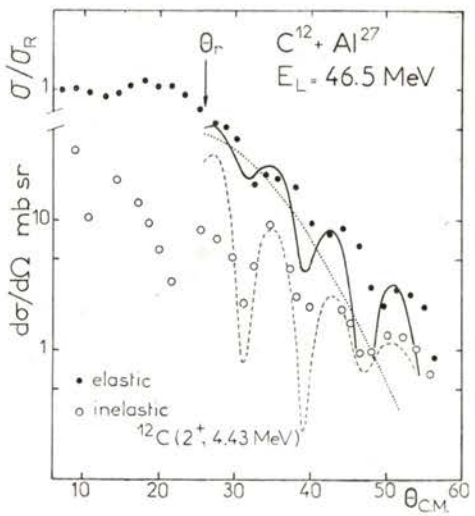

Fig. 5 — Cross-sections of elastic and inelastic 2^+ (4.43 MeV) excitation of ^{12}C in scattering of ^{12}C on ^{27}Al at EL = 46.5 MeV. The elastic cross-section is defined by expression (2.31) with (full curve) and without (dotted curve) the negative branch contribution; the inelastic one is defined by the expression (2.30) (broken curve). Experimental results are from ref. [15].

happens for heavy ion projectiles. The deformation obtained for the ion-ion potential will be smaller than the one of the target nuclear state involved. This effect has already been observed in $\alpha - \alpha$ scattering [22]. Taking into account the first order size correction [23] one may deduce the target deformation from the potential one, using the relation $\beta_L^V R_0 \equiv \beta_L^T R_T$ where $\beta_L^V, \beta_L^T, R_0, R_T$ are the deformation parameters of (L) multipolarity and the radii of the ion-ion potential and

TABEE I

^{11}B ^{208}Pb $E_L = 72.2$ MeV

	ion-ion potential parameters						*Deflection function parameters*			
	V_0	W_0	r_0	r_c	a	(a)	θ_r	l_r	l_a	q
(1)	40.	0.	1.25	1.20	0.4	4.08	61.5	39.5	35.5	0.0064
(2)	50.	0.	1.20	1.20	0.6	4.	60.4	39.5	35.4	0.0052
(3)	45.	0.	1.25	1.20	0.5	4.28	61.5	39.5	35.5	0.0064

^{12}C ^{27}AL $E_L = 46.5$ MeV

ion-ion potential parameters						*Deflection function parameters*			
V_0	W_0	r_0	r_c	a	(a)	θ_r	l_r	l_a	q
35.	0.	1.15	1.20	0.55	1.6	26.2	25	20.5	0.0045

$\beta_2^V = 0.30$

of the target respectively. We use the relations $R_0 = r_0(A_T^{1/3} + A_P^{1/3})$ and $R_T = r_T A_T^{1/3}$ (Table II). We test two descriptions of the excitation processes, they correspond to the choice of $\beta_L^V R_0$ or $\beta_L^V R_T$ as nuclear deformation parameter in the excitation potential. The potential and target deformation parameters obtained by fit of the inelastic results are in good agreement with values defined by other experimental results and theoretical DWBA analysis.

TABLE II

Deformation parameters in ^{208}Pb

3^- 2.61 MeV		$r^{(a)}$	r_0^T	β_L^V	β_L^T	$\beta_L^{(d)}$	$BE_{L\,e^2b^2}$	*Reference*
	(1)	1.25	1.18$^{(b)}$	0.07	—	0.102	0.49	(^{11}B , ^{11}B′) this work
	(2)	1.20	1.18	—	0.06	0.061	0.18	id.
	(3)	1.25	1.18	0.09	—	0.13	0.75	id.
other works		1.31	1.27	0.06	—	0.085	0.35	(^{16}O , ^{16}O′) [7]
		1.34	1.04	0.07	—	0.09	0.40	(^{11}B , ^{11}B′) [9]
							0.58	[24]

2^+ 4.10 MeV		$r^{(a)}$	r_0^T	β_L^V	β_L^T	$\beta_L^{(d)}$	$BE_{L\,e^2b^2}$	*Reference*
	(1)	1.25	1.18$^{(b)}$	0.0425	—	0.062	0.36	(^{11}B , ^{11}B′) this work
	(2)	1.20	1.18	—	0.048	0.049	0.23	id.
	(3)	1.25	1.18	0.06	—	0.087	0.69	id.
other works		1.31	1.27	0.03	—	0.043	0.18	(^{16}O , ^{16}O′) [7]
		1.34		0.042	—	0.06	0.35	(^{11}B , ^{11}B′) [9]
							0.30	[24]

5^- 3.20 MeV		$r^{(a)}$	r_0^T	β_L^V	β_L^T	$\beta_L^{(d)}$	*Reference*
	(1)	1.25	1.18$^{(b)}$	0.036	—	0.05	(^{11}B , ^{11}B′) this work
	(3)	1.20	1.18	—	0.06	0.06	id.
other works		1.34	1.04	—	0.05	0.06	(^{11}B , ^{11}B′) [9]
		—	—	—	0.043	0.055	(p , p') [24]

4^+ 4 31 MeV		$r^{(a)}$	r_0^T	β_L^V	β_L^T	$\beta_L^{(d)}$	*Reference*
	(1)	1.25	1.18$^{(b)}$	0.05	—	0.07	(^{11}B , ^{11}B′) this work
	(3)	1.20	1.18	—	0.08	0.08	id.
other works		1.34	1.04	—	0.07	0.09	(^{11}B , ^{11}B′) [9]
		—	—	—	0.062	0.08	(p , p') [24]

(a) $r = r_0$ in case (1) and (3); $r = r^T$ in case (2) with $\beta_L^V r_0 (A_P^{1/3} + A_T^{1/3}) = \beta_L^T r^T A^{1/3}$.

(b) r_0^T is the value difined in [25]:

(d) β_L deformation parameter difined by $\beta_L^V R_0 = \beta_L r_0 A_T^{1/3}$ or by $\beta_L^T R^T = \beta_L r_0^T A_T^{1/3}$.

5 — CONCLUSION

The aim of this paper has been to gain insight into the physical understanding of the different oscillatory behaviours which are observed in the elastic and inelastic heavy ions scattering cross-sections.

In the lit region, the observed phase rule results from the quantal interference effect between the classical trajectories deviated by one side of the nucleus.

In the dark region, a different oscillatory behaviour appears; it is due to an additional interference effect resulting from the trajectories deviated by the opposite side of the nucleus. At higher energies, when Coulomb effects are negligeable, the scattering is dominated by Fraunhøfer diffraction and then, the Blair phase rule applies.

The authors wish to thank Drs. J. Knoll and R. Schaeffer for helpful discussions.

REFERENCES

[1] C. LECLERCQ-WILLAIN, *Journ. the Phys.* **32**, (1971) 833.
[2] R. A. BROGLIA and A. WINTHER, *Phys. Rev.* **4**, (1972) 153.
[3] R. A. BROGLIA, S. LANDOWNE and A. WINTHER, *Phys. Lett.* **40B** (1972) 293.
[4] F. D. BECCHETTI et al., *Phys. Rev.* **C6** (1972) 2215.
[5] V. K. LUKYANOV, A. I. TITOV, J. I. N. R. DUBNA (1973) Preprint E4—6989.
[6] F. VIDEBAEK, I. CHERNOV, P. R. CHRISTENSEN and E. E. GROSS, *Phys. Rev. Lett.* **28** (1972) 1072.
[7] F. D. BECCHETTI, P. R. CHRISTENSEN, V. I. MANKO, R. J. NICKLES *Nucl. Phys.* **A203** (1973) 1.
F. D. BECCHETTI, LBL 1653 «Inelastic scattering of heavy ions».
[8] P. R. CHRISTENSEN, I. CHERNOV, E. E. GROSS, R. STOCKSTAD and F. VIDEBAEK, *Nucl. Phys.* **A207** (1973) 433.
[9] J. L. C. FORD et al., Contributed papers 5.52 in «Proceedings of the Intern. Conf. on Nuclear Physics» (Münich 1973), Eds. J. the BOER and H. J. MANG, North-Holland Publ. Co, Amsterdam.
J. L. C. FORD et al. *Phys. Rev.* **C8** (1973) 1912.
[10] K. W. FORD and J. A. WHEELER, Annals of Physics **7** (1959) 259-287.
[11] W. H. MILLER, *Journ. Chem. Phys.* **48** (1968) 464.
[12] M. V. BERRY, *Proc. Phys. Soc.* **89** (1966) 479.
[13] R. da SILVEIRA, *Phys. Lett.* **45B** (1973) 211.
[14] R. A. MALFLIET, S. LANDOWNE and V. ROSTEKIN, *Phys. Lett.* **44B** (1973) 238.

[15] F. POUGHEON, C. DETRAZ, G. ROTBARD and P. ROUSSEL, Proceedings of the Intern. Conf. on Reactions between Complex Nuclei, Nashville (1974) Supplt. to Vol. 1, p. 4.
R. da SILVEIRA, CH. LECLERCQ-WILLAIN and F. POUGHEON, Proceedings of the Intern. Conf. on Reactions between Complex Nuclei, Nashville (1974) Supplt. to Vol. 1, p. 5.
[16] R. da SILVEIRA and CH. LECLERCQ-WILLAIN, Preprint Orsay IPNO/TH 73-52.
[17] CH. LECLERQ-WILLAIN, Thesis on «Etude théorique de l'interférence des excitations coulombienne et nucléaire», Bruxelles (1968).
[18] K. ALDER, A. BOHR, T. HUUS, B. MOTTELSON, A. WINTHER, *Rev. Mod. Phys.* **28** (1956) 432.
[19] M. ABRAMOWITZ and I. A. STEGUN, «Handbook of Mathematical Functions with Formulas, Graphs and Mathematical Tables», Ed. Dover Publications, New-York — 1965.
[20] F. T. BAKER and R. TICKLE, *Phys. Rev.* **C5** (1972) 544.
[21] J. C. HIEBERT and G. T. GARVEY, *Phys. Rev.* **135** (1964) B346.
[22] A. M. BERNSTEIN, «Advances in Nuclear Physics», Vol. 3, Eds. M. BARANGER et E. Vogt, Plenum Press - New-York — 1969.
[23] D. L. HENDRIE, *Phys. Rev. Lett.* **3** (1972) 478.
[24] Nuclear Data Sheets **B5** (1971) 266.
[25] L. R. B. ELTON, «Nuclear Sizes», Oxford University Press — 1961.
[26] J. S. BLAIR, *Phys. Rev.* **115** (1959) 928.

Toute la correspondance concernant la rédaction de PORTUGALIAE PHYSICA doit être adressée à

PORTUGALIAE PHYSICA
Laboratório de Física da Faculdade de Ciências
LISBOA-2 (Portugal)

Prix de l'abonnement:	250 escudos (US $8.50) par volume
Prix des volumes déjà parus:	300 escudos (US $10)
Prix du fascicule:	75 escudos (US $2.50)

Les membres de la «Sociedade Portuguesa de Química e Física» ont une réduction de 50 % sur les prix indiqués.

Les Universités, les Laboratoires de Physique, les Académies, les Sociétés Scientifiques et les Revues de Physique sont invités à recevoir cette revue en échange de leurs publications.

PORTUGALIAE PHYSICA donnera un compte-rendu detaillé de tous les ouvrages soumis à la rédaction en deux exemplaires.

All mail concerning PORTUGALIAE PHYSICA to be addressed to:

PORTUGALIAE PHYSICA
Laboratório de Física da Faculdade de Ciências
LISBOA-2 (Portugal)

Subscription rates:	250 escudos (US $8.50) per volume
Price of past volumes:	300 escudos (US $10)
Price of copy:	75 escudos (US $2.50)

Members of the «Sociedade Portuguesa de Química e Física» may obtain *Portugaliae Physica* at a reduced price (50 %).

Universities, Physics Laboratories, Academies, Scientific Societies and Physics Publications are invited to receive this review in exchange for their publications.

PORTUGALIAE PHYSICA will give a detailed report of any book if two copies have been submitted.

Composto e impresso na Tip. Matemática, Lda. — R. Diário de Notícias, 134-1.º-Esq. — Lisboa-2

PORTUGALIAE PHYSICA

VOLUME 9
FASCÍCULO 4
1975

INSTITUTO DE ALTA CULTURA
CENTROS DE ESTUDOS DE FÍSICA DAS UNIVERSIDADES PORTUGUESAS

PORTUGALIAE PHYSICA

Fundadores: A. Cyrillo Soares, M. Telles Antunes, A. Marques da Silva M. Valadares.

VOLUME 9 1975 FASCÍCULO 4

VOLUMES PUBLICADOS:

Vol. 1 — 1943-45 — 326 pp.

Vol. 2 — 1946-47 — 256 pp.

Vol. 3 — 1949-54 — 173 pp.

Vol. 4 — 1965-66 — 304 pp.

Vol. 5 — 1967-70 — 194 pp.

Vol. 6 — 1970-71 — 316 pp.

Vol. 7 — 1971-72 — 210 pp.

Vol. 8 — 1972-73 — 266 pp.

Vol. 9 — 1974-75 — 182 pp.

Redacção: Laboratório de Física da Faculdade de Ciências — Lisboa-2 (PORTUGAL)

Comissão de redacção:

J. Moreira de Araújo — Carlos Braga — Carlos Cacho — A. Pires de Carvalho — M. Abreu Faro — J. Gomes Ferreira — F. Bragança Gil — Manuel Laranjeira. Amaro Monteiro — J. Pinto Peixoto — J. da Providência — Lídia Salgueiro — J. de Almeida Santos — José Sarmento — António da Silveira — J. Veiga Simão.

ÍNDICE

(Table des matières)

Pauli correction to the deuteron folded potential, by A. M. GONÇALVES and F. D. SANTOS 117

Simple molecular statistical interpretation of the nematic viscosity γ_1, by A. F. MARTINS and A. C. DIOGO 129

La correspondance entre modeles microscopiques et macroscopiques, par E. MATAGNE 141

Liste des publications reçues actuellement en échange avec Portugaliae Physica 177

Instructions pour les auteurs 181

GONÇALVES, A. M. and SANTOS, F. D.

Laboratório de Física,
Faculdade de Ciências, Lisboa

Pauli correction to the deuteron folded potential.

Portgal. Phys. — 9 (4): 117-128, 1975

The correction to the deuteron-nucleus effective interaction in deuteron elastic scattering resulting from the Pauli exclusion principle was calculated following the method proposed by Soper [5], using the infinite nuclear matter approximation and the separable nuclear potential of Yamaguchi [14]. The resulting Pauli potential is repulsive and has a magnitude of few percent of the deuteron folded potential real part. Its radial dependence, determined with the local density approximation, shows a pronounced peak at the nuclear surface.

MARTINS, A. F. and DIOGO, A. C.

Centro de Física da Matéria
Condensada (INIC)
Av. Gama Pinto-2,
Lisboa-4, Portugal

Simple molecular statistical interpretation of the nematic viscosity γ_1.

Portgal. Phys. — 9 (4): 129-140, 1975

We present a theoretical analysis of the rotational viscosity $\gamma_1(T)$ of nematic liquid crystals based on the theory of rate processes and Maier and Saupe's molecular theory. We derive:

$$\gamma_1(T) = c \; S^2 \exp(\varepsilon S/kT)$$

where $\varepsilon = 3A/2mV_N^2$ and $c \simeq$ const. (explicitly given). This relation fitts very well the compiled experimental data for p-azoxyanisole (PAA), with $c = 0.177$

MATAGNE, E.

Bâtiment Maxwell Faculté des
Sciences Appliquées
Louvain-la-Neuve

La correspondance entre modeles microscopiqnes et macroscopiques.

Portgal. Phys. — 9 (4): 141-176, 1975

The purpose of this paper is to show how to derive macroscopic quantities by taking the average of microscopic quantities without using either vectorial type integrals or volume integrals.

In contrast with the usual methods [3], [8], [11], [12], it follows that the method developed here is compatible with theories referring to a curved space (e. g. general relativity). However, since these theories could not yet have been put in agreement with quantum theories, this study is achieved at a purely classical (non-quantified) level, in spite of an analogy with the quantum theories.

poise and $\varepsilon = 0.879$ kcal/mole, and for anisaldazine (AD), with $c = 0.111$ poise and $\varepsilon = 0.890$ kcal/mole. From these values of ε we get the nearest-neighbour coordination numbers $m = 6.3$ for PAA and $m = 6.8$ for AD. The agreement between our theory and experience extends over the entire nematic range including the region close to T_c.

An approximate method of calculation, which is derived almost automatically from the definition of macroscopic quantities, is also developed.

By using a spherical approximation, an approximate calculation is finally carried out on three classical examples, which are

— the evaluation of the conductivity of an emulsion

— the calculus of the dielectric permeability of a polar gas, and

— the derivation of the properties of a «cold plasma» in the general relativity theory.

Although the results of these calculations are not very original, especially as far as the two first examples are concerned, we found it interesting to recalculate them by this method which is more deductive than usually presented methods, and which opens the way to more general results.

CDU 53 (469) (05)

PORTUGALIAE PHYSICA

VOLUME 9
FASCÍCULO 4
1975

PAULI CORRECTION TO THE DEUTERON FOLDED POTENTIAL (*)

A. M. Gonçalves and F. D. Santos
Laboratório de Física, Faculdade de Ciências, Lisboa

ABSTRACT — The correction to the deuteron-nucleus effective interaction in deuteron elastic scattering resulting from the Pauli exclusion principle was calculated following the method proposed by Soper [5], using the infinite nuclear matter approximation and the separable nuclear potential of Yamaguchi [14]. The resulting Pauli potential is repulsive and has a magnitude of few percent of the deuteron folded potential real part. Its radial dependence, determined with the local density approximation, shows a pronounced peak at the nuclear surface.

RESUMÉ — La correction resultante du principe de l'exclusion de Pauli qui s'applique à l'interaction effective deuteron-noyau pour la diffusion elastique fut calculée par la methode de Soper [5], utilisant l'approximation de matière nuclaire infinie et le potentiel nucleaire separable de Yamaguchi [14]. Le potentiel de Pauli ainsi obtenu est repulsif avec une intensité de l'ordre de quelques pour-cent de la partie réelle du potentiel du deuteron de Watanable [6]. La dependence radiale de ce potentiel, determinée avec l'approximation de densité locale, nous montre un pic pronouncé à la surface nucléaire.

1 — INTRODUCTION

The Pauli exclusion principle plays a dominant role in atomic collisions, due to the exchange forces set up in the overlapping electron clouds of the colliding atoms. This effect has been recognized for several years, and recently reported by Laubert and Brandt [1]. An analogous but less pronounced effect will be present in nuclear reactions involving multinucleon bound projectiles and targets. However even for the nucleon-nucleus optical potential the calculation of Pauli

(*) Received 26 June 1975.

exclusion principle effects presents considerable difficulties. This problem has been considered by Bell and Squires [2] and by Van Giai, Sawicki and Vinh Mau [3] in terms of a linked cluster expansion neglecting the target recoil energy and assuming the ground-state to be non-degenerate. The same method has been used by Junkin and Villars [4] to derive an expression for the deuteron optical potential. The linked cluster perturbation series for the effective interaction 2 nucleons-nucleus has two terms: the first is a one-body operator, where the leading term is just the Hartree-Fock (H-F) potential, and corresponds to the sum of two single-nucleon optical potentials calculated off the energy shell at roughly half the deuteron kinetic energy; the second is a two-body operator, part of which comes from the exclusion principle. Soper [5] derived from the full antisymmetrized hamiltonian an equation which describes two nucleons outside a closed shell interacting with each other via the 2-nucleon interaction and with the core through their H-F potentials. The solution of this equation is a 2-nucleon state containing only particle-states ortogonal to the bound H-F orbitals. Note however that the most general 2-nucleon state satisfying the asymptotic boundary condition of an incoming deuteron with momentum $\vec{K}$ also has hole-states in its expansion. The effective interaction in that equation is the sum of the H-F potentials plus the 2-body potential which is the lowest order approximation to the 2-body potential of Junkin and Villars [4]. Neglecting the coupling to the break-up channel, the correction to the folded potential of Watanable [6] due to the Pauli exclusion principle is just the mean value of a 2-body potential in the deuteron internal wave function.

Using this approximation Johnson and Soper [7] have calculated deuteron break-up effects in deuteron stripping reactions using an adiabatic model and obtained improved agreement with differential cross section data. Recently, Gambhir and Griffin [8, 9] investigated explicitly the deuteron break-up due to Pauli exclusion effects in deuteron elastic scattering and Austern [10] proposed a simple procedure for the calculation of antisymmetrization effects. Using this model Gambhir and Griffin [11] have discussed the qualitative features of Pauli break-up from the configuration space viewpoint.

In the present paper we analyse the Pauli correction to the deuteron folded potential, proposed by Soper [5], in particular the variation of its radial shape with deuteron incident energy and target nucleus mass number.

2 — PAULI CORRECTION TO THE DEUTERON FOLDED POTENTIAL

2. 1. *General formalism*

The terms in the deuteron-nucleus effective interaction corresponding to Pauli exclusion principle effects [5] can be written as

$$V_p(1,2) = [E - h(1) - h(2)]\,[1 - P(1)\,P(2)] + \qquad (1)$$
$$[P(1)\,P(2)\,v(1,2)\,P(1)\,P(2) - v(1,2)]$$

where E is the total energy of the system and $v(1,2)$ the 2-nucleon interaction. $P(i)$ is the projection operator into the eigenstates of the 1-body hamiltonian.

$$h(j) = T + V_H\,,\; j = 1,2$$

belonging to the eigenvalue $\varepsilon_i > \varepsilon_F$. Here V_H is the self-consistent H-F potential for A nucleons and ε_F the Fermi energy. In order to obtain the Pauli correction to the deuteron-nucleus folded potential we must calculate the average of the interaction $V_p(1,2)$ over the internal motion of the deuteron. The equivalent local potential will be calculated considering the momentum space representative of the $V_p(1,2)$ interaction

$$\langle \vec{K}\,\varphi_0 \,|\, V_p(1,2) \,|\, \vec{K}'\,\varphi_0 \rangle$$

where φ_0 is the deuteron internal wave function. We now represent the nucleus by infinite nuclear matter which, strictly speaking, means that the correction only applies to the nucleus center. In this approximation the H-F states became plane waves and the projection operators into particle states have the form

$$P(j) = \sum_{\sigma_i\,\tau_i} \int_{k_i > k_F} d\vec{k}_i \,|\, \vec{k}_i\,\sigma_i\,\tau_i \rangle \langle \vec{k}_i\,\sigma_i\,\tau_i \,| \qquad (3)$$

where σ_i and τ_i represent the spin and isospin variables. Further-

more the H-F potentials must be diagonal in momentum space. We choose as usual [12] a quadratic dependence in $\vec{k}_i$

$$<\vec{k}_1 \,|\, \mathrm{V}(1) \,|\, \vec{k}'_1> = \delta(\vec{k}_1 - k'_1)\,(\omega_0 + \omega_1 k_1^2) \tag{4}$$

which is equivalent to assume an effective nucleon mass m^* inside nuclear matter given by

$$\frac{1}{2\,m^*} = \frac{1}{2\,m} + \omega_1 \tag{5}$$

where m is the nucleon mass. The constants ω_0 and ω_1 are estimated from the energy dependence of the depth of the real part of the phenomenological nucleon optical potential $\mathrm{V}(\mathrm{E_N})$. Using the relation

$$\mathrm{E_N} = \frac{\hbar\, k_1^2}{2\,m} + \mathrm{V}(\mathrm{E_N})$$

where $\mathrm{E_N}$ is the kinetic energy of the nucleon outside the nucleus and the average nucleon optical potentials of Bechetti and Greenlees [13] we obtain

$$\omega_0 = -(81.10 + 0.29\ \mathrm{ZA}^{-1/2})\ \mathrm{MeV}$$
$$\omega_1 = 9.75\ \mathrm{MeV}\ fm^2$$

where A and Z are, respectively the mass and atomic number of the target.

A separable potential to represent the 2-nucleon interaction is particularly convenient in view of the structure of eq. (1). We use the potential of Yamaguchi [14] which fits the low energy 2-nucleon data. This potential also has the advantage that it gives a Hulthén type wave function for the deuteron which is particularly convenient for the required momentum space integration. The restricted domain of integration for the individual nucleon momenta k_i imposes conditions on the deuteron internal momentum k which is therefore subjected to the relations;

$$\frac{\mathrm{K}}{2} - k_\mathrm{F} \geqq k \geqq \frac{\mathrm{K}}{2} + k_\mathrm{F}$$

and

$$\frac{\mathrm{K}}{2} - k_\mathrm{F} < k < \frac{\mathrm{K}}{2} + k_\mathrm{F}$$

where in the latter case the angle θ between K and k must satisfy

$$\frac{K^2 - 4k_F^2}{4Kk} - \frac{k}{K} < \cos\theta < \frac{K^2 - 4k_F^2}{4Kk} + \frac{k}{K}.$$

We represent by an over bar the integrations in k over the allowed momentum space and by $\overline{N}$ the integral of the Hulthén wave function over that space. Using this notation we have;

$$<\vec{K}\,\varphi_0 \,|\, V_p(1,2) \,|\, \vec{K}'\,\varphi_0> = (\vec{K} - \vec{K}')\, V_p(K)$$

where

$$V_p(K) = \left[E_0 - \frac{\hbar^2 K^2}{4m} - 2\left(\omega_0 + \omega_1\left(\frac{K^2}{4} + <k^2>\right)\right)\right](1-\overline{N})$$

$$+\left[\overline{<v>} + \left(\frac{\hbar^2}{m} + 2\omega_1\right)\overline{<k^2>} - \left(<v> + \frac{\hbar^2}{m}<k^2>\right)\overline{N}\right]$$

$$-2\omega_1\overline{N}<k^2> \qquad (8)$$

and E_0 is the deuteron incident energy which is the difference between the total energy and the deuteron binding energy ε_0. The latter can be written

$$\varepsilon_0 = <v> + \frac{\hbar^2}{m}<k^2>$$

where

$$<v> = \int d\vec{k}\, d\vec{k}'\, \varphi_0(k)\, v(k,k')\, \varphi_0(k')$$

$$<k^2> = \int d\vec{k}\, \varphi_0(k)\, k^2\, \varphi_0(k).$$

The choice of K corresponding to a given deuteron incident energy E_0 is made in a self consistent way [15] through the equation

$$E_0 - \frac{\hbar^2 K^2}{4m} - 2\left[\omega_0 + \omega_1\left(\frac{K^2}{4} + <k^2>\right)\right] - V_p(K) = 0. \qquad (10)$$

Using eqs. (8), (9) and (10) we obtain

$$V_p(E_0) = \varepsilon_0^* - \varepsilon_0' \qquad (11)$$

where

$$\varepsilon_0^* = \frac{\overline{< v >}}{\overline{N}} + \left(\frac{\hbar^2}{m} + 2\,\omega_1 \right) \frac{\overline{< k^2 >}}{\overline{N}} \tag{12}$$

may be interpreted as an internal energy of the neutron proton system inside nuclear matter and

$$\varepsilon_0' = < v > + \left(\frac{\hbar^2}{m} + 2\,\omega_1 \right) < k^2 > \tag{13}$$

is the binding energy of a «deuteron» with an effective nucleon mass given by eq. (5). By substitution of eq. (11) into eq. (10) we finally get

$$E = \left(\frac{\hbar^2}{m} + 2\,\omega_1 \right) \frac{K^4}{4} + 2\,\omega_0 + \varepsilon_0^* . \tag{14}$$

Thus the total energy of the system «deuteron inside nuclear matter» is the sum of the deuteron center of mass energy corresponding to a nucleon effective mass m^*, the potential energy and the internal energy ε_0^*. We emphasize that the Pauli potential V_p is a function of the incident energy E_0 through ε_0^*. In fact note that the allowed momentum space for the k integrations is a function of K and therefore of E_0.

The eq. (11) has the same structure of the Pauli potential of Gambhir and Griffin [8]

$$V_x = Q\,H_i\,Q - H_i \tag{15}$$

where Q projects into the allowed momentum space and H_i is the free deuteron hamiltonian.

We can investigate the radial dependence of the Pauli potential V_p using the local density approximation. The Fermi momentum k_F is then determined by the value of the nuclear density form factor at radius R through the relation

$$k_F^3 = \frac{3\,\pi^2}{2}\,\rho\,(R) . \tag{16}$$

For consistency we also assume that ω_0 and ω_1 in eq. (4) have the same radial dependence as the nucleon optical potential of Bechetti and Greenless [13].

2. 2. *Results of calculation*

The present calculations of the Pauli potential V_p given by eq. (11) were made using for the deuteron a Hulthén wave function with parameter $\beta = 1.36\,\mathrm{fm}^{-1}$, the nucleon optical potentials from Ref. [13] and the nuclear density form factor $\rho(R)$ from Ref. [16] to determine its radial dependence. As shown in Fig. 1 V_p is repulsive and decreases

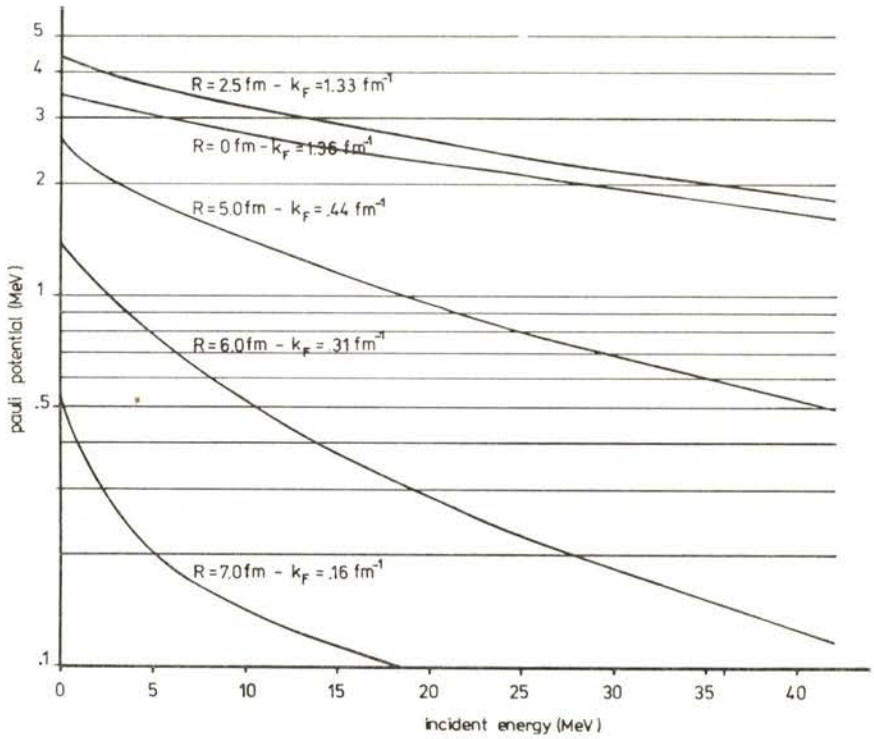

Fig. 1 — Variation of the Pauli potential in ^{40}Ca with deuteron incident energy for different values of k_F. The values of R are determined from eq. (16).

roughly exponentially with incident deuteron energy. We find that V_p has generally a larger radius than the nuclear optical potential. The difference is about 0.7 fm in ^{40}Ca for $E_0 = 10\,\mathrm{MeV}$ and increases for smaller energies. A distinctive feature of V_p is a depression in the nuclear center.

The various contributions to the Pauli potential for ^{40}Ca at $E_0 = 5$ MeV are plotted in Figs. 2 and 3 for ω_1 equal to 0,5, 9.75 and 13.2 MeV fm^2. The quantities ε_0^* and ε_0' have different radial forms. ε_0' being proportional to the nucleon optical potential since it depends linearly on ω_1. The two terms in ε_0^* have a ratter complicated dependence on R and ω_1 but their sum always has a mean radius

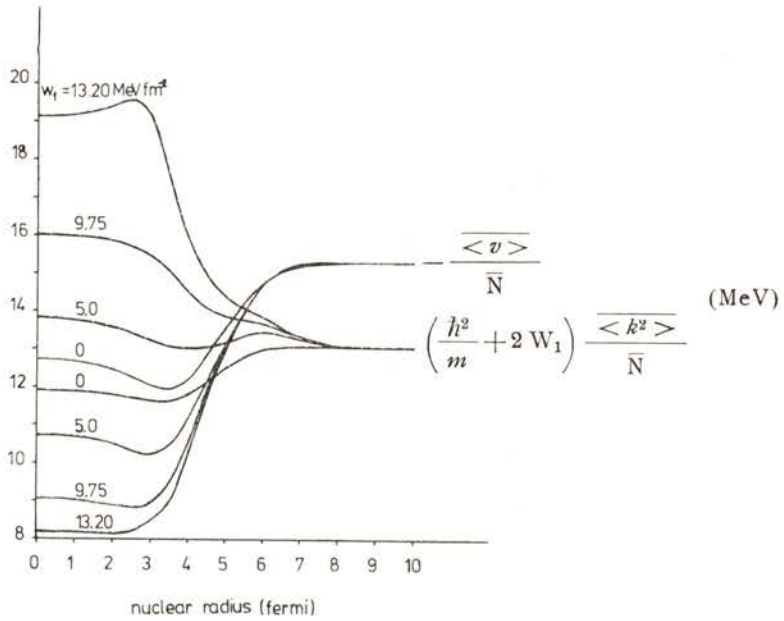

Fig. 2 — Radial dependence of the two terms in the expression (12) which gives the internal energy of the neutron-proton system inside nuclear matter for different vallues of ω_1. The target is ^{40}Ca and the deuteron incident energy $E_0 = 5$ MeV.

greather then ε_0' as shown in Fig. 3. Further, with $\omega_1 = 0$ and 13.2 MeV fm^2, ε_0^* presents a little surface peak, which is not present at intermediate values of ω_1. These two facts, namely the difference in radius and the surface peak in ε_0^*, lead to a pronounced surface peak in the Pauli potential. The increase of V_p with ω_1 shown in Fig. 4 is mainly due to the pronounced dependence of the ε_0^* term.

The behaviour of V_p as a function of the deuteron incident energy is represented in Fig. 5. As expected, V_p decreases with deuteron

incident energy, but this variation is less pronounced in the nuclear interior. In fact, in this region of space K varies slowly with E_0, because it is mainly determined by $2\omega_0$ (eq. (10)). However, at the nuclear surface this variation is much more pronounced, and therefore the domain of integration in k is drastically increased.

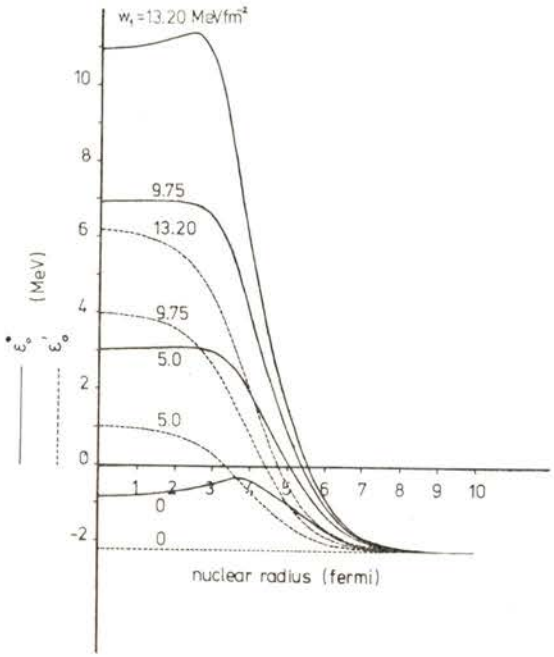

Fig. 3 — Radial dependence of the two terms in the expression (11) which gives the Pauli potential V_P for different values of ω_1. The target and incident energy is as in Fig. 2.

Fig. 6 represents the radial dependence of V_P for various nuclei. We note that the variation with A is less pronounced in the nuclear interior. This is due to the fact that V_P is invariant with A in the infinite nuclear matter approximation if we neglect the weak dependence of ω_0 on A and Z.

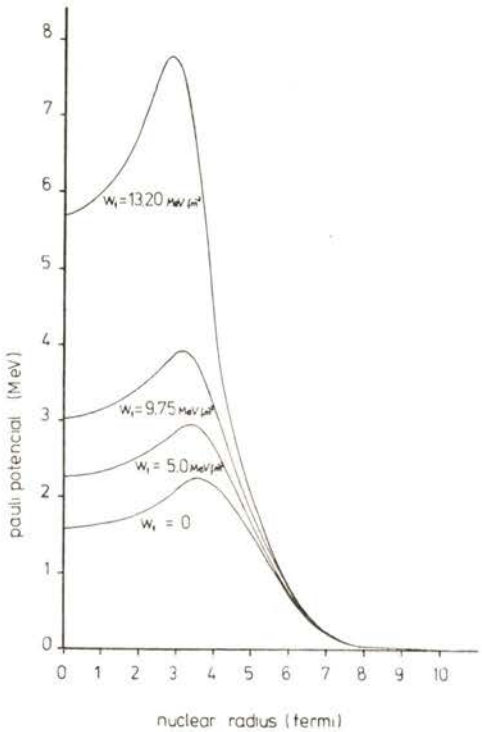

Fig. 4 — Radial dependence of the Pauli potential in ^{40}Ca for a deuteron incident energy $E_0 = 5$ MeV and for different values of ω_1.

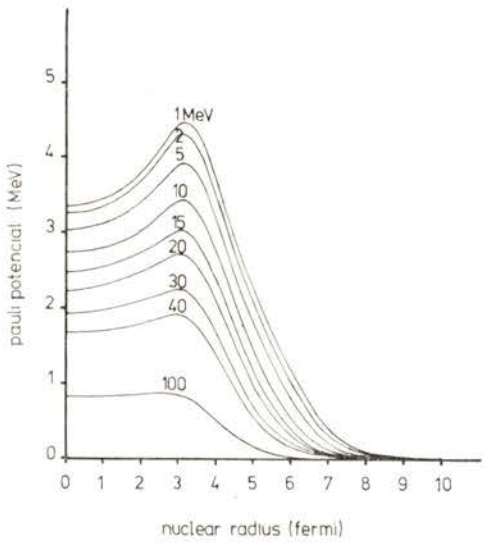

Fig. 5 — Radial dependence of the Pauli potential in ^{40}Ca for different deuteron incident energies and assuming $\omega_1 = 9.75$ MeV fm^{-2}.

3 — CONCLUSIONS

The Pauli correction to the deuteron folded potential is found to be repulsive and to decrease with deuteron incident energy as it should be expected from simple physical grounds. The same type of behaviour is reported by Gambhir and Griffin [11]. The magnitude of V_p is of the

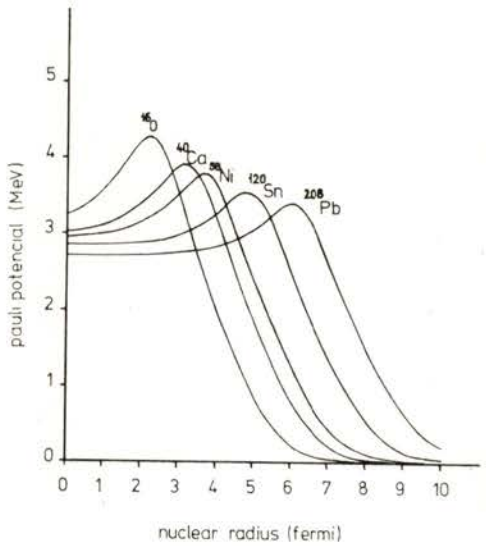

Fig. 6 — The Pauli potential in different target nuclei for a deuteron incident energy $E_0 = 5$ MeV and assuming $\omega_1 = 9.75$ MeV fm^{-2}.

order of 5% of the depth of the real part of the folded potential [17] and its radius is larger. As regards the radial dependence we find a marked surface peak particularly in light nuclei. This therefore does not give support to the assumption of Ref. [11] of uniformity of V_p over the nuclear volume.

The deuteron becomes unbound at a radius where the nuclear density is only few percent of the value in the center. This radius is found to be appreciably sensitive to the coefficient ω_1 which gives the nucleon optical potential energy dependence. For the value of ω_1 taken from [13] the deuteron reaches an unbound state even for relatively

high energies of the order of 100 MeV. However if we take $\omega_1 = 0$ the deuteron is never unbound for an incident energy $E_0 > 5$ MeV.

We note that in the calculations of Ref. [9] the deuteron is unbound in nuclear matter unless it has a kinetic energy of the order of 100 MeV. These predictions are significantly altered in the present more realistic calculations of the intrinsic energy of the $n-p$ system inside nuclear matter.

ACKNOWLEDGEMENTS

We are thankful to Dr. R. C. Johnson and Dr. P. J. R. Soper for many helpfull discussions and their interest in this work.

REFERENCES

[1] R. LAUBERT and W. BRANDT, *Phys. Rev. Letters* **24**, 1037 (1970).
[2] J. S. BELL and E. J. SQUIRES, *Phys. Rev. Letters* **3**, 96 (1959).
[3] N. VAN GIAI, J. SAWICKI and N. VINH MAU, *Phys. Rev.* **141**, 913 (1966).
[4] W. F. JUNKIN and F. VILLARS, *Ann. Phys.* (N. Y.) **45**, 93 (1967).
[5] P. J. R. SOPER, Ph. D. Thesis, University of Surrey, unpublished.
[6] S. WATANABLE, *Nucl. Phys.* **8**, 484 (1958).
[7] R. C. JOHNSON and P. J. R. SOPER, *Phys. Rev.* **C1**, 976 (1970).
[8] B. L. GAMBHIR and J. J. GRIFFIN, *Phys. Rev.* **C5**, 1856 (1972).
[9] B. L. GAMBHIR and J. J. GRIFFIN, *Phys. Rev.* **C7**, 590 (1973).
[10] N. AUSTERN, *Phys. Lett.* **46B**, 49 (1973).
[11] B. L. GAMBHIR and J. J. GRIFFIN, *Phys. Lett.* **50B**, 407 (1974).
[12] K. KIKUCHI and M. KAWAI, *Nuclear Matter and Nuclear Reactions* (Amsterdam: North-Holland, 1968), pag. 5.
[13] F. D. BECHETTI and G. W. GREENLESS, *Phys. Rev.* **182**, 1190 (1969).
[14] Y. YAMAGUCHI, *Phys. Rev.* **95**, 1628 (1954).
[15] D. J. THOULESS, *Nucl. Phys.* **75**, 128 (1966).
[16] P. E. HODGSON, *Nuclear Reaction and Nuclear Structure* (London: Oxford University Press, 1971), pag. 28.
[17] J. R. ROOK, *Nucl. Phys.* **61**, 219 (1965).

SIMPLE MOLECULAR STATISTICAL INTERPRETATION OF THE NEMATIC VISCOSITY γ_1 (*) (**)

A. F. Martins and A. C. Diogo
Centro de Física da Matéria Condensada (INIC)
Av. Gama Pinto-2, Lisboa-4, Portugal

ABSTRACT — We present a theoretical analysis of the rotational viscosity $\gamma_1(T)$ of nematic liquid crystals based on the theory of rate processes and Maier and Saupe's molecular theory. We derive:

$$\gamma_1(T) = c\ S^2\ \exp(\varepsilon S/kT)$$

where $\varepsilon = 3A/2mV_N^2$ and $c \simeq$ const. (explicitly given). This relation fitts very well the compiled experimental data for p-azoxyanisole (PAA), with $c = 0.177$ poise and $\varepsilon = 0.879$ kcal/mole, and for anisaldazine (AD), with $c = 0.111$ poise and $\varepsilon = 0.890$ kcal/mole. From these values of ε we get the nearest-neighbour coordination numbers $m = 6.3$ for PAA and $m = 6.8$ for AD. The agreement between our theory and experience extends over the entire nematic range including the region close to T_c.

RESUMÉ — Nous présentons une analyse théorique du coefficient de viscosité rotationelle $\gamma_1(T)$ des cristaux liquides nématiques qui nous permet de trouver la relation suivante:

$$\gamma_1(T) = c\ S^2\ \exp(\varepsilon S/kT)$$

où $\varepsilon = 3A/2mV_N^2$ est défini dans le cadre de la théorie moléculaire de Maier et Saupe et c est une constante dont la forme explicite est donnée. La relation ci-dessus s'accorde très bien avec les résultats expérimentaux relatifs au p-azoxyanisole (PAA), avec $c = 0{,}177$ poise et $\varepsilon = 0{,}879$ kcal/mole, et avec les résultats relatifs à l'anisaldasine (AD), avec $c = 0{,}111$ poise et $\varepsilon = 0{,}890$ kcal/mole. À partir des valeurs du paramètre ε nous obtenons les nombres de coordination $m = 6{,}3$ pour le PAA et $m = 6{,}8$ pour l'AD. L'accord de cette théorie avec l'expérience s'étend sur toute la plage nématique, en particulier il se vérifie tout près de T_c.

(*) Received 14 October 1976.

(**) This is a slightly modified version of a paper first presented at the fifth International Liquid Crystal Conference, Stockholm, June 17-21, 1974.

I — INTRODUCTION

The fundamental equations for viscous flow in nematic liquid crystals have first been written down by Leslie [1] and have proved to be consistent with many experimental observations. Essentially, the hydrodynamic equations of Leslie give the motions of two *coupled* fields, the velocity field $\vec{v}(\vec{r}, t)$ and the director field $\vec{n}(\vec{r}, t)$. If the velocity gradients are negligible, the coupling between these fields vanishes and we may separate the equation of motion for the director:

$$\sigma \frac{d\vec{\Omega}}{dt} + \gamma_1 \vec{\Omega} - \vec{N} = 0 . \tag{1}$$

Here $\vec{\Omega} = \vec{n} \times (d\vec{n}/dt)$ is the rotational velocity of the director, $\vec{N} = \vec{n} \times \vec{h}$ is a restoring torque due to the *molecular field* $\vec{h}$ [2], σ is an inertial coefficient associated with director reorientations, and γ_1 is a pure *rotational* viscosity. The effect of an external magnetic field is included in $\vec{N}$.

The viscosity $\gamma_1(T)$ may be measured in a way derived from the application of Leslie equations to the Tsvetkov's experiment [3]. The measurement is performed under stationary conditions such that the director fied $\vec{n} \equiv \vec{n}(t)$ makes a constant angle with an external rotating magnetic fied $\vec{H} \equiv \vec{H}(t)$, and it is assumed that $\vec{n}(t)$ is homogeneous in space, $\vec{v} = 0$, and the temperature is constant.

The inertial term in equation (1) is completely negligible for motions in the frequency range compatible with the continuum theory [2]. To this approximation, equation (1) describes a rotational motion of the director with a definite velocity under given conditions. This is typical of a rate process [4].

In the following part of this paper we will outline a molecular statistical theory of $\gamma_1(T)$ which takes advantage of these facts.

In part III the main results of the theory are contrasted with different interpretations of $\gamma_1(T)$ that have been proposed so far and with experimental data available for *p*-azoxyanisole (PAA) and anisaldazine (AD). These data strongly support our theory.

In the conclusion we briefly refer to expected extensions and improvements of this work.

II — MOLECULAR THEORY OF $\gamma_1(T)$

As it is well known the director $\vec{n}$ is a unit vector used to specify, in equilibrium, the preferred direction of molecular orientation.

When rotational motion is set in a portion of the nematic liquid, as expressed by equation (1), the molecules at each point of the moving liquid will be, on the average, parallel to the director at that point if the condition $\omega\tau \ll 1$ is fulfilled. Here ω is the frequency characterizing the time variation of $\vec{\Omega}$ and τ is a characteristic molecular decay time. Therefore, under such a condition we may interpret the motion of $\vec{n}$ as a collective motion of the molecules (or, perhaps in some cases, more complex «particles» formed by several molecules).

Besides the collective reorientations represented by the motion of $\vec{n}$, there are single-particle motions in the nematic phase with characteristic times of order τ, most likely to molecular motions in the isotropic liquids.

Single-particle reorientations take place against a potential barrier due to the local field created by all other molecules in the fluid. The instantaneous form of this potential depends on the configuration of the surrounding molecules and its calculation is a formidable task. However, to a good approximation, we may use the smooth form of the potential as given by the Maier and Saupe's mean-field theory [5]:

$$D(\theta) = -\frac{A}{m V_N^2} S P_2(\cos\theta) \tag{2}$$

where S is the degree of order, A is a molecular constant, m is a cluster parameter, V_N is the nematic volume, and θ is the angle made by the long molecular axis with the equilibrium direction. The minima of the potential (2) are separated by π thus reflecting the experimental fact that the directions $\vec{n}$ and $-\vec{n}$ are physically equivalent in all known nematics. The height of the potential barrier is given by

$$E = D(\theta)_{max} - D(\theta)_{min} = \frac{3}{2}\frac{A}{m V_N^2} S = \varepsilon S . \tag{3}$$

The actual packing of the molecules in the nematic state, and their long shape, do not allow for single-particle reorientations over large angles (e. g. rotational jumps of π) unless a previous local «lattice» expansion occurs. The probability of a rotational jump should then be given by the probability of the molecule finding the *necessary free volume* times the probability of attaining *sufficient energy* to cross over the potential barrier, as the two events must happen simultaneously. In equilibrium, the frequencies of molecular jumps clockwise and counter-clockwise are the same, and, within the framework of the rate theory [4], they are given by the following expression:

$$\nu_0 = \frac{k\,T}{h}\,\Pi\,(Z^e\,,Z)\exp\,(-\,\varepsilon\,S/k\,T) \tag{4}$$

where $\Pi\,(Z^e\,,Z)$ is a probability or «steric» factor depending on the partition functions of the molecule in the excited and normal states, k and h are the Boltzmann and Planck constants, and T is the temperature.

In the conditions of the Tsvetkov's experiment, as described above, an external torque due to the magnetic field is constantly applied to the molecules and the frequencies of molecular jumps forward and backward are no more the same. We then have, according to Boltzmann statistics:

$$\nu_{\pm} = \nu_0 \exp\,(\pm\,W/k\,T) \tag{5}$$

for the frequencies of molecular jumps in the forward (+) and backward (—) directions. In expression (5), W is the work done by the external torque; it should be computed between normal ($\theta = 0$) and excited ($\theta = \pi/2$) states of the jumping molecule. Note that we are concerned only with molecular rotational jumps of π for these jumps *conserve* the direction of $\vec{n}$ relative to the external field (cf. Tsvetkov's experiment).

Taking into account the distance between minima of the potential barrier, and expression (5), we may introduce a (relative) *mean rotational velocity* of the jumping molecule in the following manner:

$$\Omega^* = \pi\,(\nu_+ - \nu_-) = 2\,\pi\,\nu_0\,\sinh\,(W/k\,T)\,.$$

In actual experiments we always have $W \ll k\,T$ so that:

$$\Omega^* = 2\pi\nu_0 \frac{W}{kT}. \tag{6}$$

The work W may be written as:

$$W = N^* V_i^* \frac{\pi}{2} \tag{7}$$

where N^* is the *mean value* (for $\theta = 0 \to \pi/2$) of the torque density per molecule, and V_i^* is the volume available for the jumping molecule after the local lattice expansion referred to above. V_i^* is roughly the volume which should dispose each molecule if they were isotropically distributed. If ΔV^* represents the local expansion we may write:

$$V_i^* = V_N^* + \Delta V^* \tag{8}$$

where V_N^* is the volume per molecule in the nematic phase. The change in volume at the nematic-isotropic transition is only a very small fraction of the nematic volume V_N and the temperature variations of V_N and V_I are very similar. V_I is the actual volume in the isotropic phase. As we expect $V_i \simeq V_I^e$ (V_I^e being equal to V_I as extrapolated from the isotropic phase) it is clear that ΔV^* should be nearly temperature independent. On the other hand, the internal pressure variation Δp necessary to produce this volume expansion ΔV^* should be strongly dependent on temperature and increase as the crystalisation point is approached. In fact, the mean field theory of Maier and Saupe [5], predict:

$$\Delta p = \left(\frac{\partial U_{ord}}{\partial V_N}\right)_S = \frac{N_A}{m} \frac{A}{V_N^3} S^2 \tag{9}$$

where U_{ord} is the internal energy associated with nematic order and S is the usual order parameter.

From expressions (6) and (7) we have:

$$\gamma_1 = \frac{N^*}{\Omega^*} = \frac{kT}{\pi^2 V_i^*} \frac{1}{\nu_0}. \tag{10}$$

In order to write this formula in a more convinient way, we now remember the following thermodynamic relation

$$V_i^* \chi_i = \Delta V^* / \Delta p$$

where, according to the definition of V_i^* given above, the quantity χ_i denotes the isothermal compressibility of the state with an isotropic distribution of the molecular axes (at the temperature corresponding to V_N). On substituting V_i^* taken from this relation into the expression (10) we get:

$$\gamma_1 = \frac{k\,T\,\chi_i}{\pi^2\,(\Delta\,V^*)}\,(\Delta\,p)\,\frac{1}{\nu_0}\,.$$

If we finally substitute here the value of ν_0 as given by (4) and the value of Δp taken from (9) we find:

$$\gamma_1 = c\,S^2 \exp\,(\varepsilon\,S/k\,T) \tag{11}$$

where c is a roughly temperature independent factor given by:

$$c = \frac{N_A}{m}\,\frac{h\,A\,\chi_i}{\pi^2\,(\Delta\,V^*)\,V_N^3\,\Pi}\,. \tag{12}$$

Here N_A is the Avogadro's number, and Π is the probability factor introduced in expression (4); the meaning of the other symbols was given above.

Expression (11) is our central result. It was first published in a previous Note by one of us, Ref. [6], without detailed demonstration (only the principle of our reasoning was given).

The *activation energy* which appears in (11) is proportional to the order parameter S and thus varies strongly with temperature. This behaviour contrasts with what is usual in isotropic liquids, for which E is constant over most practical temperature ranges. Expression (11) also shows that the *rotational* viscosity $\gamma_1(T)$ vanishes in the isotropic phase $(S = 0)$.

To complement the theory we have just outlined, a final remark is in order. In the foregoing discussion we have considered simple nematics where intermolecular position-correlations are not too strong, and the molecules *do not* form well defined clusters or cybotactic groups. If nematic molecules associate to form cybotactic groups or clusters composed of a great number of molecules some deviation from the curve (11) may occur. This point will be discussed elsewhere.

III — EXPERIMENTAL DATA AND DISCUSSION

An expression similar to (11) but with E = constant was first proposed empirically by Martins [7]. Helfrich proposed $\gamma_1 = b_1 S^2$ with b_1 = constant, for $|S| << 1$, which is not the current case [8].

It may be fruitful to contrast our results with a theory developed by Imura and Okano. From their paper we get:

$$\gamma_1 = 2 C_1 S + 2 C_2 S^2 \qquad (13)$$

where C_1 and C_2 are «constants which are expected to depend on temperature very weakly» [9]. Moreover, the term proportional to S^2 in expression (13) should be negligible as compared to the first.

We have used the least squares method to fit the experimental data on PAA and AD to equation (13) and have found that the contribution of the term in S^2 is dominant. We may conclude that $\gamma_1(T)$ as given by expression (13) cannot be approximated to first order in S. A similar situation is expected for some other viscosities of nematic liquid crystals [6].

On the other hand, the equations proposed by Imura and Okano contain only one activation energy which is defined in the isotropic phase by the usual Arrhenius' law. The theory outlined here predicts one more activation energy which is characteristic of rotational motions. The activation energy measured in the isotropic phase is characteristic of translational motions (as is the usual shear viscosity).

Let us now compare the predictions of our theory with experimental data. We start with the case of PAA and consider first expression (10) which is equivalent but simpler than expression (11). As $V_i \approx V_1^e$, and the volume change at the nematic-isotropic transition is $\Delta V_c = 0.0035\, V_{N,c}$ [5], we may write $V_i^* \simeq 1.0035\, V_N^* = 3.712 \times \times 10^{-22}\,cm^3/molec$. On the other hand we expect, to a good approximation that $1/\nu_o \simeq \tau_d^{(1)}$, where $\tau_d^{(1)}$ is a dielectric relaxation time relative to the orientational motion of the component of the permanent electric dipole parallel to the long molecular axis. With $\tau_d^{(1)} = 4.3 \times 10^{-9}$ s at 125° C [10] expression (10) gives $\gamma_1 = 0.064$ poise which is in excelent agreement with experience (see Fig. 1).

The experimental data on $\gamma_1(T)$ so far reported for PAA have yet been analysed in Ref. [6] in terms of expression (11). These

data are again displayed in Fig. 1 and their analysis repeated here for a matter of completeness. The data have been fitted to equation (11) by the least squares method, giving $c = 0.177$ poise and $\varepsilon = 0.879$ kcal/mole. In this calculation we have used the values of S as given by Chandrasekhar, which have been successfully contrasted with experience [11]. The data agree very well with our theoretical

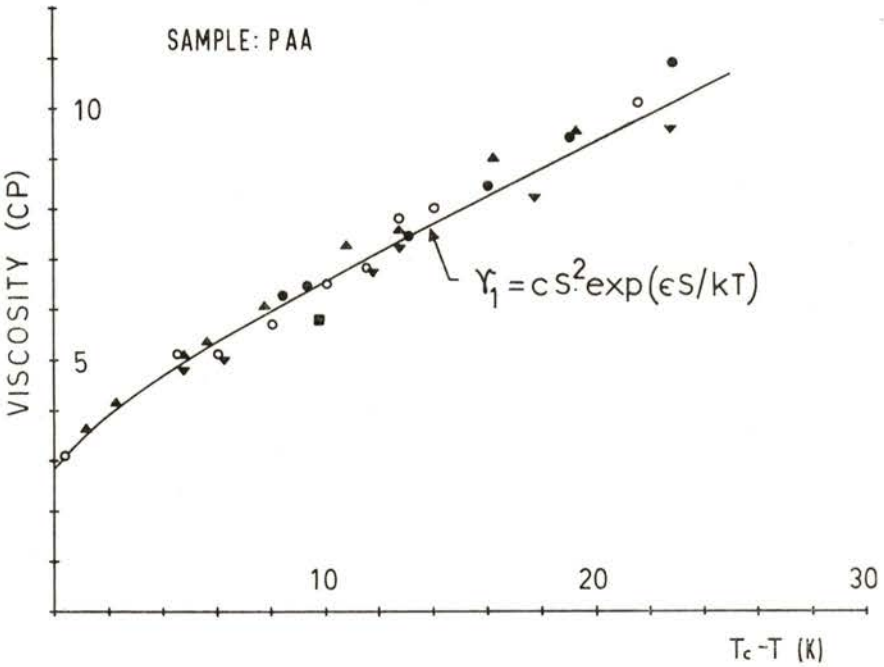

Fig. 1 — Rotational viscosity γ_1 (T) of PAA. Experimental points: open circles from ref. [3]; triangles from ref. [14]; full circles from ref. [16]; square from ref. [17].

prediction over the entire nematic range. Substituting in expression (10) the foregoing value of ε and the value of A/V_N^2 as given by Maier and Saupe [5] we find $m = 6.3$ for the nearest-neighbour coordination number. This seems to be a meaningful result. It is to be compared with the value $m = 6$ characteristic of a simple-cubic lattice considered by Lebwohl and Lasher in their Monte Carlo calculation [12]. Although this calculation gives very good results, we expect the actual value of m to be slightly larger than 6 because of the contribution of incoherent diffusion not considered in the lattice

model. This contribution should have a rather little effect in this case because the diffusion correlation time of PAA is about one order of magnitude greater than the correlation time characteristic of molecular reorientations [7]. Translational diffusion should be completely negligible if the time required for a molecule to diffuse through a distance comparable with the inter-molecular separation were much longer

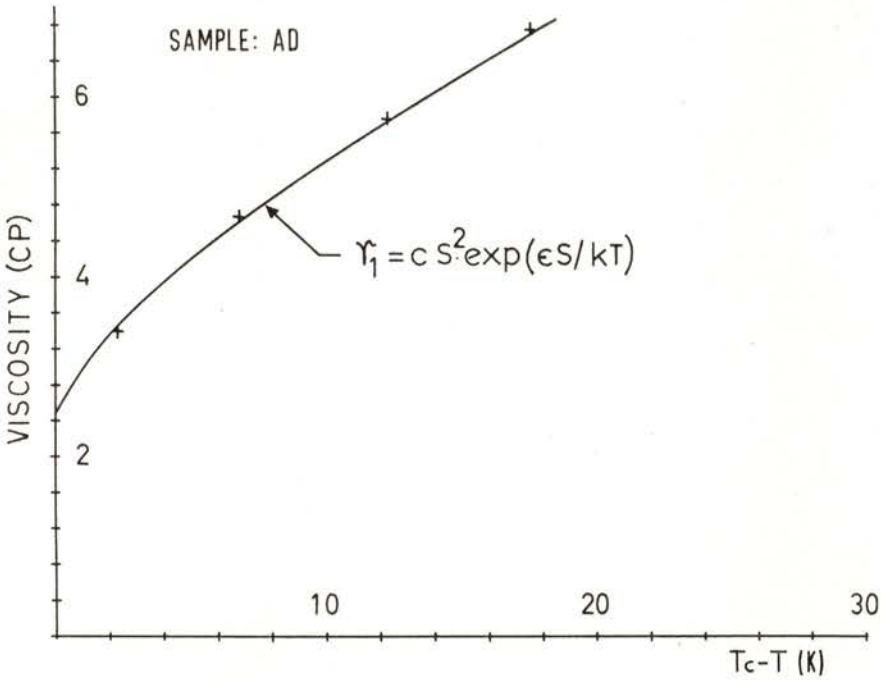

Fig. 2 — Rotational viscosity $\gamma_1(T)$ of AD. Experimental points from ref. [14].

than the characteristic time of reorientation. In such a situation the molecules could be treated as fixed at the lattice points.

In Fig. 2 are displayed the results we have obtained for anisaldazine (AD). This material clears at 454 K and its order parameter is known from the work of Madhusudana et al. [13]. The data on $\gamma_1(T)$ were reported by Yun [14]. Again, the agreement between expression (11) and experimental data is very good. We find now $c = 0.111$ poise and $\varepsilon = 0.890$ kcal/mole. From the equation $A = 4.55\,k\,T_c\,V_{N,c}^2$ established by Maier and Saupe [5] the value

$T_c = 454$ K, and the value $V_{N,c} = 257.775$ cm³/mole computed from the density data of Porter and Johnson [15], we find $m = 6.8$. This result compares well with that found for PAA. It may be less accurate as it has been computed from much less experimental data.

IV — CONCLUSION

We have outlined a molecular theory of the nematic rotational viscosity $\gamma_1(T)$ in the spirit of the theory of rate processes. Although established along very simple lines, our theory furnishes a new expression for $\gamma_1(T)$ which is strongly supported by the experimental data available for *p*-azoxyanisole and anisaldazine. Of particular importance is the agreement obtained near T_c.

It is our hope that this theory should be reformulated more rigorously and applied to other cases. Materials with a smectic A-nematic transition should be studied with particular interest near this transition. In any case, precise measurements of the degree of order are required, together with the measurements of $\gamma_1(T)$. We should also try a molecular interpretation of the other viscosities characterizing nematics. Preliminary arguments on this problem have been already presented elsewhere [6, 9].

REFERENCES

[1] LESLIE, F. M., *Arch. Rational Mech. Anal.* **28** (1968) 265.

[2] DE GENNES, P. G., *The Physics of Liquid Crystals* (Oxford University Press) 1974.

[3] GASPAROUX, H., PROST, J., *J. Physique* **32** (1971) 953.

[4] GLASSTONE, S. N., LAIDLER, K., EYRING, H., *The theory of Rate Processes* (Mc Graw Hill) 1941.

[5] MAIER, W., SAUPE, A., *Z Naturforchg.* **14a** (1959) 882; **15a** (1960) 287.

[6] MARTINS, A. F., *Portg. Phys.* **9**, 1 (1974) 1.

[7] MARTINS, A. F., Thesis, U. Grenoble (1972), published in *Portg. Phys.* **8**, 1-2 (1972) 1-166 and by French Atomic Energy Comission: Rapport CEA-R-4492.

[8] HELFRICH, W., *J. Chem. Phys.* **56** (1972) 3187.

[9] IMURA, H., OKANO, K., *Jap. J. Appl. Phys.* **11** (1972) 1440.

[10] MARTIN, A. J., MEIER, G., *Symposia of the Faraday Society*, n.º 5 (1971) 119.

[11] CHANDRASEKHAR, S., MADHUSUDANA, N. V., *Mol. Cryst. Liquid Cryst.* **10** (1970) 151.

[12] LEBWOHL, P. A., LASHER, G., *Phys. Rev.* **A6** (1972) 426. Note that the ε's definition of Lebwohl and Lasher is not the same as that given by expression (3) in this paper: within the mean field approximation we have $\varepsilon_{LL} = -(2/3)\varepsilon$.

[13] MADHUSUDANA, N. V., SHASHIDHAR, R., CHANDRASEKHAR, S, *Mol. Cryst. Liquid Cryst.* **13** (1971) 61.

[14] YUN, C. K., *Phys. Lett.* **43A** (1973) 369.

[15] PORTER, R. S., JOHNSON, J. F., *J. Appl. Phys.* **34** (1963) 51.

[16] MEIBOOM, S., HEWITT, R. C., *Phys. Rev. Lett.* **30** (1973) 261.

[17] ORSAY LIQUID CRYSTAL GROUP, *Mol. Cryst. Liquid Cryst.* **13** (1971) 187.

LA CORRESPONDANCE ENTRE MODELES MICROSCOPIQUES ET MACROSCOPIQUES (*)

E. MATAGNE

Bâtiment Maxwell Faculté des Sciences Appliquées
Louvain-la-Neuve

ABSTRACT — The purpose of this paper is to show how to derive macroscopic quantities by taking the average of microscopic quantities without using either vectorial type integrals or volume integrals.

In contrast with the usual methods [3], [8], [11], [12], it follows that the method developed here is compatible with theories referring to a curved space (e. g. general relativity). However, since these theories could not yet have been put in agreement with quantum theories, this study is achieved at a purely classical (non-quantified) level, in spite of an analogy with the quantum theories.

An approximate method of calculation, which is derived almost automatically from the definition of macroscopic quantities, is also developed.

By using a spherical approximation, an approximate calculation is finally carried out on three classical examples, which are

— the evaluation of the conductivity of an emulsion
— the calculus of the dielectric permeability of a polar gas, and
— the derivation of the properties of a «cold plasma» in the general relativity theory.

Although the results of these calculations are not very original, especially as far as the two first examples are concerned, we found it interesting to recalculate them by this method which is more deductive than usually presented methods, and which opens the way to more general results.

RESUMÉ — Le propos de cet article est de montrer comment l'on peut obtenir des grandeurs macroscopiques comme moyennes effectuées sur des grandeurs microscopiques *sans avoir recours* à des intégrales de type vectoriel, ni à des intégrales de volume.

La définition proposée présente dès lors l'avantage sur les méthodes habituelles [3], [8], [11], [12] d'être compatible avec les théories qui font intervenir un espace courbe (par exemple la relativité générale).

(*) Received 19 November 1976.

Par contre, ces dernières théories n'ayant pas encore pu être conciliées avec les théories quantiques, l'étude ci-dessous reste purement classique (non-quantique), ce qui n'empêchera pas de relever une analogie avec les théories quantiques.

Une méthode de calcul approchée, qui dérive presque trivialement de la définition des grandeurs macroscopiques, sera aussi présentée.

Finalement, en faisant usage d'une approximation sphérique, le calcul approché sera fait à propos de trois exemples classiques, à savoir le calcul de la conductivité d'une émulsion, le calcul de la perméabilité diélectrique d'un gaz polaire et le calcul des propriétés d'un «plasma froid» en relativité générale.

Bien que les résultats eux-mêmes manquent d'originalité, spécialement en ce qui concerne les deux premiers exemples, il nous a semblé intéressant de les retrouver par cette méthode plus déductive que ce qui est habituellement présenté et d'ouvrir ainsi la voie à une généralisation possible.

1. INTRODUCTION

Dans beaucoup de cas, un même phénomène peut être décrit par plusieurs modèles dont certains, dits microscopiques, entrent dans le détail d'inhomogénéités que d'autres, dits macroscopiques, ne considèrent pas.

En électromagnétisme, Maxwell lui-même [1] s'attacha à calculer la conductivité d'une émulsion. Il est clair que cette notion n'a de sens que si l'on considère l'émulsion comme un milieu homogène. Le calcul s'effectue en mettant ce modèle «macroscopique» en correspondance avec un modèle «microscopique» où le milieu comprend deux phases de conductivités différentes.

Lorsque Carter [2] [5] tint compte de l'influence des encoches dans une machine électrique en remplaçant l'entrefer par un entrefer moyen (et donc le champ magnétique microscopique par un champ macroscopique), il effectuait une démarche du même genre.

A une autre échelle, la théorie de l'électron [3] met en correspondance un modèle microscopique formé de particules et un modèle macroscopique des milieux électromagnétiques matériels.

Plus près de nous, l'électromécanique étudie couramment les machines à courant continu en utilisant non pas un modèle de circuits filiformes à commutation mais un modèle «macroscopique» de circuits à contacts glissants dont les phénomènes de commutation ont été exclus ainsi que les fluctuations des tensions de période inférieure à l'intervalle de commutation [15].

On le voit, les mots «macroscopique» et «microscopique» sont tout relatifs. Pour le cosmologue, l'univers est empli d'une densité continue de matière et, si l'on veut déduire cette densité continue

d'un modèle «microscopique», c'est à l'échelle des amas de galaxies que la moyenne doit être faite [17].

A partir de cet extrême, on pourrait considérer de multiples intermédiaires dans la descente vers l'infiniment petit en considérant l'échelle des galaxies, des systèmes planétaires, des astres, des atomes (mot assez malheureux), des particules élémentaires (mot probablement tout aussi malheureux car le foisonnement de ces particules donne à penser qu'elles ne sont pas si élémentaires).

Finalement, on songe à un milieu «subquantique».

Nous pouvons donc seulement, puisque nous ne disposons pas d'un modèle «le plus microscopique possible», ordonner les modèles existants en disant que l'un est plus microscopique que l'autre.

Souvent, les deux modèles (l'un microscopique et l'autre macroscopique) que l'on souhaite mettre en correspondance font appel à une même théorie physique. Ainsi, Maxwell [1] utilise deux fois l'électromagnétisme quasistatique galvanique et Carter [2] utilise seulement l'électromagnétisme quasistatique magnétique.

D'autres fois, la théorie microscopique est un cas particulier de la théorie macroscopique. Ainsi Lorentz [3] utilise au niveau microscopique l'électromagnétisme dans le vide, où l'on peut identifier les champs et les inductions puisque ε_0 et μ_0 sont prises comme constantes universelles, alors que la théorie macroscopique utilise des perméabilités dépendant du milieu considéré.

On pourrait également imaginer que les théories microscopiques et macroscopiques n'aient que de lointains rapports (Wheeler 1970, repris en [17]).

2. LIMITATIONS DES DEFINITIONS COURANTES

Lorsque les deux modèles à mettre en correspondance font appel à des théories se déroulant dans un même cadre spatio-temporel plat, c'est à dire lorsqu'elles sont du niveau de la relativité galiléenne ou de la relativité restreinte d'Einstein, le passage peut s'effectuer d'une façon simple, au moins conceptuellement, en utilisant des moyennes obtenues par intégration spatiale et temporelle.

Catte méthode a été utilisée par Lorentz et portée à son apogée par de Groot [11] [12]. Elle est pourtant sujette à des critiques du point de vue conceptuel car on voit mal comment un effet microscopique *de volume* pourrait influencer un observateur macroscopique. Cela ne devrait jouer un rôle fondamental que pour une théorie

admettant l'action instantanée à distance, hypothèse peu fructueuse en physique.

La méthode est également limitée dans ses applications. Puisqu'elle fait appel à l'intégration de grandeurs vectorielles, elle ne peut pas être généralisée à un espace-temps courbe et se trouve donc en défaut à l'échelle de l'univers (red-shift) et de l'astrophysique (trous noirs).

Elle est également discutable à l'échelle des particules élémentaires. En effet, celles-ci apparaissent alors comme une simple idéalisation des sphères chargées dont se servaient les premiers expérimentateurs; tout au plus les réduit-on, par un passage à la limite, à des répartitions de source en delta de Dirac [8].

Or ce point de vue n'est pas exempt de contradictions; Lorentz lui-même faisant remarquer qu'une particule ponctuelle chargée serait entourée d'une énergie infinie.

En relativité spéciale, cette particule aurait alors une inertie infinie et il serait impossible de la faire dévier de sa trajectoire rectiligne. On peut donc supposer qu'il existe, au voisinage des particules, des densités d'énergie suffisantes pour incurver l'espace: c'est à la relativité générale qu'il faudrait alors avoir recours.

Ainsi, les géométries des modèles microscopique et macroscopique peuvent être différentes, la première présentant des courbures très fortes là où la seconde est presque plate.

3. ESSAI DE DEFINITION DE LA CORRESPONDANCE ENTRE MODELES

Considérons deux modèles décrivant un même phénomène physique. Ces modèles peuvent faire intervenir des géométries spatio-temporelles différentes: nous supposerons seulement que la dimension est 4 dans les deux modèles.

Divisons les espaces en cellules dont les frontières évitent les singularités éventuelles.

Ces frontières de cellules sont donc des sous-espaces à trois dimensions, ordinairement deux dimensions spatiales et une dimension temporelle.

Les frontières des cellules sont supposées avoir la même topologie dans les deux modèles (à deux cellules contigues dans un modèle correspondent deux cellules contigues de l'autre) et nous pouvons donc les mettre en correspondance biunivoque continue. Ces opérations

mathématiques peuvent s'interpréter physiquement comme le choix d'une échelle de grandeur.

Nous dirons que les deux modèles se correspondent à l'échelle des cellules considérées si tous le flux que l'on peut définir sur les interfaces séparant les cellules sont identiques, qu'ils soient calculés en suivant l'un ou l'autre modèle.

Cette définition suppose évidemment une définition de ce que nous appellons un flux sur un interface : il s'agira d'un nombre *scalaire* obtenu par intégration sur l'interface considéré de grandeurs intrinsèques à cet interface.

Ainsi, nous n'avons besoin ni de moyennes vectorielles, ni d'intégrales de volume. Ce point de vue est plus satisfaisant pour notre esprit anthropomorphique (on ne peut déplacer un objet qu'en le touchant, c'est-à-dire à travers une surface de séparation entre notre corps et l'objet considéré) qui nous conduit à nier l'action instantanée à distance.

Bien que les idées ci-dessus n'aient jamais fait l'objet, à notre connaissance, d'un exposé systématique, on peut en trouver les germes chez des auteurs aussi disparates que Carter [2] [5], Lorentz [3], Wigner-Seitz [6] et Lindquist-Wheeler [9].

Il reste à expliquer ce que nous appellerons une grandeur intrinsèque.

Tout d'abord, cette grandeur doit pouvoir être décrite en utilisant seulement la structure interne de l'interface ; si nous admettons que cet interface est une variété différentiable de dimension 3, il s'agira donc d'objets géométriques sur cette variété, par exemple des vecteurs ou des tenseurs de dimension 3.

En outre, les grandeurs intrinsèques doivent pouvoir être calculées à partir des champs sur l'espace à 4 dimensions voisin de la frontière. Plus précisement, à partir de ceux de ces champs qui interviennent dans les conditions aux limites d'un problème de Cauchy. En effet, ces grandeurs doivent prendre une valeur unique, qu'elles soient calculées d'un côté ou de l'autre de la frontière.

Lorsque l'on considère une théorie dont le formalisme distingue nettement les équations d'évolution des relations constitutives (tel est par exemple le cas de l'électromagnétisme de Minkowski), nous dirons qu'une grandeur est intrinsèque à un interface si elle est astreinte *de par les équations d'évolution* à rester continue lors de la traversée de l'interface considéré.

Ainsi, le champ électrique $E_\perp$ perpendiculaire à une surface n'est pas une grandeur intrinsèque parce qu'il peut prendre des valeurs

différentes de part et d'autre de cette surface si celle-ci correspond à une discontinuité de la perméabilité diélectrique.

Même si l'on élimine du modèle ces discontinuités, nous ne considérerons pas $E_\perp$ comme une grandeur intrinsèque parce que sa continuité n'est alors garantie que par une relation constitutive. En fait, les relations d'évolution

$$\nabla \times \vec{E} + \partial \vec{B}/\partial t = 0 \quad \text{et} \quad \nabla \cdot \vec{B} = 0 \tag{1}$$

$$\nabla \times \vec{H} - \partial \vec{D}/\partial t = \vec{J} \quad \text{et} \quad \nabla \cdot \vec{D} = \rho \tag{2}$$

entraînent seulement la continuité de $\vec{E}_{//}$ et $B_\perp$ d'une part, $D_\perp$ et $\vec{H}_{//}$ de l'autre, ces grandeurs étant désormais considérées comme intrinsèques.

Le problème est plus confus lorsque l'on a affaire à une théorie comme la théorie de la gravitation d'Einstein où les relations d'évolution ne se dégagent pas entièrement des relations constitutives. On peut trouver des éléments de réponse dans les travaux de Lichnerowicz [7] et de Misner (par exemple [17]).

Selon Lichnerowicz, la condition de raccordement à vérifier en théorie d'Einstein est l'existence d'un système de coordonnées admissible au voisinage de la frontière et tel que la métrique $g_{\mu\nu}$ et ses dérivées premières y soient de classe C_1. Les données de Cauchy sont donc les potentiels $g_{\mu\nu}$ et leurs dérivées premières.

Cette condition est fort concise mais souvent difficile à appliquer parce qu'elle impose la construction d'un tel système de coordonnées. Il est préférable de remplacer la condition de Lichnerowicz par l' existence de grandeurs intrinsèques que l'on puisse comparer de façon algébrique.

Soit donc $\{x^i\}$ $(i = 1, 2, 3)$ un système de coordonnées décrivant la frontière et le repère naturel

$$e^\mu_i = \frac{\partial x^\mu}{\partial x^i} . \tag{3}$$

On peut montrer en passant au système de coordonnées de Gauss (cfr par exemple [17]) que la donnée de $g_{\mu\nu}$ et de ses dérivées revient à la donnée de la métrique intrinsèque

$$g_{ij} \underset{\text{déf}}{=} g_{\mu\nu} e^\mu_i e^\nu_j \tag{4}$$

et du tenseur accélération-courbure extérieure

$$K_{ij} \underset{\text{déf}}{=} \hat{n}_\mu \, a^\mu_{ij} \tag{5}$$

où, n_μ étant la forme (de poids -1) normale à la frontière

$$n_\mu \underset{\text{déf}}{=} \varepsilon_{\mu\nu\rho\sigma} \, e_1^\nu \, e_2^\rho \, e_3^\sigma , \tag{6}$$

on a défini

$$\hat{n}_\mu = \frac{n_\mu}{\sqrt{g^{\varepsilon\eta} \, n_\varepsilon \, n_\eta}} \tag{7}$$

tandis que les a^μ_{ij} sont les accélérations-courbures associées aux x^i :

$$a^\mu_{ij} \underset{\text{déf}}{=} \frac{d^2 x^\mu}{d x^i \, d x^j} + \Gamma^\mu_{\nu\rho} \, e_i^\nu \, e_j^\rho . \tag{8}$$

Nous n'avons considéré comme fondamentales, ni en électromagnétisme ni en gravitation, la continuité des sources, c'est à dire du courant perpendiculaire à la frontière dans le premier cas, du flux d'énergie (ou de matière?) et des tensions tangentielles dans le second.

Ces conditions sur les sources se trouvent en effet vérifiées automatiquement lorsque les conditions sur les champs le sont. Ainsi, en électromagnétisme, la continuité du champ magnétique et éventuellement du courant de déplacement suffit à garantir la continuité du courant.

En outre, la composante du vecteur de Poynting perpendiculaire à la surface, $\vec{E}_{//} \times \vec{H}_{//} \cdot \vec{n}$, est continue en même temps que $\vec{E}_{//}$ et $\vec{H}_{//}$.

De même, en théorie d'Einstein, Lichnerowicz [7] a montré que les données de Cauchy suffisent à déterminer la partie du tenseur d'Einstein normale à la frontière.

En pratique, il sera cependant souvent avantageux de remplacer certaines conditions sur les champs par des conditions sur les sources, procédé qui sera utilisé à la section VI.

4. DISTINCTION ENTRE MODELES MACROSCOPIQUE ET MICROSCOPIQUE

A l'échelle *d'une division en cellules donnée*, un modèle sera dit macroscopique si les grandeurs auxquelles il fait appel sont constantes

d'un point à l'autre de la cellule (en particulier, aucune singularité ne peut être contenue dans les cellules).
Dans certains cas, cette condition d'homogénéité n'est pas tout à fait respectée. Je me permettrai donc d'appeller macroscopique un modèle tel que les dimensions des cellules soient plus petites qu'une distance caractéristique de variation des champs (par exemple un quart de longueur d'onde).

Cependant, lorsque les dimensions des cellules sont comparables à la distance caractéristique, on arrive à ce résultat désagréable que les relations constitutives dépendent de la répartition des champs. C'est ainsi qu'aux petites longueurs d'onde, la perméabilité diélectrique varie rapidement en fonction de la fréquence jusqu'au moment où cette notion perd toute signification, la longueur d'onde étant inférieure aux dimensions des cellules.

De même, en ferromagnétisme, les domaines de magnétisation peuvent être de dimensions comparables à celles de l'échantillon : les dimensions de l'échantillon interviennent alors dans les relations constitutives.

En électromécanique, la distance entre deux encoches et la distance entre deux sections de bobinage ne sont inférieures que d'un ordre de grandeur aux dimensions de la machine. Il n'y a donc rien d'étonnant à ce que certains paramètres macroscopiques dépendent de la répartition des champs (c'est-à-dire, dans ce cas, du pas polaire).

Enfin, un modèle sera dit microscopique s'il n'est pas macroscopique.

A noter que la distinction entre modèles microscopiques et macroscopiques est indépendante de la distinction faite en physique entre les théories corpusculaires et celles de type «continuum». En particulier, un modèle microscopique peut être basé sur une théorie de type milieu continu comme ce sera d'ailleurs le cas pour l'exemple de la section 6.

5. PROCEDES DE CALCUL

Les définitions données aux sections précédentes ne permettent guère en général d'effectuer de façon exacte le calcul des grandeurs macroscopiques en fonction des grandeurs microscopiques, car on ne dispose pas d'une méthode générale permettant de choisir une disposition des cellules rendant possible la mise en correspondance avec un modèle macroscopique.

Trouver le découpage en cellules adéquat est en fait la plus grande difficulté rencontrée dans l'application des définitions ci-dessus.

Pratiquement, ou supposera que le modèle microscopique présente de fortes symétries. Le découpage en cellules pourra alors se faire en fonction d'un nombre réduit de paramètres, après quoi il ne restera plus qu'à écrire les grandeurs macroscopiques en fonction d'un certain nombre (heuristique) de paramètres et à déterminer tous ces paramètres en identifiant les flux calculés selon les deux modèles.

Il est clair que l'on ne peut découper l'espace en cellules sphériques, mais l'approximation sphérique constitue néanmoins une bonne approximation dans les cas isotropes. On se permet même de prendre un modèle microscopique à symétrie sphérique (par exemple un corpuscule au centre d'une cellule sphérique comme à la section 7).

On trouve dans les articles dê Wigner-Seitz [6] et Lindquist--Wheeler [9] des considérations permettant de se faire une idée de la gravité des erreurs dues à l'approximation sphérique.

Pour traiter les cas légérement anisotropes, nous proposerions l'utilisation de cellules ellipsoïdales, le découpage en cellules permettant alors d'introduire deux ou trois paramètres (au lieu d'un seul rayon pour une cellule sphérique).

Pour ces cellules, sphériques ou ellipsoïdales, à haut degré de symétrie, il peut arriver que les grandeurs intrinsèques à la surface de la cellule coïncident point par point dans les deux modèles (et non p'us seulement par leurs intégrales de flux).

En pareil cas, on peut d'ailleurs concevoir le problème comme un problème de raccordement entre une solution microscopique valable à l'intérieur de la cellule et une solution macroscopique valable à l'extérieur.

Nous examinerons aux sections suivantes des exemples de ce type où le calcul analytique sera possible.

6. CONDUCTIVITE D'UNE EMULSION

Proposons nous de calculer «la conductivité d'un milieu homogène comportant une phase continue de conductivité σ_1 et une phase dispersée sous forme de sphères de conductivité σ_2, en fonction du taux de la second phase, soit α» .

Tel est le programme défini par Maxwell dès 1891.

6. 1. *Modèle microscopique*

Ce modèle utilise l'électromagnétisme au niveau galvanique.

Considérons une cellule sphérique de rayon a, dont l'intérieur comprend les deux phases de conductivité σ_1 et σ_2. Pour permettre le calcul analytique, nous supposerons que la phase dispersée occupe une sphère située au centre de la cellule. Afin que le volume de cette phase soit bien une fraction α du volume total de la cellule, il faut lui donner un rayon $a\sqrt[3]{\alpha}$.

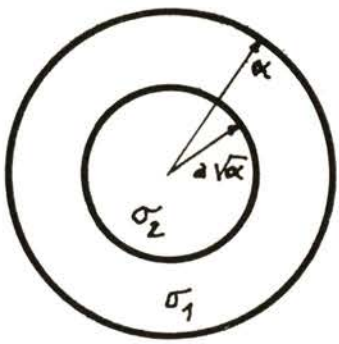

Fig. 1

En phase continue, nous allons essayer un potentiel comportant un terme dipolaire :

$$\phi = (A\,r + B\,r^{-2})\cos\theta\,. \tag{11}$$

Par contre, en phase dispersée, nous devons adopter un potentiel dépourvu de singularité en $r = 0$. Soit donc un champ homogène

$$\phi = e\,r\cos\theta\,. \tag{12}$$

Comme ces potentiels doivent coïncider en $r = a\,\alpha^{\frac{1}{3}}$ on obtient une première relation entre les paramètres :

$$e = A + B/(\alpha\,a^3)\,. \tag{13}$$

La conservation du courant normal à la frontière, que nous utiliserons à la place de la continuité du champ magnétique tangentiel, fournit une seconde relation:

$$\sigma_1 \frac{\partial \phi_1}{\partial r}\bigg|_{r=a\sqrt[3]{\alpha}} = \sigma_2 \frac{\partial \phi_2}{\partial r}\bigg|_{r=a\sqrt[3]{\alpha}} \tag{14}$$

dont on tire

$$\sigma_1 (A - 2B/(\alpha a^3)) = \sigma_2 e . \tag{15}$$

On peut éliminer B et e entre (13) et (15) et obtenir le potentiel en phase continue en fonction d'un seul paramètre A:

$$\phi = A\left(r + \frac{\sigma_1 + \sigma_2}{2\sigma_1 + \sigma_2}\alpha a^3/r^2\right)\cos\theta . \tag{16}$$

A la frontière ($r = a$), on a donc un potentiel

$$\phi = A\,a\left(1 + \alpha\frac{\sigma_1 - \sigma_2}{2\sigma_1 + \sigma_2}\right)\cos\theta \tag{17}$$

et une densité de courant radiale:

$$J_r = \sigma_1 A\left(1 - 2\alpha\frac{\sigma_1 - \sigma_2}{2\sigma_1 + \sigma_2}\right)\cos\theta . \tag{18}$$

6. 2. *Modèle macroscopique*

Macroscopiquement, l'émulsion sera considérée comme un milieu isotrope, de conductivité σ. La théorie macroscopique est donc la même que la théorie microscopique, à savoir l'électromagnétisme galvanique.

Nous supposons un champ uniforme (ce qui est normal pour une théorie macroscopique considérée à l'échelle des cellules):

$$\phi = E\,r\cos\theta . \tag{19}$$

Le choix de l'échelle ne pose aucune difficulté ici: on peut en effet adopter la même géométrie et le même système de coordonnées pour les modèles microscopique et macroscopique, ainsi que la même cellule sphérique de rayon a (pour être strict, il faudrait ne procéder à l'identification qu'au paragraphe suivant).

Le potentiel sur la frontière est

$$\phi = E\, a \cos\theta \tag{20}$$

et la densité de courant radiale :

$$J_r = \sigma E \cos\theta . \tag{21}$$

6. 3. *Mise en correspondance*

Il est possible, en éliminant E et A, d'identifier les potentiels (17) et (20), ainsi que les courants (18) et (21).

Le fait que cette identification soit possible justifie d'ailleurs à posteriori le choix de l'expression (11) pour le potentiel microscopique.

L'identification impose la valeur de la conductivité macroscopique

$$\sigma = \sigma_1 \frac{1 - 2\alpha(\sigma_1 - \sigma_2)/(2\sigma_1 + \sigma_2)}{1 + \alpha(\sigma_1 - \sigma_2)/(2\sigma_1 + \sigma_2)} \tag{22}$$

indépendamment de la taille des cellules.

6. 4. *Commentaire*

La loi (22) a été obtenue par Maxwell [1] en suivant une méthode différente, mais faisant également appel à une approximation sphérique. Elle rend compte de l'expérience dans une large plage de variation du taux α [16].

Signalons que la méthode de calcul utilisée ici pourrait se généraliser facilement au cas anisotrope où la phase dispersée ne se présente plus sous forme sphérique.

Cette situation se rencontre lorsque l'une des deux phases est soumise à un gradient de pression auquel l'autre phase échappe. Ainsi, si une émulsion composée de phases de densités différentes est soumise à l'action d'un champ de gravitation (ou, ce qui revient au même, à un champ d'accélération), la phase dispersée sera en mouvement relatif par rapport à la phase continue et ce mouvement se traduira par un aplatissement des bulles.

Une situation analogue se rencontre dans les machines magnétohydrodynamiques à emulsion, car la phase la plus conductrice subira alors davantage la force de Lorentz

$$\vec{F} = \vec{J} \times \vec{B} \tag{23}$$

où $\vec{F}$ est la densité de force, $\vec{J}$ la densité de courant et $\vec{B}$ l'induction magnétique.

Ces anisotropies peuvent s'étudier en ajoutant aux potentiels (11) des termes supplémentaires du développement en harmoniques sphériques et en modifiant la forme des cellules de façon à pouvoir encore identifier les différentes expressions des potentiels et des courants normaux sur les frontières. Pour des taux de phase dispersée importants, il faut abandonner ces formes ellipsoïdales au profit de formes polygonales.

Ces différentes généralisations feront l'objet d'une autre étude.

7. PERMEABILITE DIELECTRIQUE

Dans cette section, nous nous proposons de calculer la perméabilité diélectrique d'un milieu homogène, composé de dipôles identiques, orientés dans la même direction et répartis au hasard.

L'historique de cet ancien problème peut être trouvée dans le livre d'Elliott [14].

7. 1. *Modèle microscopique*

Ce modèle utilise l'électromagnétisme quasistatique électrique du vide; la perméabilité diélectrique y est donc une constante ε_0 permettant d'éliminer l'induction $\vec{D}$ en fonction du champ $\vec{E}$.

Au voisinage d'un dipôle, nous adopterons une solution du type (11), qui superpose un champ uniforme au champ propre du dipôle:

$$\phi := \left(e\, r - \frac{1}{4\pi\varepsilon_0} \frac{p}{r^2} \right) \cos\theta \tag{24}$$

où e est le champ «local» vu par le dipôle et p la valeur du dipôle, supposé orienté dans la direction $\vec{a}_z$.

En ce qui concerne le choix de l'échelle, nous nous tournons à nouveau vers une cellule sphérique de rayon a, contenant un seul dipôle situé en son centre.

A la frontière, on obtient donc un potentiel

$$\phi = \left(e\, a - \frac{1}{4\pi\varepsilon_0} \frac{p}{a^2} \right) \cos\theta \tag{25}$$

et une composante radiale de l'induction électrique :

$$D_r = \varepsilon_0 \left(e + \frac{1}{2\pi\varepsilon_0} \frac{p}{a^3} \right) \cos\theta . \tag{26}$$

7. 2. *Modèle macroscopique*

A l'extérieur de la cellule, le modèle utilisé sera celui de Maxwell-Minkowski, qui fait appel comme variables électriques à la fois au champ $\vec{E}$ et à l'induction $\vec{D}$.

Ces grandeurs sont évidemment supposées homogènes à l'échelle des cellules, de sorte que le champ dérivera d'un potentiel

$$\phi = E r \cos\theta \tag{27}$$

et nous supposons à cause de l'isotropie du problème l'introduction orientée comme le champ selon l'axe des z.

La cellule est bien entendu une sphère de rayon a dont nous pouvons maintenant donner l'expression :

$$a = \left(\frac{3}{4 r n} \right)^{\frac{1}{2}} \tag{28}$$

n étant la densité de cellules (supposées identiques) donc finalement de dipôles.

Le potentiel à la surface de la cellule vaut évidemment

$$\phi = E a \cos\theta \tag{29}$$

tandis que la composante radiale de l'induction est

$$D_r = D \cos\theta . \tag{30}$$

7. 3. *Mise en correspondance*

L'identification de (25) et (27) fournit, compte tenu de (28) :

$$E = e - \frac{1}{3} \frac{n p}{\varepsilon_0} . \tag{31}$$

Paradoxalement, c'est Lorentz lui-même qui obtint le premier cette relation [3] en utilisant également une approximation sphérique. Mais Lorentz utilisait comme intermédiaire de calcul une densité de charge de surface à la frontière de la cellule et il effectuait le calcul en supposant la cellule vide. Cette manipulation consistant à enlever le dipôle pour calculer le champ local n'est licite que parce que la théorie électromagnétique du vide utilisée ici est linéaire.

De l'identification de (26) et (30) on déduit en tenant compte de (28) la valeur de l'induction :

$$\mathrm{D} = \varepsilon_0 \left(e + \frac{2}{3} \frac{np}{\varepsilon_0} \right). \tag{32}$$

On notera que, contrairement à ce qui est affirmé par certains auteurs, le champ macroscopique E n'a pas à être égal au champ local e.

7. 4. *Obtention des relations macroscopiques*

De (31) et (32), on peut tirer

$$\mathrm{D} = \varepsilon_0 (\mathrm{E} + np/\varepsilon_0) \tag{33}$$

à laquelle on peut donner l'apparence d'une relation macroscopique en posant

$$\vec{\mathrm{P}} = np\vec{a}_z \tag{34}$$

ce qui permet de réécrire (33) :

$$\vec{\mathrm{D}} = \varepsilon_0 \vec{\mathrm{E}} + \vec{\mathrm{P}}. \tag{35}$$

Cette expression, souvent considérée comme une définition de $\vec{\mathrm{D}}$, est ici obtenue par voie déductive dans le cas particulier qui nous occupe.

En fait, elle fait intervenir plus de grandeurs macroscopiques que nécessaire, $\vec{\mathrm{P}}$ étant superflue.

Pour obtenir une relation macroscopique entre $\vec{\mathrm{E}}$ et $\vec{\mathrm{D}}$ seulement, on doit ajouter à (31) et (32) une relation microscopique entre e et p.

La plus simple est l'approximation linéaire due à Mossotti (1847) qui suppose p proportionnel au champ local, soit

$$p = \alpha e . \tag{37}$$

On peut alors obtenir l'expression classique

$$\frac{D}{E} = \varepsilon = \varepsilon_0 \frac{1 + 2\alpha n/3}{1 - \alpha n/3} \tag{38}$$

de la perméabilité diélectrique macroscopique.

La dépendance de α en fonction de la température a été introduite par Debye (1945) dans la relation (38) et le résultat est actuellement connu sous le nom de relation de Clausius-Mossotti.

8. PROPRIETES D'UN PLASMA FROID

Les exemples précédents faisaient intervenir des modèles microscopiques et macroscopiques se déroulant dans un cadre spatio-temporel commun.

Comme annoncé dans l'introduction, ceci n'est pas nécessaire avec les conceptions adoptées ici; je vais illustrer ce fait tout en généralisant légèrement un calcul dû à Lindquist et Wheeler [7] pour l'étendre au cas de particules chargées.

8. 1. *Modèle microscopique*

Ce modèle utilisera la théorie d'Einstein en schéma électromagnétique pur.

L'univers est supposé peuplé de corpuscules à symétrie sphérique. Cette symétrie impose à la métrique d'être, au voisinage d'un corpuscule, la métrique de Reissner-Nordström qui se trouve rappellée à l'annexe II:

$$d\sigma^2 = \Delta\, dt^{*2} - \frac{1}{c^2 \Delta}\, dr^2 - \frac{r^2}{c^2}(d\theta^2 + \sin^2\theta\, d\varphi^2) \tag{41}$$

où

$$\Delta = 1 - \frac{2M}{r} + \frac{Q^2}{r^2} . \tag{42}$$

La variable temporelle est notée t^* pour éviter toute confusion avec le temps macroscopique.

Il nous faut maintenant définir une échelle. Nous supposerons chaque corpuscule au centre d'une cellule à symétrie sphérique. En fait, ce n'est qu'à l'intérieur de cette cellule que (41) (42) sont valables.

Compte tenu de la symétrie sphérique, le mouvement de la frontière est décrit par une relation entre r et t^* que nous utiliserons sous forme paramétrique :

$$r = r(\tau) \tag{43}$$

$$t^* = t^*(\tau) . \tag{44}$$

La frontière doit donc être vue comme un sous-espace à trois dimensions de coordonnées τ, θ, φ. Nous imposerons à τ d'être un temps propre, c'est à dire :

$$\Delta \left(\frac{dt^*}{d\tau}\right)^2 - \frac{1}{c^2 \Delta}\left(\frac{dr}{d\tau}\right)^2 = 1 \tag{45}$$

de sorte que la métrique du sous-espace frontière est simplement :

$$d\sigma^2 = d\tau^2 - \frac{r^2}{c^2}(d\theta^2 + \sin^2\theta\, d\varphi^2) . \tag{46}$$

On remarquera que r a la dimension d'une longueur et est lié aux dimensions de la paroi. En effet, la circonférence vaut dans la métrique (46) $2\pi r$ et la surface $4\pi r^2/3$.

Par analogie avec les formules euclidiennes, on peut dire que $r(\tau)$ est le rayon de la cellule.

La normale à la frontière est

$$n_\mu = \varepsilon_{\mu\nu\rho\sigma} \frac{dx^\nu}{d\tau} \frac{dx^\rho}{d\vartheta} \frac{dx^\sigma}{d\varphi} = \left(\frac{dr}{d\tau}, -\frac{dt^*}{d\tau}, 0, 0\right) \tag{47}$$

que nous utiliserons normée

$$\hat{n}_\mu = \left(\frac{1}{c}\frac{dr}{d\tau}, -\frac{1}{c}\frac{dt^*}{d\tau}, 0, 0\right) . \tag{48}$$

L'accélération vaut

$$a^{\mu}_{\tau\tau} = \frac{d e_{\tau}}{d\tau} + \Gamma^{\mu}_{\nu\rho}\, e^{\nu}_{\tau}\, e^{\rho}_{\tau} = (a^{t^*}_{\tau\tau}, a^{r}_{\tau\tau}, 0, 0)^{\mathrm{T}}. \tag{49}$$

Or, puisque τ est un temps propre, l'accélération est perpendiculaire à la quadrivitesse

$$a^{t^*}_{\tau\tau}\,\Delta\,\frac{dt^*}{d\tau} - a^{r}_{\tau\tau}\,\frac{dr}{d\tau}\,\frac{1}{c^2\Delta} = 0 \tag{50}$$

ce qui permet d'éliminer les dérivées secondes de t^* :

$$a^{\mu}_{\tau\tau} = a^{r}_{\tau\tau}\left(\frac{1}{c^2\Delta^2}\,\frac{dr/d\tau}{dt^*/d\tau}, 1, 0, 0\right)^{\mathrm{T}}. \tag{51}$$

Quant à la composante $a^{r}_{\tau\tau}$, on obtient facilement

$$a^{r}_{\tau\tau} = \frac{d^2 r}{d\tau^2} + \Gamma^{r}_{t^*t^*}\left(\frac{dt^*}{d\tau}\right)^2 + 2\,\Gamma^{r}_{t^*r}\,\frac{dt^*}{d\tau}\,\frac{dr}{d\tau} + \Gamma^{r}_{rr}\left(\frac{dr}{d\tau}\right)^2 \tag{52}$$

qui s'écrit en utilisant les valeurs de la connexion affine données en annexe II et en simplifiant par (42)

$$a^{r}_{\tau\tau} = \frac{d^2 r}{d\tau^2} + c^2\left(\frac{M}{r^2} - \frac{Q^2}{r^3}\right). \tag{53}$$

Les autres «accélérations-courbures» sont plus simples :

$$a^{\mu}_{\tau\theta} = \left(0, 0, \frac{1}{r}\,\frac{dr}{d\tau}, 0\right)^{\mathrm{T}} \tag{54}$$

$$a^{\mu}_{\theta\theta} = \left(0, 0, 0, \frac{1}{r}\,\frac{dr}{d\tau}\right)^{\mathrm{T}} \tag{55}$$

$$a^{\mu}_{\theta\theta} = (0, -r\Delta, 0, 0)^{\mathrm{T}} \tag{56}$$

$$a^{\mu}_{\varphi\varphi} = (0, -r\Delta\sin^2\theta, -\sin\theta\cos\theta, 0)^{\mathrm{T}} \tag{57}$$

$$a^{\mu}_{\theta\varphi} = (0, 0, 0, \operatorname{ctg}\theta)^{\mathrm{T}}. \tag{58}$$

En contractant les expressions (51) (54) (55) (56) (57) (58) avec (48), on obtient la grandeur intrinsèque K_{ij}:

$$(59) \qquad K_{ij} = \begin{bmatrix} -\dfrac{a^r_{\tau\tau}}{c\,\Delta\, dt^*/d\tau} & 0 & 0 \\ 0 & \dfrac{r\,\Delta\, dt^*}{c\, d\tau} & 0 \\ 0 & 0 & \dfrac{r\,\Delta\, dt^*}{c\, d\tau}\sin^2\theta \end{bmatrix}$$

On peut écrire cette expression de telle sorte que la dérivée $dt^*/d\tau$ n'intervienne que par l'expression de $K_{\theta\theta}$

$$(60) \qquad K_{ij} = \begin{bmatrix} -\dfrac{r\,a^r_{\tau\tau}}{c^2 K_{\theta\theta}} & 0 & 0 \\ 0 & K_{\theta\theta} & 0 \\ 0 & 0 & K_{\theta\theta}\sin^2\theta \end{bmatrix}$$

$$(61) \qquad K_{\theta\theta} = \frac{r\,\Delta\, dt^*}{c\, d\tau}.$$

Or, on peut facilement éliminer t^* de (61) en utilisant (45):

$$(62) \qquad K_{\theta\theta} = \frac{r}{c^2}\,(c^2\Delta + (dr/d\tau)^2)^{\frac{1}{2}}.$$

Quant à $K_{\tau\tau}$, on peut lui donner une expression plus condensée que celle qu'il a en (60). On trouve en effet facilement

$$(63) \qquad K_{\tau\tau} = -\frac{1}{c^2}\,\frac{1}{dr/d\tau}\,\frac{d}{d\tau}\,(K_{\theta\theta}/r).$$

8. 2. *Modèle macroscopique*

La théorie utilisée sera cette fois la théorie d'Einstein avec terme de matière (appellée paradoxalement cas intérieur par Lichnerowicz), (cf. annexe IV).

La métrique sera isotrope et homogène :

$$d\sigma^2 = \frac{a^2}{c^2}(d\eta^2 - d\chi^2 - \sin^2\chi\,(d\theta^2 + \sin^2\theta\, d\theta^2)) \tag{64}$$

$$a = a(\eta)\,. \tag{65}$$

Définissons maintenant une cellule à symétrie sphérique de coordonnées τ, φ, θ

$$\chi = \chi(\tau) \tag{66}$$

$$\eta = \eta(\tau)\,. \tag{67}$$

Puisque nous avons supposé le plasma «froid», il faut que les différentes cellules soient immobiles les unes par rapport aux autres et nous supposerons pour que le modèle macroscopique soit homogène qu'elles ont toutes le même volume à l'instant η donné.

Les parois des cellules sont donc immobiles :

$$\chi = \chi_0 = \text{constante} \tag{68}$$

donc

$$d\chi/d\tau = 0\,. \tag{69}$$

Dans ces conditions, imposer à τ d'être un temps propre entraîne

$$c\,d\tau = a\,d\eta \tag{70}$$

de sorte que la métrique de la frontière sera

$$d\sigma^2 = d\tau^2 - \frac{a^2}{c^2}\sin\chi_0\,(d\theta^2 + \sin^2\theta\, d\varphi^2)\,. \tag{71}$$

La normale à la cellule sera simplement

$$n_\mu = \left(0, -\frac{d\eta}{d\tau}, 0, 0\right) \tag{72}$$

qui devient, une fois normée :

$$\hat{n}_\mu = (0, -a/c, 0, 0)\,. \tag{73}$$

Les accélérations-courbures se calculent facilement à partir de (68) et des expressions de la connexion affine données en annexe :

$$(74)\quad a^{\mu}_{\tau\tau} = 0$$

$$(75)\quad a^{\mu}_{\tau\theta} = \left(0, 0, \frac{\dot{a}\, d\eta}{a\, d\tau}, 0\right)^{\mathrm{T}}$$

$$(76)\quad a^{\mu}_{\tau\varphi} = \left(0, 0, 0, \frac{\dot{a}\, d\eta}{a\, d\tau}\right)^{\mathrm{T}}$$

$$(77)\quad a^{\mu}_{\theta\theta} = \left(\frac{\dot{a}}{a}\sin^2\chi, -\sin\chi\cos\chi, 0, 0\right)^{\mathrm{T}}$$

$$(78)\quad a^{\mu}_{\varphi\varphi} = \left(\frac{\dot{a}}{a}\sin^2\chi\sin^2\theta, -\sin\chi\cos\chi\sin^2\theta, -\sin\theta\cos\theta, 0\right)^{\mathrm{T}}$$

$$(79)\quad a^{\mu}_{\theta\varphi} = (0, 0, 0, \operatorname{ctg}\theta)^{\mathrm{T}}.$$

En contractant ces expressions avec (73), on obtient la grandeur intrinsèque

$$(80)\quad \mathrm{K}_{ij} = \begin{vmatrix} 0 & 0 & 0 \\ 0 & \dfrac{a}{c}\sin\chi\cos\chi & 0 \\ 0 & 0 & \dfrac{a}{c}\sin\chi\cos\chi\sin^2\theta \end{vmatrix}$$

8. 3. *Identification*

La première condition découle de l'identité des métriques intrinsèques (46) (71):

$$(81)\quad r = a\sin\chi_0 .$$

L'identification des expressions de $\mathrm{K}_{\tau\tau}$ fournit une seconde condition, à savoir, utilisant (59) ou (60)

$$(82)\quad a^{r}_{\tau\tau} = 0$$

c'est-à-dire que les parois de la cellule sont en chute radiale libre.

Le mouvement de chute libre dans le potentiel de Reissner-Nordström est étudié en annexe, mais il n'est pas nécessaire de connaître la solution pour exploiter l'identité des $K_{\tau\tau}$. On peut en effet partir de l'expression (63) de $K_{\tau\tau}$ qui, puisqu'elle est nulle pour des raisons macroscopiques, fournit l'intégrale première :

$$K_{\theta\theta}/r = \text{constante} \tag{83}$$

que l'on peut avantageusement paramétrer de la façon suivante :

$$K_{\theta\theta}/r = \frac{1}{c}\left(1-\frac{M}{r_0}\right)^{\frac{1}{2}} \tag{84}$$

car le paramètre r_0 a une interpétation simple en termes du mouvement de chute libre (cf annexe III).

Les deux conditions (81) et (82) ou (84) sont connues dans la littérature [9] mais elles ne sont pas suffisantes. Aussi les complète-t'on par une relation constitutive macroscopique qui est facile à deviner dans le cas de particules neutres, à savoir la nullité de la pression. Le cas de particules chargées serait plus difficile à traiter par cette méthode heuristique.

La méthode développée dans ce texte a l'avantage de fournir automatiquement une troisième relation, obtenue par identification des $K_{\theta\theta}$, ce qui permettra finalement de dériver les relations macroscopiques avec assurance.

L'identification des $K_{\theta\theta}$ donnés par les expressions (84) et (80) fournit compte tenu de (81) :

$$\left(1-\frac{M}{r_0}\right)^{\frac{1}{2}} = \cos\chi_0 \tag{85}$$

soit

$$r_0 = M/\sin^2\chi_0 . \tag{86}$$

Il est intéressant de remarquer que cette relation joue vis-à-vis du mouvement microscopique le rôle d'une règle de sélection. En effet, parmis tous les mouvements microscopiques qui obéissent à la loi d'inertie classique (82), seuls sont permis ceux dont le paramètre r_0 prend la valeur (86). Il y a là une analogie avec les théories quantiques ; peut-être le modèle macroscopique joue-t-il le rôle d'un «observateur» vis-à-vis du modèle microscopique.

8. 4. *Mouvement et relations macroscopiques*

Comme montré en annexe, le mouvement microscopique est hypocycloïdal. En introduisant (81) (86) dans les équations du mouvement microscopique, on obtient le mouvement macroscopique :

$$a = a_0(1 + \alpha \cos \xi) \tag{87}$$

$$\tau = \frac{a_0}{c}(\xi + \alpha \sin \xi) \tag{88}$$

$$\alpha = \left(1 - \frac{Q^2}{Mr_0}\right)^{\frac{1}{2}} \tag{89}$$

où l'on a posé

$$a_0 \underset{\text{déf}}{=} \frac{r_0}{\sin \chi_0} \tag{90}$$

En dérivant (88) et en utilisant (87), il vient

$$c\, d\tau = a\, d\xi \tag{91}$$

qu'il suffit de comparer à (70) pour constater que l'on peut, par un choix convenable des origines, identifier ξ et η.

Notons, à l'intention de ceux qui croient à la cosmologie, que la solution (87) ne contient pas de «big bang» originel, le rayon de l'univers ne pouvant descendre en dessous de la valeur limite.

$$a_{\min} = a_0(1 - \alpha) \tag{92}$$

qui est strictement positive dans le cas de particules chargées.

En vue d'obtenir les valeurs de l'énergie et de la pression, calculons tout d'abord les dérivées de a :

$$\dot{a} = \frac{da}{d\eta} = -a_0 \alpha \sin \xi \tag{93}$$

donc

$$\dot{a}^2 = (a_0 \alpha)^2 - (a_0 - a)^2 \tag{94}$$

$$\ddot{a} = -a_0 \alpha \cos \xi = a_0 - a \tag{95}$$

Il suffit d'introduire ces valeurs dans les expressions du tenseur d'Einstein données à l'annexe IV pour obtenir :

$$G_\eta^\eta = \frac{3c^2}{a^4}(2aa_0 - a_0^2(1-\alpha^2)) \tag{96}$$

$$G_\chi^\chi = G_\theta^\theta = G_\varphi^\varphi = \frac{c^2}{a^4} a_0^2(1-\alpha^2)\,. \tag{97}$$

Nous pouvons interpréter (96) (97) en utilisant le volume de l'univers [13],

$$V = 2\pi^2 a^3 \tag{98}$$

donc

$$dV = 6\pi^2 a^2 \, da \tag{99}$$

on obtient alors facilement :

$$d(G_\eta^\eta V) = G_\chi^\chi \, dV \tag{100}$$

qui n'est autre que la conservation de l'énergie, et

$$\left(G_\chi^\chi + \frac{1}{3} G_\eta^\eta\right) V = (2\pi a_0 c)^2 = \text{constante} \tag{101}$$

à rapprocher de la loi de Boyle-Mariotte.

ANNEXE I: COURBURE D'UN ESPACE-TEMPS A SYMETRIE SPHERIQUE

Nous reprenons ici une partie du théorème de Birkhoff (1923) (cf. [17]) mais sans faire l'hypothèse d'un espace vide. Cette présentation est à peine différente de celle de Landau-Lifchitz [13].

La symétrie sphérique suffit pour garantir l'existence d'un système de coordonnées où l'on puisse écrire la métrique sous la forme

$$d\sigma^2 = A\,dt^2 - (B\,dr^2 + r^2(d\theta^2 + \sin^2\theta\,d\varphi^2))/c^2 \tag{1}$$

σ et t seront tous deux mesurés en secondes, de sorte que A est sans dimensions. Il en est évidemment de même de B. c sera une constante dimensionnelle, et donc universelle, à laquelle on pourrait attribuer par définition une valeur proche de $3\,10^8$ m/sec, de sorte que la coordonnée r a la dimension d'une longueur (mesurée en mètres).

Nous désignerons par $\cdot$ la dérivée temporelle $\partial/\partial t$ par $'$ la dérivée radiale $\partial/\partial r$.

Par un choix judicieux de la coordonnée t, il est toujours possible de rendre A indépendant de t.

$$\dot{A} = 0. \tag{2}$$

Par contre, B dépend en général à la fois de t et de r.

A cause de la symétrie sphérique, aucun coefficient ne dépend de θ ni de φ.

Afin de faciliter les écritures, il est d'usage de poser

$$A = e^{2\nu(r)} \tag{3}$$

$$B = e^{2\lambda(r,t)}. \tag{4}$$

Les seules composantes non nulles de la métrique sont alors:

$$g_{tt} = e^{2\nu} \tag{5 a}$$

$$g_{rr} = -(e^{2\lambda})/c^2 \tag{5 b}$$

$$g_{\theta\theta} = -r^2/c^2 \tag{5 c}$$

(5 d) $$g_{\varphi\varphi} = -r^2 \sin^2\theta / c^2$$

et la racine de son déterminant est donnée par

(6) $$\sqrt{-g} = e^{\nu+\lambda} r^2 |\sin\theta| / c^3 .$$

Les seules composantes non nulles de la connexion affine sont

(7)
$$\Gamma^r_{tt} = c^2 \nu' e^{2\nu-2\lambda} \qquad \Gamma^t_{rt} = \Gamma^t_{tr} = \nu'$$
$$\Gamma^t_{rr} = \dot{\lambda}(e^{2\lambda-2\nu})/c^2 \qquad \Gamma^r_{tr} = \Gamma^r_{rt} = \dot{\lambda}$$
$$\Gamma^r_{rr} = \lambda'$$
$$\Gamma^r_{\theta\theta} = -r e^{-2\lambda} \qquad \Gamma^\theta_{r\theta} = \Gamma^\theta_{\theta r} = r^{-1}$$
$$\Gamma^r_{\varphi\varphi} = -r e^{-2\lambda} \sin^2\theta \qquad \Gamma^\varphi_{r\varphi} = \Gamma^\varphi_{\varphi r} = r^{-1}$$
$$\Gamma^\theta_{\varphi\varphi} = -\sin\theta\cos\theta \qquad \Gamma^\varphi_{\theta\varphi} = \Gamma^\varphi_{\varphi\theta} = \operatorname{cotg}\theta$$

donc

(8)
$$\Gamma_t = \dot{\lambda}$$
$$\Gamma_r = \nu' + \lambda' + 2r^{-1}$$
$$\Gamma_\theta = \operatorname{cotg}\theta$$
$$\Gamma_\varphi = 0 .$$

Les relations (8) auraient d'ailleurs pu être tirées directement de (6).

A partir de (7) et en s'aidant éventuellement de (8) on peut calculer le tenseur de Ricci. Les seules composantes non nulles de celui-ci sont :

(9)
$$R_{tt} = \ddot{\lambda} + \dot{\lambda}^2 - c^2 e^{2\nu-2\lambda}(\nu'' + \nu'^2 - \nu'\lambda' + 2\nu' r^{-1})$$
$$R_{rt} = R_{tr} = -2\dot{\lambda} r^{-1}$$
$$R_{rr} = \nu'' + \nu'^2 - \lambda'\nu' - 2\lambda' r^{-1} - e^{2\lambda-2\nu}(\ddot{\lambda} + \dot{\lambda}^2)/c^2$$
$$R_{\theta\theta} = -1 + e^{-2\lambda}(+1 - r\lambda' + r\nu')$$
$$R_{\varphi\varphi} = \sin^2\theta\,(-1 + e^{-2\lambda}(+1 - r\lambda' + r\nu'))$$

soit, en montant le premier indice :

(10)
$$R_t^t = e^{-2\nu}(\lambda^{\cdot\cdot} + \lambda^{\cdot 2}) - c^2 e^{-2\lambda}(\nu'' + \nu'^2 - \nu'\lambda' + 2\nu' r^{-1})$$
$$R_t^r = 2c^2 e^{-2\lambda}\lambda^{\cdot} r^{-1}$$
$$R_r^t = -e^{-2\nu}\left(\frac{2\lambda^{\cdot}}{r}\right)'$$
$$R_r^r = -c^2 e^{-2\lambda}\left(\nu'' + \nu'^2 - \lambda'\nu' - 2\frac{\lambda'}{r}\right) + e^{-2\nu}(\lambda^{\cdot\cdot} + \lambda^{\cdot 2})$$
$$R_\theta^\theta = R_\varphi^\varphi = c^2 r^{-2} - c^2 e^{-2\lambda}(r^{-2} - \lambda' r^{-1} + \nu' r^{-1}).$$

La courbure scalaire vaut donc

(11)
$$\tfrac{1}{2}R = e^{-2\nu}(\lambda^{\cdot\cdot} + \lambda^{\cdot 2}) - c^2 e^{-2\lambda}(\nu'' + \nu'^2 - \nu'\lambda' + 2\nu' r^{-1} - 2\lambda' r^{-1} + r^{-2}) + c^2 r^{-2}.$$

Le tenseur d'Einstein de poids 1, à savoir

(12)
$$G_\nu^\mu = \sqrt{-g}\,(R_\nu^\mu - \tfrac{1}{2}R)$$

vaut alors

(13)
$$G_t^t = |\sin\theta|\,(e^{\nu-\lambda}(1 - 2\lambda' r) - e^{\nu+\lambda})/c$$
$$G_t^r = |\sin\theta|\,e^{\nu-\lambda}2\lambda^{\cdot} r/c$$
$$G_r^t = -|\sin\theta|\,e^{\lambda-\nu}2\lambda^{\cdot} r/c^3$$
$$G_r^r = |\sin\theta|\,(e^{\nu-\lambda}(1 + 2\nu' r) - e^{\nu+\lambda})/c$$
$$G_\theta^\theta = G_\varphi^\varphi = -r^2 c^{-3}|\sin\theta|\,e^{\lambda-\nu}(\lambda^{\cdot\cdot} + \lambda^{\cdot 2}) + c^{-1}|\sin\theta|\,r^2 e^{\nu-\lambda}(\nu'' + \nu'^2 - \nu'\lambda' + (\nu' - \lambda')r^{-1}).$$

En divisant (13) par la constante d'Einstein, on obtient de G_t^t une densité d'énergie, de G_t^r un flux d'énergie, de G_r^t un moment et les trois autres composantes sont des tensions.

Parfois, on cherche à obtenir des relations supplémentaires en faisant usage de la conservation de l'énergie. Le procédé, rigoureusement appliqué, ne conduit en fait à aucune relation nouvelle car (13) vérifie automatiquement une loi de conservation de par l'identité de Bianchi.

D'ailleurs, aussi longtemps que la métrique dépend du temps ($\lambda^{\cdot} \neq 0$), il n'y a pas de raison pour que l'énergie soit une intégrale première.

ANNEXE II: LA METRIQUE DE REISSNER-NORDSTROM

Nous allons reprendre la métrique à symétrie sphérique de l'annexe I avec la condition supplémentaire d'une courbure interprétable comme due uniquement à un champ électromagnétique dans le vide.

Cette condition entraine (Rainich [4])

$$R = 0 \tag{1}$$

$$R^{\mu}_{\alpha} R^{\alpha}_{\nu} = k \, \delta^{\mu}_{\nu} \tag{2}$$

Compte tenu de l'annulation de nombreuses composantes par suite de la symétrie sphérique, l'équation (2) se réduit dans notre système de coordonnées à

$$R^{t2}_{t} + R^{t}_{r} R^{r}_{t} = R^{r}_{t} R^{t}_{r} + R^{r2}_{r} = R^{\theta 2}_{\theta} = R^{\varphi 2}_{\varphi} \tag{3}$$

$$R^{t}_{t} R^{t}_{r} + R^{t}_{r} R^{r}_{r} = R^{t}_{r} (R^{t}_{t} + R^{r}_{r}) = 0 \tag{4}$$

$$R^{r}_{t} (R^{t}_{t} + R^{r}_{r}) = 0 . \tag{5}$$

De (3), on tire

$$R^{t}_{t} = \pm R^{r}_{r} \tag{6}$$

Limitons nous au premier cas (signe +), qui correspond à l'électromagnétisme classique.

Alors, la condition (1) entraîne

$$R^{t}_{t} = R^{r}_{r} = - R^{\theta}_{\theta} = - R^{\varphi}_{\varphi} \tag{7}$$

de sorte que, par (3), R^{t}_{r} et R^{r}_{t} doivent être nuls, ce qui annule identiquement (4) et (5) et donne, par les expressions de l'annexe I:

$$\lambda^{\bullet} = 0 \tag{8}$$

Ainsi, la première solution de (6) est stationnaire.

En utilisant (7), on obtient aisément

$$\nu' + \lambda' = 0 \tag{9}$$

ainsi que

$$r^2 e^{-2\lambda}(-\lambda'' + 2\lambda'^2 - 4\lambda' r^{-1} + r^{-2}) = 1 \tag{10}$$

que l'on peut écrire

$$\left(\tfrac{1}{2} r^2 e^{-2\lambda}\right)'' = 1 . \tag{11}$$

L'intégration de (11) est triviale et fournit

$$e^{-2\lambda} = 1 - 2\,\mathrm{M}\, r^{-1} + \mathrm{Q}^2 r^{-2} = \Delta \tag{12}$$

où M et Q sont des longueurs caractéristiques de la singularité centrale. Pour ne pas préjuger en écrivant (12) du signe du dernier terme, il faudrait admettre que Q puisse être purement imaginaire.

Par (9), $e^{2\nu}$ ne peut différer de (12) que par une constante multiplicative. Cette dernière peut être réduite à l'unité par un choix convenable de la coordonnée temporelle t, de sorte que l'on obtient la métrique de Reissner-Nordström :

$$d\sigma^2 = \Delta\, dt^2 - c^{-2}\Delta^{-1} dr^2 - c^{-2} r^2 (d\theta^2 + \sin^2\theta\, d\varphi^2) . \tag{13}$$

Dans cette métrique, on a

$$e^{-2\lambda} = e^{2\nu} = \Delta \tag{14}$$

donc

$$\lambda' = 0 \tag{15}$$

$$\lambda' = (-\mathrm{M} r^{-2} + \mathrm{Q}^2 r^{-3})/\Delta \tag{16}$$

$$\nu' = (\mathrm{M} r^{-2} - \mathrm{Q}^2 r^{-3})/\Delta \tag{17}$$

En introduisant ces valeurs dans les expressions de l'annexe I, on obtient :

$$\Gamma^r_{tt} = c^2 (\mathrm{M} r^{-2} + \mathrm{Q}^2 r^{-3})\Delta \tag{18}$$

$$\Gamma^t_{rt} = \Gamma^t_{tr} = (\mathrm{M} r^{-2} - \mathrm{Q}^2 r^{-3})/\Delta \tag{19}$$

$$\Gamma^{r}_{rr} = (-M r^{-2} + Q^2 r^{-3})/\Delta \tag{20}$$

$$\Gamma^{r}_{\theta\theta} = -r\Delta \tag{21}$$

$$\Gamma^{\theta}_{r\theta} = \Gamma^{\theta}_{\theta r} = r^{-1} \tag{22}$$

$$\Gamma^{r}_{\varphi\varphi} = -r\Delta \sin^2\theta \tag{23}$$

$$\Gamma^{\varphi}_{r\varphi} = \Gamma^{\varphi}_{\varphi r} = r^{-1} \tag{24}$$

$$\Gamma^{\theta}_{\varphi\varphi} = -\sin\theta \cos\theta \tag{25}$$

$$\Gamma^{\varphi}_{\theta\varphi} = \Gamma^{\varphi}_{\varphi\theta} = c\,t\,g\,\theta \tag{26}$$

Les autres composantes de la connexion sont nulles.

ANNEXE III: MOUVEMENT RADIAL DANS LA METRIQUE DE REISSNER-NORDSTROM

Nous nous intéressons au mouvement d'une particule test *neutre* dont le mouvement est donc donné par la nullité de l'accélération (par rapport au temps propre τ)

$$a^{\mu}_{\tau\tau} = 0\,. \tag{1}$$

En utilisant les expressions de la connexion données à l'annexe II, on obtient cette accélération

$$0 = \frac{d^2 r}{d\tau^2} + c^2 (M r^{-2} - Q^2 r^{-3}) \left(\Delta \left(\frac{dt}{d\tau} \right)^2 - \frac{1}{c^2 \Delta} \left(\frac{dr}{d\tau} \right)^2 \right) \tag{2}$$

soit, puisque τ est un temps propre et le mouvement radial,

$$0 = \frac{d^2 r}{d\tau^2} + c^2 (M r^{-2} - Q^2 r^{-3})\,. \tag{3}$$

L'équation (3) fournit facilement l'intégrale première:

$$\left(\frac{dr}{d\tau} \right)^2 + c^2 (-2 M r^{-1} + Q^2 r^{-2} + c^{te}) = 0\,. \tag{4}$$

Lorsque $Q=0$, c'est-à-dire pour un potentiel purement gravitationnel, on sait que le mouvemment est cycloïdal.

Aussi est-il tentant d'essayer une solution hypo- ou épi-cycloïdale de (3). Posons

$$r = r_0(1 + \alpha \cos \xi) \tag{5}$$

$$\tau = \tau_0(\xi + \alpha \sin \xi)\,. \tag{6}$$

On tire de (5) (6):

$$\frac{dr}{d\tau} = \frac{dr/d\xi}{d\tau/d\xi} = -\frac{r_0 \alpha \sin \xi}{\tau_0(1 + \alpha \cos \xi)}\,. \tag{7}$$

On pourrait dériver une seconde fois et introduire le résultat en (3), mais il est plus facile d'éliminer ξ de (7) en utilisant (5) (6)

$$\left(\frac{dr}{d\tau}\right)^2 = -\left(\frac{r_0}{\tau_0}\right)^2 + \frac{2r_0^3}{\tau_0^2 r} - \frac{(1-\alpha^2)r_0^4}{\tau_0^2 r^2} \tag{8}$$

et de constater que l'on peut identifier (8) et (4), ce qui élimine deux paramètres sur trois:

$$\tau_0 = \frac{r_0}{c}\left(\frac{r_0}{M}\right)^{\frac{1}{2}} \tag{9}$$

$$\alpha = \left(1 - \frac{Q^2}{M r_0}\right)^{\frac{1}{2}}\,. \tag{10}$$

Dans tous les cas «physiques», le rapport $\dfrac{Q^2}{M r_0}$ est petit de sorte que l'expression (10) a un sens.

Lorsque $Q=0$, $\alpha=1$ et le mouvement est cycloïdal.

Si Q est réel et différent de 0, $\alpha<1$ et le mouvement est hypo-cycloïdal.

Si Q était imaginaire pur, le mouvement serait épi-cycloïdal.

Notons encore que l'identification de (8) et (4) fixe la valeur de la constante utilisée en (4), qui devient ainsi:

$$\left(\frac{dr}{d\tau}\right)^2 = -c^2(M r_0^{-1} - 2M r^{-1} + Q^2 r^{-2})\,. \tag{11}$$

Contrairement à ce qui se passe lorsque $Q=0$, une solution statique est possible. Il suffit pour cela d'avoir en (5) et (6)

$$\alpha = 0 . \tag{12}$$

En ce cas, r_0 et τ_0 sont imposés par (10) et (9):

$$r = r_0' = Q^2/M \tag{13}$$

$$\tau = \tau_0' \xi = \frac{Q^5}{c\,M^2}\,\xi . \tag{14}$$

r_0' n'est autre que le rayon classique d'une particule chargée. Quant à τ_0', il s'agit de la période des oscillations au voisinage du point d'équilibre.

A titre indicatif, on aurait pour un proton

$$r_0' = 1.55\ \ 10^{-18}\,\mathrm{m}$$

$$\tau_0' = 3.61\ \ 10^{-8}\,\mathrm{sec}$$

et pour un électron

$$r_0' = 2.84\ \ 10^{-14}\,\mathrm{m}$$

$$\tau_0' = 0.121\ \mathrm{sec} .$$

ANNEXE IV: METRIQUE D'UN MILIEU ISOTROPE ET HOMOGENE

La forme générale de cette métrique est, du moins dans le modèle fermé (cf. [13])

$$d\sigma^2 = dt^2 - a^2[d\chi^2 + \sin^2\chi\,(d\theta^2 + \sin^2\theta\, d\varphi^2)]/c^2 \tag{1}$$

avec

$$a = a(t) . \tag{2}$$

Cette métrique est à symétrie sphérique et est donc étudiable par les méthodes de l'annexe I.

Malheureusement, l'expression (1) prend alors une forme très compliquée de sorte qu'il est préférable de recommencer entièrement l'étude. Auparavant, on effectue souvent le changement de variable

(3) $$d\eta = c\,dt/a$$

qui fait de la métrique :

(4) $$d\sigma^2 = a^2[d\eta^2 - d\chi^2 - \sin^2\chi(d\theta^2 + \sin^2\theta\, d\varphi^2)]/c^2$$

(5) $$a = a(\eta)$$

soit

(6) $$g_{\eta\eta} = a^2/c^2$$

(7) $$g_{\chi\chi} = -a^2/c^2$$

(8) $$g_{\theta\theta} = -a^2\sin^2\chi/c^2$$

(9) $$g_{\varphi\varphi} = -a^2\sin^2\chi\sin^2\theta/c^2$$

(10) $$\sqrt{-g} = a^4\sin^2\chi\,|\sin\theta|/c^4\,.$$

Les seules composantes non nulles de la connexion affine sont alors, le $\cdot$ dénotant une dérivation selon η:

(11) $$\Gamma^{\eta}_{\eta\eta} = \dot{a}/a$$

(12) $$\Gamma^{\eta}_{\chi\chi} = \dot{a}/a$$

(13) $$\Gamma^{\chi}_{\chi\eta} = \Gamma^{\chi}_{\eta\chi} = a/a$$

(14) $$\Gamma^{\eta}_{\theta\theta} = \dot{a}\sin^2\chi/a$$

(15) $$\Gamma^{\theta}_{\theta\eta} = \Gamma^{\theta}_{\eta\theta} = \dot{a}/a$$

(16) $$\Gamma^{\chi}_{\theta\theta} = -\sin\chi\cos\chi$$

(17) $$\Gamma^{\theta}_{\theta\chi} = \Gamma^{\theta}_{\chi\theta} = \operatorname{cotg}\chi$$

(18) $$\Gamma^{\eta}_{\varphi\varphi} = \dot{a}\sin^2\chi\sin^2\theta/a$$

(19) $$\Gamma^{\varphi}_{\varphi\eta} = \Gamma^{\varphi}_{\eta\varphi} = \dot{a}/a$$

(20) $$\Gamma^{\chi}_{\varphi\varphi} = -\sin\chi\cos\chi\sin^2\theta$$

(21) $$\Gamma^{\varphi}_{\varphi\chi} = \Gamma^{\varphi}_{\chi\varphi} = \operatorname{cotg}\chi$$

(22) $$\Gamma^{\theta}_{\varphi\varphi} = -\sin\theta\cos\theta$$

(23) $$\Gamma^{\varphi}_{\varphi\theta} = \Gamma^{\varphi}_{\theta\varphi} = \operatorname{cotg}\theta$$

donc

$$\Gamma_\eta = 4\,\dot{a}/a \tag{24}$$

$$\Gamma_\chi = 2\,\mathrm{cotg}\,\chi \tag{25}$$

$$\Gamma_\theta = \mathrm{cotg}\,\theta \tag{26}$$

$$\Gamma_\varphi = 0 \tag{27}$$

que l'on aurait pu tirer directement de (10).

Les seules composantes non nulles du tenseur de Ricci sont:

$$R_\eta^\eta = -3\,c^2(a\,\ddot{a} - \dot{a}^2) \tag{28}$$

$$R_\chi^\chi = R_\theta^\theta = R_\varphi^\varphi = -c^2(a\,\ddot{a} + \dot{a}^2 + 2\,a^2)/a^4\,. \tag{29}$$

La courbure scalaire vaut donc

$$R = -6\,c^2(a + \ddot{a})/a^3 \tag{30}$$

et le tenseur d'Einstein (de poids nul)

$$G_\eta^\eta = 3\,c^2(\dot{a}^2 + a^2)/a^4 \tag{31}$$

$$G_\chi^\chi = G_\theta^\theta = G_\varphi^\varphi = c^2(2\,a\,\ddot{a} - \dot{a}^2 + a^2)/a^4\,. \tag{32}$$

REFERENCES

[1] MAXWELL, J. C.: A treatise on electricity and magnetism *Clarendon Press* (1891).

[2] CARTER, F. W.: Air-gap induction *Electrical World and Engineer* Vol. 38, **22**, 884-888 (1901).

[3] LORENTZ, H. A.: The theory of electrons (sect. 117), Teubner Leipzig (1906) Reprinted by Dover Publications, Inc. N. Y. 1952.

[4] RAINICH, G. Y.: Electrodynamics in the general relativity theory *Trans. Am. Math. Soc.* **27**, 106 (1925).

[5] CARTER, F. W.: The magnetic field of the dynamo electric machine *J. of the Inst. of Electrical Engineers* Vol. 64, 1115-1118 (1926).

[6] WIGNER, E. P., SEITZ, F.: On the constitution of metallic sodium *Physical Rev.* **43**, 804 (1933).

[7] LICHNEROWICZ, A.: Théories relativistes de la gravitation et de l'électromagnétisme Masson (1955).

[8] MAZUR, P., DE GROOT, S. R.: On pressure and ponderomotive force in a dielectric *Physica* **22**, 657-669 (1956).

[9] LINDQUIST, R. W., WHEELER, J. A.: Dynamics of a lattice universe by the Schwarzschild cell method *Rev. Mod. Phys.* **29**, 432-433 (1957).
[10] MISNER, C., WHEELER, J. A.: Classical physics as geometry *Ann. Phys.* (U. S. A.) **2**, 525-603 (1957).
[11] DE GROOT, S. R., VLIEGER, J.: Derivation of Maxwell equations *Physica* **31**, 125-140, 254-268 (1965).
[12] DE GROOT, S. R.: The Maxwell equations: non-relativistic multipole expansion of all orders *Physica* **31**, 953-958 (1965).
[13] LANDAU, L., LIFCHITZ, E.: Théorie du champ Ed. Mir U. R. S. S. (1966).
[14] ELLIOT, R. S.: Electromagnetics Mc Graw-Hill (1966).
[15] GARRIDO, M. S.: Contribution à la théorie dynamique des systèmes électromécaniques. Thèse, Nancy (1968).
[16] HANSEN, J. P.: Contribution à l'étude de la production magnétohydrodynamique d'énergie électrique en veine liquide. Thèse présentée à l'université de Paris VI (1974).
[17] MISNER, C., THORNE, K., WHEELER, J. A.: Gravitation. Freeman (1974).

LISTE DES PUBLICATIONS REÇUES ACTUELLEMENT EN ENCHANGE AVEC PORTUGALIAE PHYSICA

ALEMANHA
- *Physikertagung (Physikalisch-Technische Bundesanstalt)*
- *Physikertagung-Plenarvortrage (Physikalisch-Technische Bundesanstalt)*
- *Physikertagung-Voradbrucke der Fachberichte (Physikalisch-Technische Bundesanstal)*
- *Sitzungberichte der Sachsischen Akademie der Wissenschaften zu Leipzig*
- *Verhandlungen der Deutschen Physikalischen Gesellschaft*

ARGENTINA
- *Anales de la Sociedad Cientifica Argentina*
- *Mathematicae Notae (Boletin del Instituto de Matematica «Beppo*
- *Levi»)*
- *Revista de la Union Matematica Argentina*

AUSTRÁLIA
- *Journal and Proceedings of the Royal Society of New South Wales*

BÉLGICA
- *Annuaire de l'Académie Royale de Belgique*
- *Bulletin de la Classe des Sciences de l'Académie Royale de Bélgique*
- *Mededelingen uit het Natuurkundig Laboratorium der Universiteit te Gent*
- *Recueil de Travaux de Laboratoire de Physique de l'Université de Louvain*
- *Scientific Report (Centre d'Etude de l'Energie Nucleaire)*

BRASIL
- *Boletim do Gabinete Português de Leitura de Porto Alegre*
- *Noticia (Centro Latino Americano de Fisica)*

BULGÁRIA
- *Annuaire de l'Université de Sofia*

CANADÁ
- *Canadian Journal of Physics*

E. U. A.
- *Bulletin of the Scripps Institution of Oceanography (University of California*
- *Bulletin of the Seismographic (University of California)*
- *Journal of the Franklin Institute*
- *Report of the publications and Theses (Mass. Institute of Technology)*
- *Research in Materials (Mass. Institute of Technology)*
- *Solid-State and Molecular Theory Group (Mass. Institute of Technology)*
- *The General Radio Experimenter*

EQUADOR	— *Anales de la Universidad Central del Ecuador*
ESPANHA	— *Revista de Geofisica (Instituto Nacional de Geofísica)*
FINLANDIA	— *Annales Academiae Scientiarum Fennicae*
	— *Commentationes Physico-Mathematicae (Societas Scientiarum Fennica)*
FRANÇA	— *Annalles de Physique*
	— *Bulletin de la Société Scientifique de Bretagne*
	— *Cours de l'École Polytechnique*
HOLANDA	— *Communications from the Kamerlingh Onnes Laboratory of the University of Leiden*
HUNGRIA	— *Atomki Közlemények (Inst. of Nuclear Research of the Hung. Acad. of Sciences*
ÍNDIA	— *Proceedings of the Indian Academy of Sciences*
INGLATERRA	— *Asta (The Assoc. of Short Circuit Testing Authorities-Inc)*
	— *Comments on Solid State Physics*
	— *Contributions from the Cambridge Observatories*
	— *Educations in Science (Ass. for Science Education)*
	— *Electrical Review*
	— *Electricol Times*
	— *Journal of Science & Technology*
	— *Notes on Applied Science (National Physical Labaratory*
	— *Proceedings of the Royal Society of Edinburgh*
	— *Report (National Physical Laboratory)*
	— *Revue de la Société English Electric*
	— *Thin Films*
	— *The School Science Review (Ass. for Science Education)*
IRLANDA	— *Procedings of the Royal Irish Academy*
	— *The Scientific Proceedings of the Royal Dublin Society*
ITÁLIA	— *Annali dell'Istituto Superiore di Sanità*
	— *Congressi, Convegni e Simposi Scientifici (Consiglio Nazionale delle Richerche)*
	— *La Ricerca Scientifica (Consiglio Nazionale delle Richerce)*
	— *La Scienza del Pensare (UTEP)*
	— *Quaderni de «La Ricerca Scientifica»*
	— *Raporti dei Laboratori di Fisica dell'Istituto Superiore di Sanità*
	— *Rendiconti del Seminario della Facoltà di Scienze dell'Università de Cagliari*
JUGOSLÁVIA	— *Fizika (Editorial Office)*
	— *Glasnik Matenaticko-Fizicki i Astronomski*
	— *Publikacije Elektrotehnickog Fakulteta Univerziteta u Beogradu*
	— *Radovi Zavoda za Fiziku*
	— *Reports — (Nuklearni Institut Jozef Stefan)*
NORUEGA	— *Arkiv for det Fysiske Seminar i Trondheim (Institutt for Teoretisk Fysikk)*
POLÓNIA	— *Acta Physica Polonica*
	— *Prace Komisji Nauk Techniczych (Académie Polonaise des Sciences)*

PORTUGAL	— *Agronomia Lusitana*
	— *Arquivo do Instituto Gulbenkian de Ciência*
	— *Cursos e Seminários do Instituto Gulbenkian de Ciência*
	— *Estudos de Programação e Análise Numérica do Instituto Gulbenkian de Ciência*
	— *Gazeta de Física*
	— *Gazeta de Matemática*
	— *Revista da Faculdade de Ciências de Coimbra*
	— *Revista Portuguesa de Química*
ROMÉNIA	— *Buletinul (Institutului Politehnic din Iasi)*
RÚSSIA	— *Referativnyi Zhurnal Fizika (Institut de l'Information Scientifique de l'Académie des Sciences de l'U. R. S. S.)*
SUÉCIA	— *Arkiv för Fysik*
SUÍÇA	— *Information Bulletin (International Union of Pure and Applied Chemistry)*
TURQUIA	— *Bulletin of the Turkish Physical Society*
	— *Communications de la Faculte des Sciences de l'Université d'Ankara Fen Fakültesi Mecmuasi (İstambul Üniversitesi)*

PORTUGALIAE PHYSICA

Instructions pour les auteurs

PORTUGALIAE PHYSICA est la seule publication périodique portugaise consacrée exclusivement à la divulgation des recherches dans le domaine des Sciences Physiques. Les travaux pourront être présentés sous forme d'articles ou de brèves communications. Des articles de mise au point seront encore publiés, par invtiation. Les travaux à publier devront être rédigés soit en Français, soit en Anglais, et avoir un résumé dans les deux langues. Ils seront dactylographiés à deux espacements sur une seule face du papier, l'original étant envoyé à la rédaction accompagné d'une copie.

Les figures et les tableaux devront être présentés sur des feuilles séparées. Les dessins devront être soigneusement faits à l'encre de Chine et avoir au moins le double des dimensions définitives. Les photographies seront faites sur du papier blanc brillant.

Les références bibliographiques seront indiquées dans le texte par un numéro entre parenthèses, en exposant, et groupées à la fin de l'article par l'ordre de citation. Les références à des articles dans des publications périodiques devront préciser les noms des auteurs, le titre abrégé de la revue selon le code international d'abréviation de titres de périodiques, le numéro du volume, le numéro de la première page de l'article en référence et l'année de publication. En ce qui concerne les livres, il faut indiquer les auteurs, le titre de l'ouvrage, le lieu d'impression, l'éditeur, l'année de l'édition et la page.

Les auteurs devront vérifier soigneusement le texte et les figures de leurs travaux car la rédaction ne peut pas accepter des altérations ou additions au texte original.

L'auteur d'un article ou communication recevra gratuitement 50 tirages à part. Ce nombre est réduit à 25 par auteur lorsque le même article aura l'intervention de plusieurs auteurs.

Toute correspondance doit être addressée à

PORTUGALIAE PHYSICA
Laboratório de Física da Faculdade de Ciências
Lisboa-2 (PORTUGAL)

PORTUGALIAE PHYSICA

Instructions to the authors

PORTUGALIAE PHYSICA is the only Portuguese review exclusively dedicated to the publication of research papers concerning the Physical Sciences. The papers may be presented under the form of articles or research notes. Review articles will also be published, by invitation.

The papers to be published may be written in French or in English with abstracts in both languages. They should be typed with two spaces, on one side of the page only, and the original and one copy must be submitted.

The figures and tables must be presented in separate sheets. Drawings should be carefully done in Indian ink and be at least double the definitive size. Photographs must be executed in white, glossy paper.

Bibliographical references should be indicated in the text by a number between brackets, in exponent, and grouped at the end of the article in the order they are mentioned. References to articles published in periodical publications should include the names of the authors, the abbreviated title of the publication according to the international code of abbreviation of the titles of periodicals, the issue number, the number of the first page of the article mentioned, and the year of publication. As for books, the authors, title of the work, place of the edition, editor, year of the edition, and page should be indicated.

The authors should carefully check their text and figures before submitting them, as the editor cannot accept any changes or additions to the original text.

The author of an article or research note is entitled to 50 free reprints. This number is reduced to 25 per author whenever more than one author intervene in a paper.

All mail to be addressed to

PORTUGALIAE PHYSICA
Laboratório de Física da Faculdade de Ciências
Lisboa-2 (PORTUGAL)

Composto e impresso na Tip. Matemática, Lda. — R. Diário de Notícias, 134-1.º-Esq. — Lisboa-2

Toute la correspondance concernant la rédaction de PORTUGALIAE PHYSICA doit être adressée à

PORTUGALIAE PHYSICA
Laboratório de Física da Faculdade de Ciências
LISBOA-2 (Portugal)

Prix de l'abonnement:	250 escudos (US $8.50) par volume
Prix des volumes déjà parus:	300 escudos (US $10)
Prix du fascicule:	75 escudos (US $2.50)

Les membres de la «Sociedade Portuguesa de Química e Física» ont une réduction de 50 °/₀ sur les prix indiqués.

Les Universités, les Laboratoires de Physique, les Académies, les Sociétés Scientifiques et les Revues de Physique sont invités à recevoir cette revue en échange de leurs publications.

PORTUGALIAE PHYSICA donnera un compte-rendu detaillé de tous les ouvrages soumis à la rédaction en deux exemplaires.

All mail concerning PORTUGALIAE PHYSICA to be addressed to

PORTUGALIAE PHYSICA
Laboratório de Física da Faculdade de Ciências
LISBOA-2 (Portugal)

Subscription rates:	250 escudos (US $8.50) per volume
Price of past volumes:	300 escudos (US $10)
Price of copy:	75 escudos (US $2.50)

Members of the «Sociedade Portuguesa de Química e Física» may obtain *Portugaliae Physica* at a reduced price (50 °/₀).

Universities, Physics Laboratories, Academies, Scientific Societies and Physics Publications are invited to receive this review in exchange for their publications.

PORTUGALIAE PHYSICA will give a detailed report of any book if two copies have been submitted.